FINAL PROJECT – ME141502

ANALYSIS OF STALL NACA 23021 PHENOMENON ON APPLICATION HYDROFOIL

Fitri Puspita Dewi
NRP. 4213 101 005

Supervisor
Irfan Syarif Arief, S.T., M.T.
Edi Jadmiko, S.T., M.T.

DOUBLE DEGREE PROGRAM OF MARINE ENGINEERING DEPARTMENT
FACULTY OF MARINE ENGINEERING
INSTITUT TEKNOLOGI SEPULUH NOPEMBER
SURABAYA
2017

"This page is intentionally left blank"

TUGAS AKHIR – ME141502

ANALISA FENOMENA STALL NACA 23021 APLIKASI PADA HIDROFOIL

Fitri Puspita Dewi
NRP. 4213 101 005

Dosen Pembimbing :
Irfan Syarif Arief, S.T., M.T.
Edi Jadmiko, S.T., M.T.

DOUBLE DEGREE PROGRAM OF MARINE ENGINEERING DEPARTMENT
FAKULTAS TEKNOLOGI KELAUTAN
INSTITUT TEKNOLOGI SEPULUH NOPEMBER
SURABAYA
2017

"This page is intentionally left blank"

APPROVAL SHEET

ANALYSIS OF STALL NACA 23021 PHENOMENON ON APPLICATION HYDROFOIL

FINAL PROJECT

Submitted to Comply One of The Requirements to Obtain a Bachelor Engineering Degree
on
Laboratory of Marine Manufacture and Design (MMD) Bachelor Degree Program of Marine Engineering Department Faculty of Marine Technology Institut Teknologi Sepuluh Nopember

Prepared by :
FITRI PUSPITA DEWI
NRP. 4213101005

Approved by
Supervisor of Final Project :

Irfan Syarif Arief, S.T., M.T.
NIP. 1969 1225 1997 02 1001 ( )

Edi Jadmiko, S.T., M.T.
NIP. 1978 0706 2008 01 1012 ( )

SURABAYA
Juli 2017

"This page is intentionally left blank"

APPROVAL SHEET

ANALYSIS OF STALL NACA 23021 PHENOMENON ON APPLICATION HYDROFOIL

FINAL PROJECT

Submitted to Comply One of The Requirements to Obtain a Bachelor Engineering Degree

on

Laboratory of Marine Manufacture and Design (MMD)

Bachelor Degree Program of Marine Engineering Department

Faculty of Marine Technology

Institut Teknologi Sepuluh Nopember

Prepared by :

FITRI PUSPITA DEWI

NRP. 4213101005

Approved by

Head of Marine Engineering Department

Dr. Eng. M. Badrus Zaman, S.T., M.T.

NIP. 1977 0802 2008 01 1007

SURABAYA

Juli 2017

"This page is intentionally left blank"

APPROVAL SHEET

ANALYSIS OF STALL NACA 23021 PHENOMENON ON APPLICATION HYDROFOIL

FINAL PROJECT

Submitted to Comply One of The Requirements to Obtain a Bachelor Engineering Degree

on

Laboratory of Marine Manufacture and Design (MMD)
Bachelor Degree Program of Marine Engineering Department
Faculty of Marine Technology
Institut Teknologi Sepuluh Nopember

Prepared by :

FITRI PUSPITA DEWI
NRP. 4213101005

Approved by
Representative Hochschule Wismar in Indonesia

Dr.-Ing Wolfgang Busse

SURABAYA
Juli 2017

"This page is intentionally left blank"

DECLARATION OF HONOR

I, who signed below hereby confirm that:

This bachelor thesis report has written without any plagiarism act, and confirm consciously that all the data, concepts, design, references, and material in this report own by Marine Manufacturing and Design (MMD) in Department of Marine Engineering ITS which are the product of research study and reserve the right to use for further research study and its development.

Name	: Fitri Puspita Dewi
NRP	: 4213 101 005
Bachelor Thesis Title	: Analysis of Stall NACA 23021 Phenomenon On Aplication Hydrofoil
Department	: Double Degree Program in Marine Engineering

If there is plagiarism act in the future, I will fully responsible and receive the penalty given by ITS according to the regulation applied.

Surabaya, July 2017

Fitri Puspita Dewi

ANALYSIS OF STALL NACA 23021 PHENOMENON ON APPLICATION HYDROFOIL

Student Name : Fitri Puspita Dewi
NRP : 4213101005
Department : Marine Engineering
Supervisor : 1. Irfan Syarif Arief, S.T., M.T.
2. Edi Jadmiko, S.T., M.T.

ABSTRACT

Hydrofoil is a ship with hull that has foil which is mounted on a strut under the hull. One of the hydrofoil characteristics is the position of hydrofoil angle which named angle of attack. Angle of attack is an angle that formed by chord hydrofoil and flow velocity vector of frestream fluid. The aim from angle of attack is to optimized lift force and drag ratio. Then, the stall condition in hydrofoil ship is the result of strem separation at high angle of attack with lift force reduction and drag force get bigger because of drag pressure. In this research will find the optimal lift force on NACA 23021 by using CFD simulation. In this simulation will get the pressure distribution and drag coefficient. There are several variables in this research that angle of attack used 5 °, 10 °, 15 °, 20 ° and 25 °; Aspect ratio used 0.05, 0.25, 0.45, 0.65, and 0.85; And Froude number used 0.1, 0.2, 0.3, 0.4, and 0.5. The result of this simulation is the comparison between CL chart, CD chart, and CL / CD chart with angle of attack. With the result are Aspect ratio 0.05 maximum value CL / CD at an angle of attack 20 ° with Fn 0.1, Aspect ratio 0.25 maximum value CL / CD at an angle of attack 15 ° with Fn 0.3, Aspect ratio 0.45 maximum value CL / CD at an angle of attack 15 ° with Fn 0.1, Aspect ratio 0.65 maximum value CL / CD at an angle of attack 15 ° with Fn 0.1, Aspect ratio 0.85 maximum value CL / CD at an angle of attack 15 ° with Fn 0.1.

Keywords : Hydrofoil, NACA 23021, Angle of Attack, Stall, lift

"This page is intentionally left blank"

ANALISA FENOMENA STALL NACA 23021 APLIKASI PADA HYDROFOIL

Nama	: Fitri Puspita Dewi
NRP	: 4213101005
Departemen	: Marine Engineering
Dosen Pembimbing	: 1. Irfan Syarif Arief, S.T., M.T.
	2. Edi Jadmiko, S.T., M.T.

ABSTRAK

Hidrofoil merupakan kapal dengan lambung yang memiliki sayap (foil) yang dipasang pada penyangga (strut) di bawah lambung kapal. Salah satu karakteristik hydrofoil adalah posisi sudut hydrofoil yang bisa disebut juga dengan sudut serang. Sudut serang merupakan sudut yang dibentuk antara chord hydrofoil dengan vector kecepatan aliran fluida freestream. Tujuan dari sudut serang untuk mengoptimalkan gaya angkat pada rasio drag. Kondisi stall pada hydrofoil ship merupakan akibat dari perpisahan aliran pada sudut serang tinggi dengan pengurangan gaya angkat dan bertambah besarnya gaya hambat akibat drag pressure. Pada penelitian ini akan menemukan gaya angkat yang optimal pada NACA 23021 dengan menggunakan simulasi CFD. Dalam simulasi ini akan mendapatkan ditribusi tekanan dengan koefisien drag. Ada beberapa variable dalam penelitian ini yaitu sudut serang yang digunakan 5°, 10°, 15°, 20° dan 25°; Aspect ratio yang digunakan 0.05 , 0.25 , 0.45 , 0.65 , dan 0.85; dan Froude number yang digunakan 0.1 , 0.2, 0.3, 0.4, dan 0.5 . Hasil dari simulasi ini berupa perbandingan antara grafik CL, grafik CD, dan grafik CL/CD dengan sudut serang. Dengan hasil yaitu ketika Aspek rasio 0.05 nilai maksimal CL/CD pada sudut serang 20° dengan Fn 0.1, AR pada 0.25 nilai maksimal CL/CD pada sudut serang 15° dengan Fn 0.3, AR pada 0.45 nilai maksimal CL/CD pada sudut serang 15° dengan Fn 0.1, AR pada 0.65 nilai maksimal CL/CD pada sudut serang 15° dengan Fn 0.1, AR pada 0.85 nilai maksimal CL/CD pada sudut serang 15° dengan Fn 0.1.

Kata kunci : Hidrofoil, NACA 23021, Sudut serang, Stall, gaya angkat

"This page is intentionally left blank"

PREFACE

The author is grateful to The Almighty God, Allah SWT who has given His grace and blessing so the thesis entitled **"Analysis of Stall NACA 23021 Phenomenon on Application Hydrofoil"** can be well finished. This final project can be done well by author because the support from my family and colleague. Therefore, the author would like to thank to:

1. My father, Achmad Budiyono (alm) and my mother, Satinah and my brother, Ahmad Maulana Saputra and for all of my family who have given love, support, and prayers.
2. Dr. Eng M. Badruz Zaman, S.T, as the Head of Marine Engineering Department
3. Prof. Semin, ST., MT., Ph.D as the Secretary of Marine Engineering Department
4. My Lecture Advisor, Dr. I. Made Ariana, S.T., M.T., for his motivation, guidance, support and kindness thorugh the learning process.
5. Mr. Irfan Syarif Arief, S.T., M.T. and Mr. Edi Jadmiko, S.T., M.T. as academic advisor who have been guiding and giving a lot of suggestion during my writing the final project.
6. Mr. Ir. Dwi Priyanta, MSE as Double Degree of Marine Engineering Secretary who has advised provided beneficial advisory and motivation.
7. Dr.-Ing Wolfgang Busse as coordinator of Hochschule Wismar in Indonesia and marine engineering lecturer who has been guiding, helping, and teaching the double degree student and giving motivation to all student of the first batch of marine engineering student in double degree program.
8. All of my friends BARAKUDA'13 who have given many stories over the author completed education in Department of Marine Engineering FTK - ITS.
9. All of my BARACUTE'13 who had help, cooperate, and support the author.
10. All of my The Five friends (Winnie, Nahed, Ahda, dan Amira) who gave me huge support & motivation to done my bachelor and made many discussions about grateful life.
11. All of my friends particulary member of MMD who gave me huge support & motivation to done my bachelor.
12. All parties were unable author mentioned.

The author realizes that in the writing of this final project is still far from perfect. Therefore, any suggestions are very welcomed by the author for the improvement and advancement of this thesis. Hopefully, this final project report can be useful for the readers and reference to write next final project.

Surabaya, Juli 2017

Penulis

"This page is intentionally left blank"

TABLE OF CONTENTS

TABLE OF FIGURES

"This page is intentionally left blank"

TABLE OF TABLES

"This page is intentionally left blank"

CHAPTER I
INTRODUCTION

1.1. Background

In Maritime world industry, both management and operations of the development of marine based industry need supporting facilities, such as ships with a variety of specific types which are capable of serving the interest. The technology used in ship-building have a high comfort level and able to fulfill the needs of time travel efficiency. In this case, hydrofoil ship could be one of the options. The travel time in hydrofoil ship is influenced by the foil. Foil or wing is a tool that used as aerodynamic force generator to controls object during in the medium fluid, either gases (especially) or liquids. Foil is divided into two form, that are airfoil and hydrofoil. Airfoil is wing (airplane) that connected at each fuselage and it is a surface that lifts airplane in the air [10] Hydrofoil is a ship with hull that has foil which is mounted on a strut under the hull. The foil will lift the ship when its vessel increases the velocity so that the hull was lifted in and out of the water. This leads to a reduction of resistance and increases the velocity of hydrofoil ship. One of hydrofoil series is NACA hydrofoil which is developed by the National Advisory Committee for Aeronautics.

One of the hydrofoil characteristics is the position of hydrofoil angle which named angle of attack. Angle of attack is an angle that formed by chord hydrofoil and flow velocity vector of frestream fluid. The aim from angle of attack is to optimized lift force and drag ratio. Then, the stall condition in hydrofoil ship is the result of strem separation at high angle of attack with lift force reduction and drag force get bigger because of drag pressure. Dynamic stall occurs when the lifting surface is subjected to a quick motion of fluid or change in its direction. Any dynamic change in flow or a blade that leads to variations in angle of attack (AOA) or free stream velocity causes dynamic stall[8].

The reason of application wing (foil) in hydrofoil ship is because it will produce lift force during the ship increasing speed so that the hull is lifted and out from the water. Therefore, in this research we more focus to stall phenomenon at NACA 230201 with the application of hydrofoil ship by using CFD simulation.

1.2. Problems Statement

The problems that would be concerned on this research are:

a. How is the time estimation of stall NACA 23021 condition that needed by hydrofoil at each Froude number.

b. How is the flow phenomenal on hydrofoil analyzed at each Froude number.

1.3. Research Scope

Scope of problems on this research are:

a. Analysis would be focused only on foil, not including ship.
b. The Froude number of hydrofoil determined by 0.1, 0.2, 0.3, 0.4, and 0.5.
c. The aspect ratio of hydrofoil determined by 0.05, 0.25, 0.45, 0.65 and 0.85
d. The angle of attack of hydrofoil determined by 5°, 10°, 15°, 20° and 25°
e. Analysis would be done on technical analysis but not economical

1.4. Research Objectives

This final report has these following objectives:

a. To determine time estimation of stall NACA 23021 condition that needed by hydrofoil at each Froude number.
b. To know flow phenomenal on hydrofoil at each Froude number.

1.5. Research Benefits

The benefits from this final project as follows:

a. Knowing time estimation of stall NACA 23021 condition on ship's application at each Froude number
b. Determining flow phenomenal on hydrofoil at each Froude number.
c. The result of this final project is expected as reference on next research.

CHAPTER II
LITERATURE STUDY

2.1. Hydrofoil Theory

Hydrofoil is a form that can produce a large lifting force with obstacles as small as possible. Lift and stall of the foil are very dependent on the geometrical shape cross-section of the hydrofoil. Hydrofoil sectional geometric shapes in general can be seen in the following figure [3]:

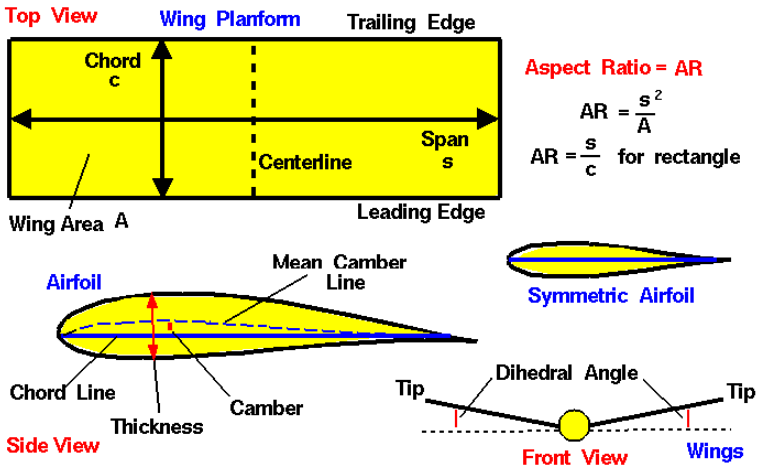

Figure 2. 1 Notation of Hydrofoil [7]

Parts of hydrofoil are as follows [7] :

Span	: the length of wing
Chord	: the width of wing
Spect ratio	: span/chord
Dihedral angle	: angle of wing from plane to wing to tip (purpose is stability)
Camber	: curve of wing
Angle of attack	: angle of wing to the oncoming air
Angle of incidence	: angle of elevators to oncoming air
Leading edge	: the front side hydrofoil
Trailing edge	: the back side hydrofoil
Chord	: distance between the leading edge and the trailing edge
Mean chamber line surfaces	: the line that divides equally between the upper and lower

Maximum chamber : the maximum distance between the line and the chord line chamber

Maximum thickness : the maximum distance between the upper and lowe surfaces.

2.2. The Aerodynamic Force

Lift (L) is a component of the fluid force on the hydrofoil is perpendicular to the direction of movement. Based on the analysis of the equation lift dimensional shapes are as follows [3]:

$$L = 1/2\ \rho V2\ ApCL$$

Where,
L : lift force
CL : lift coefficient
ρ : fluid density
V : velocity
Ap : plan area (S), area maximum : *chord* × *span*

And to calculate the resistance generated by hydrofoil is as follows:

$$D = 1/2\ \rho V2\ ApCD$$

Where,
D : drag force
CL : drag coeffecient
ρ : fluid density
V : velocity
Ap : plan area (S), area maximum : *chord* × *span*

2.3. Characteristics of Airfoil

The wing characteristics may be predicted from the known aerodynamic characteristics of the wing section if the span is large with respect to the chord, if the match number are subcritical, and if the chordwise component of velocity is large compared with the spanwise component. Thus the wing-section characteristics considered in this volume have large field of applicability. The lift is defined as the component of force acting in the plane of symmetry in a direction perpendicular to the line of flight. In addition to the lift, a force directly opposing the motion of the wing through the air is always present and is called "drag" [9].

A convenient way of describing the aerodynamic characteristics of a wing is to plot the values of the coefficients against the angle of attack, which is the angle

between the plane of the wing and direction of motion. The lift coefficient increases almost linearly with angle of attack until maximum value is reached, whereupon the wing is said to "stall". The drag coefficient has a minimum value at low lift coefficient, and the shape of the curve is approximately parabolic at angles of attack below the stall. In as much as the high-speed lift coefficient is usually substantially less than that corresponding to the best lift-drag ratio, one of the best ways of reducing the wing drag is to reduce the wing area. This reducing of area is usually limited by considerations of stalling speed or maneuverability. These considerations are directly influenced by the maximum lift coefficient obtainable. The wing should therefore have a maximum lift coefficient combined with low drag coefficient for high speed and cruising flight[9].

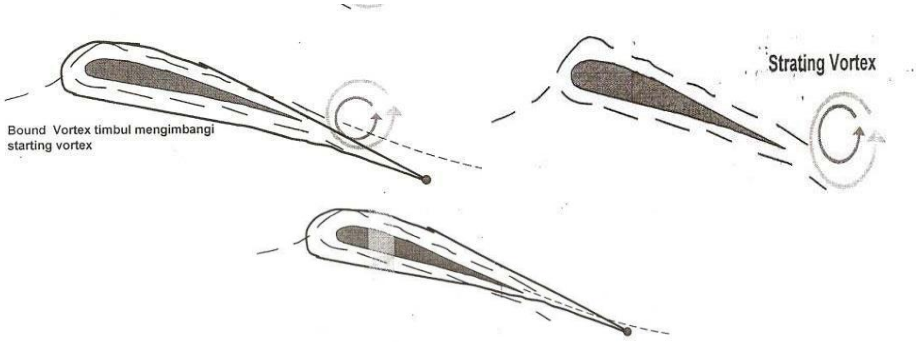

Figure 2. 2 Formation Process of Lift [4]

Here is the formation process of lift:

- The flow of air is flowing through the airflow was divided into two flows, above and below the surface of the airfoil.
- In trailing edge those flows unite again. But, because of the difference angle of direction, the two flows will make a starting vortex with the direction of rotation is counterclockwise.
- Due to the rotary momentum of initial flow is zero, then according to the law of conservation of momentum, must arise a vortex against the direction of this starting vortex. This vortex spins in a clockwise direction around the airfoil and called bound vortex.
- Starting vortex will be shifted to the rear for forward movement.
- Due to this bound vortex, the flow above the surface will get extra speed, and the flow under the surface will get a reduction in speed.
- Due to the difference of speed, according to the Bernoulli law, arise a force which the direction goes up and it's called lift.

2.4. NACA

NACA (National Advisory Committee for Aeronautics) airfoil is one form of a simple hydrodynamic which is useful to provide a certain lift against another form and with mathematical completion it is possible to predict how many the amount of lift generated by an airfoil shape. Airfoil geometry has a major influence on the characteristics of hydrodynamic with important parameters such as CL (Coefficient Lift) and then be associated with lift (lift generated).

Digit Series of NACA

a. Four Digit Series

For types of NACA's four digit series, the meaning of its numbers is:

1. The first digit states the maximum percent of chamber to the chord
2. The second digit states tenths of the maximum position of the chamber on the chord from the leading edge.
3. The last two digits expresses percent of airfoil thickness to chord.

Example of this numbering is airfoil NACA 2412, this means the airfoil has 0.02 of maximum chamber located at 0.4c from the leading edge and has 12% of maximum thickness of chord or 0.12c.

b. Five Digit Series

Mean of chamber line of this series is different than the four digits series. This change was made in order to shift the maximum of the next chamber, thereby increasing the CL max. For this type of NACA's five digit series, the meaning of its numbers is:

1. The first digit multiplied by 3/2 and then divided by ten gives design value of lift coefficient.
2. The next two digits are the maximum percent of chamber to the chord position.
3. The last two digits represent a percent thickness/thickness of the chord.

In addition to a series of four-digit and five-digit NACA still has the classification of the other series, the NACA Series-1 (Series 16), NACA Series 6, NACA Series 7 and NACA Series 8.

Table 2. 1 Characteristics Comparison of Airfoil NACA Series

Series	Advantages	Disadvantages
4-Digits	Have a good characteristic of stall	Mostly have a low lift coefficient

	The center of the pressure movement is small	Have a relatively high drag
	Not too influenced with roughness	
	Have a high maximum coefficient	Big pitching moment
5-Digits	High maximum lift coefficient	Bad stall behavior
	Small pitching moment	Have a relatively small drag
	Not influenced with roughness	
6-Digits	Drag is very low if airfoil works inside operation area	Drag is very high if airfoil works outside the operation area
	Have a high maximum coefficient	Big pitching moment
	Suitable for high wind velocity	Susceptible with roughness
7-Digits	Drag is very low if airfoil works inside operation are	Reduction of maximum lift coefficient
	Small pitching moment	Bad stall behavior
16-Digits	Avoiding low pressure peaks	Have relatively small lift force
	Low drag force at high velocity	

2.5. Computational Fluid Dynamics Method

Computational Fluid Dynamics (CFD) is an image modeling to solve problems related to fluid flow. CFD is used to simulate the interaction of fluids with surfaces (boundary condition), to predict fluid flow, heat transfer, phase change, chemical reactions and the voltage on the solid surface [3].

In the simulation process, there are three steps that must be done, namely: pre-processing, solving and post-processing.

• Pre-processing is the process of entering data. This process includes:

a. Defining the boundaries conditions (boundary) of geometry
b. Determination of domains
c. Selection of the type of fluid to be analyzed

• Solving is a counting process of the input data that has been given to the method of numerical solver. This stage is divided into several methods:

a. Finite difference method
b. Finite elements method
c. Finite volume method
d. Boundary element method

Post processing is a simulation stage to interpret conditions that have been created.

CHAPTER III
METHODOLOGY

3.1. Research Methodology

To solve these problems would be used CFD method. Experimental design could be seen on this flow chart below. On this experimental design divided by 3 primary steps i.e. preparation (identification the problems, literature review, data collection, determine variable data), analysis (make hydrofoil model, examination and modification model, data analysis), and result.

3.1.1. Step I Preparation

a. Identify the problems

Identify the problem including the estimated time of the NACA 23021 stall conditions required for hydrofoil vessel on each Froude number and state of the sea that will be used to determine the flow phenomena in each Froude number.

b. Literature review

The study of literature of my thesis is by collecting reference material to be studied as a supporting material such research activities is to find some reference books, journals, papers or on the internet relating to the stall condition of the hydrofoil and Froude number.

c. Data Collecting

Collecting data on the ocean wave conditions related with sailling that will be performed by hydrofoil ship.

Design hydrofoil

NACA Type : NACA 23021

Angle of attack : 5°, 10°, 15°, 20° and 25°

d. Determining Veriable Test

Determination of parameters test in Computational Fluid Dynamics include:

- Control variable : The Froude Number, angle of attack, and aspect ratio
- Free variable : Flow type
- Fixed variable : Hydrofoil design and specification

3.1.2. Step II Analysis

a. Making Model of Foil in Software

Making model of foil standard is NACA 23021 with the existing data by using software. NACA 23021 has the best quality on the previous studies have calculated a series of NACA and determined that the NACA 23021 has a ratio X / C is better than others NACA series when used for hydrofoil.

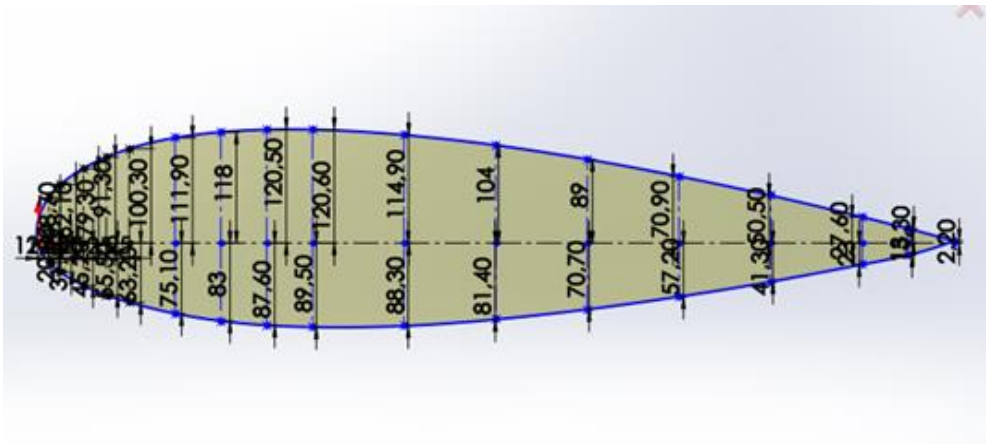

Figure 3. 1 Hydrofoil NACA 23021

b. Testing and Model Modification

Testing and model modification is performed by simulating the model using Computational Fluid Dynamics software. In this study, the model simulated variations hydrofoil Froude number, attack angle and aspect ratio to determine the time estimation of stall condition.

c. Data Analysis

Data analysis is obtained from model testing in each variable and showing that data in the grafik and the visual. Results obtained in the form:

- Distribution of pressure on the foil
- 2The total force each direction on the foil
- Visualization flow hydrofoil

3.1.3. Step III Conclusion

After data analysis and the conclusions obtained then determined foil configurations that give the results of time when the stall condition is occur.

3.2. Flowchart of Research Methodology

To solve the problems above, the flowchart as follows:

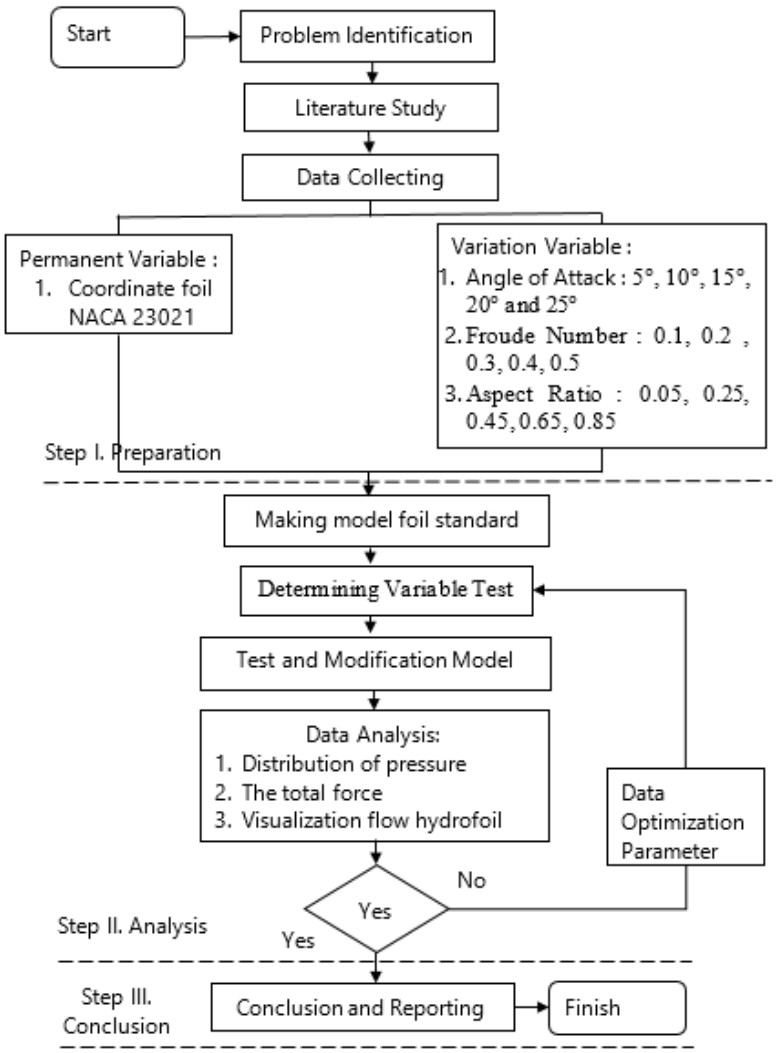

Figure 3. 2 Flowchart of Research

"This page is intentionally left blank"

CHAPTER IV
DATA ANALYSIS AND DISCUSSION

4.1. General

This chapter will explain about steps of completing the final project with the title An Analysis of Stall NACA 23021 on Application Hydrofoil. The explanation starts from the phase of modeling NACA 23021 software Computational Fluid Dynamics. In this final project, the angle of attack of foil which is varied are 5°, 10°,15°, 20° dan 25°. Aspect ratio of foil which is varied are 0.05, 0.25, 0.45, 0.65, dan 0.85. Additionally varied, the Froude number of ship also varied 0.1, 0.2,0.3,0.4, and 0.5 to determine the distribution of pressure model foil at each change velocity.

4.2. Choice of Foil

This research uses NACA 23021 with reference to the previous research.

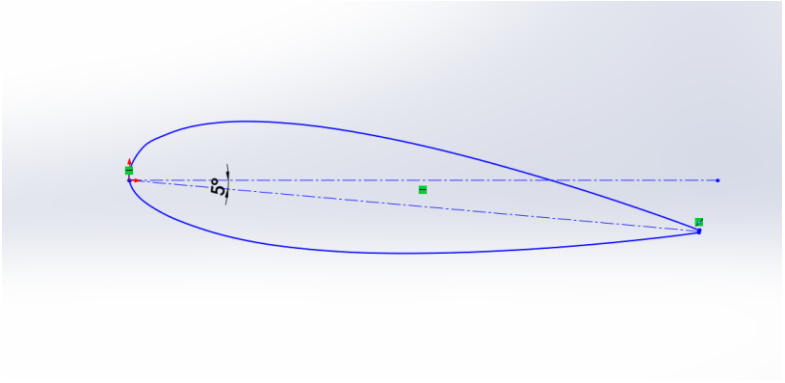

Figure 4. 1. 5 Degrees Angle

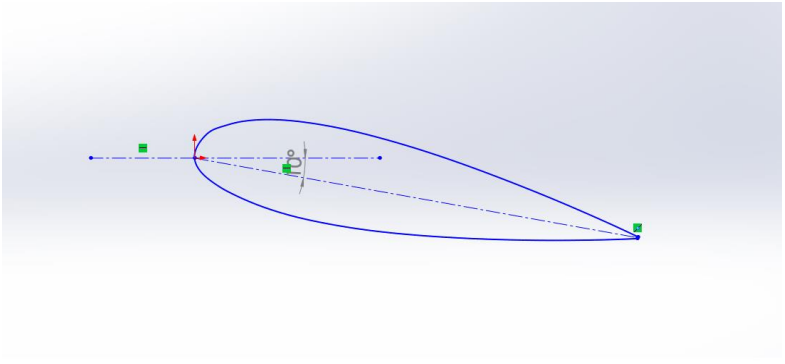

Figure 4. 2 10 Degrees Angle

Foil Geometry

The foil geometry data is shown in Table.

Table 4. 1 The Coordinate of Foil NACA 23021

#GROUP	POINT	X-CORD	Y-CORD	Z-CORD
1	1	1,0000	0,0022	0
1	2	0,9500	0,0153	0
1	3	0,9000	0,0276	0
1	4	0,8000	0,0505	0
1	5	0,7000	0,0709	0
1	6	0,6000	0,0890	0
1	7	0,5000	0,1040	0
1	8	0,4000	0,1149	0
1	9	0,3000	0,1206	0
1	10	0,2500	0,1205	0
1	11	0,2000	0,1180	0
1	12	0,1500	0,1119	0
1	13	0,1000	0,1003	0
1	14	0,0750	0,0913	0
1	15	0,0500	0,0793	0
1	16	0,0250	0,0641	0
1	17	0,0125	0,0487	0
1	18	0,0000	0,0000	0
1	19	0,0125	-0,0208	0
1	20	0,0250	-0,0314	0
1	21	0,0500	-0,0452	0
1	22	0,0750	-0,0555	0
1	23	0,1000	-0,0632	0
1	24	0,1500	-0,0751	0
1	25	0,2000	-0,0830	0
1	26	0,2500	-0,0876	0
1	27	0,3000	-0,0895	0
1	28	0,4000	-0,0883	0
1	29	0,5000	-0,0814	0
1	30	0,6000	-0,0707	0
1	31	0,7000	-0,0572	0
1	32	0,8000	-0,0413	0
1	33	0,9000	-0,0230	0
1	34	0,9500	-0,0130	0
1	35	1,0000	-0,0022	0

In this step, every coordinate of foil NACA is illustrated according to types of NACA which have been decided. The first step is to make points of coordinates in accordance with NACA hydrofoil dimension is used, in this case used NACA 23021.

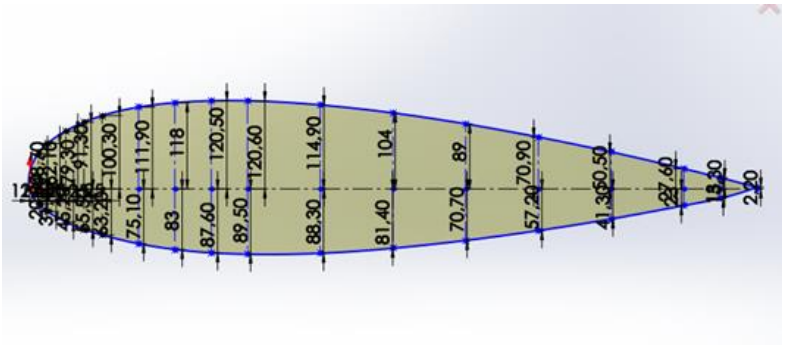

Figure 4. 3 Foil Coordinate Configuration

After that point coordinates connected with a curve, the curve is divided into top and bottom so that the next analysis step becomes easier. Furthermore, the finished shape of the curve is made into a solid by the parameter of AR are 0.05, 0.25, 0.45, 0.65, and 0.85.

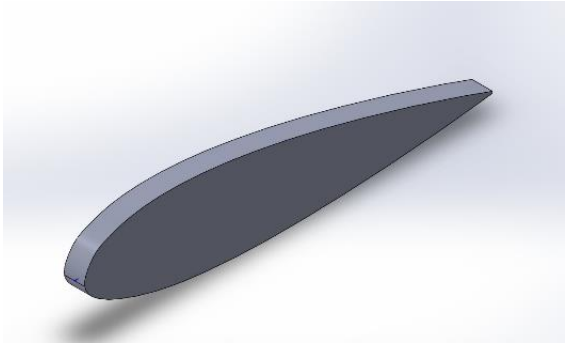

Figure 4. 4 Model Foil with AR 0.05

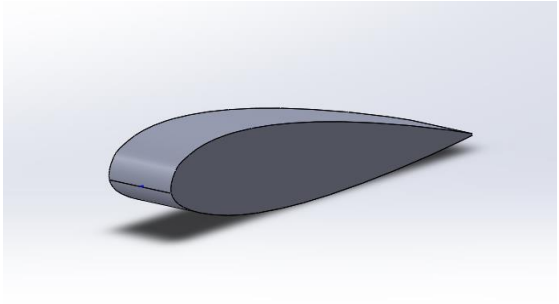

Figure 4. 5 Model Foil with AR 0.25

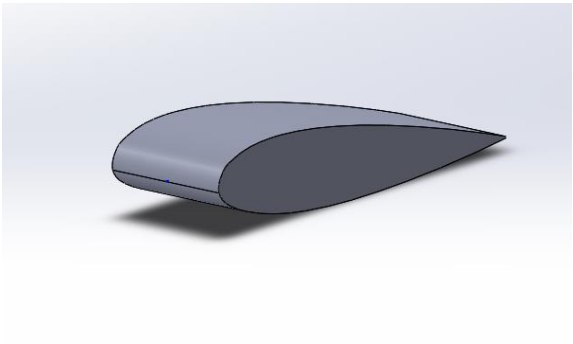

Figure 4. 6 Model Foil with AR 0.45

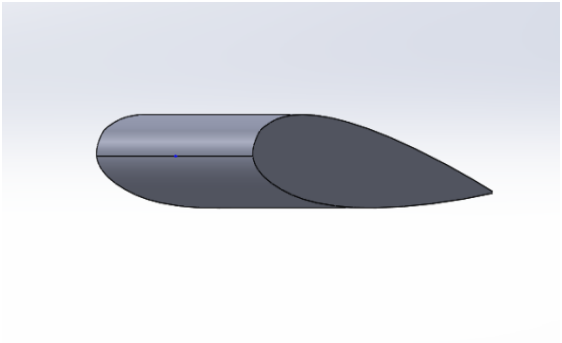

Figure 4. 7 Model Foil with AR 0.65

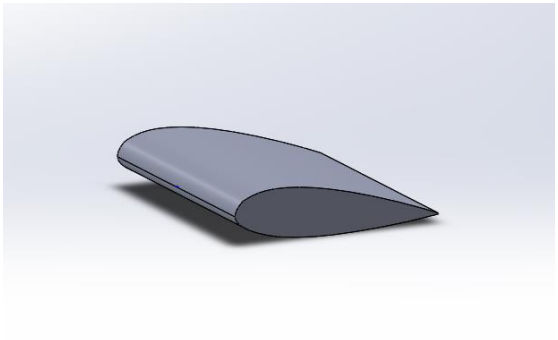

Figure 4. 8 Model Foil with AR 0.85

4.2.1. Meshing

After finishing the model geometry foil, the next step is meshing. This stage is a detailed division of geometry to be more subtle and specific by mesh sizing optimization.

Before doing meshing, first performed the domain creation process. Domain size has a standard size of a boundary so that the analysis results can correspond to the actual state of the environment.

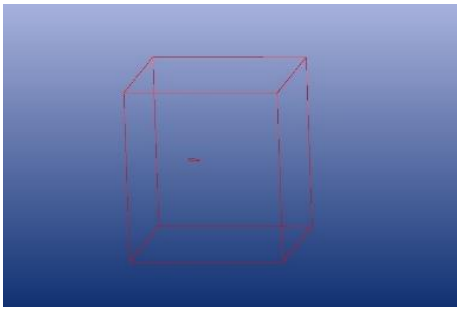

Figure 4. 9 Standard Size of Domain Boundary

The first meshing parameter is the initial mesh, where in the first parameter is defined geometry size distribution of the entire domain. Domain is divided into squares to match the domain that has been created.

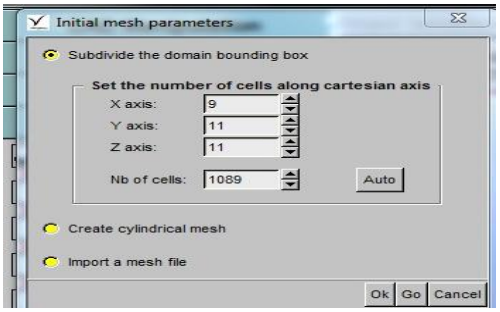

Figure 4. 10 Start of Meshing

The second parameter defines the parts that should get more improvement than others, usually found at the end of the domain.

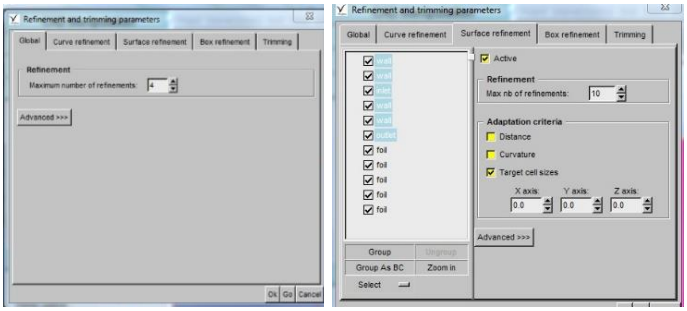

Figure 4. 11 Adaptation of Geometry

The third parameter is about repair of first and second parameter where the meshing will be more subtle and touching every part of the domain geometry. The fourth parameter is the optimization parameters that follow form part meshing domain.

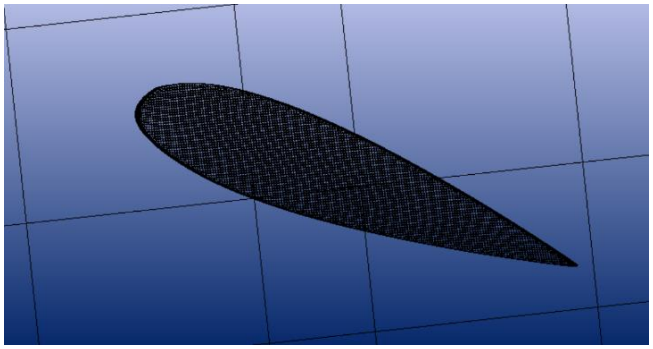

Figure 4. 12 Result of Meshing

The fifth parameter is about meshing conditions at the surface of the object. In this fifth meshing parameters, it requires the size and speed of the ship so that the result of Reynolds number and Froude numbers are influenced the size and speed of the ship.

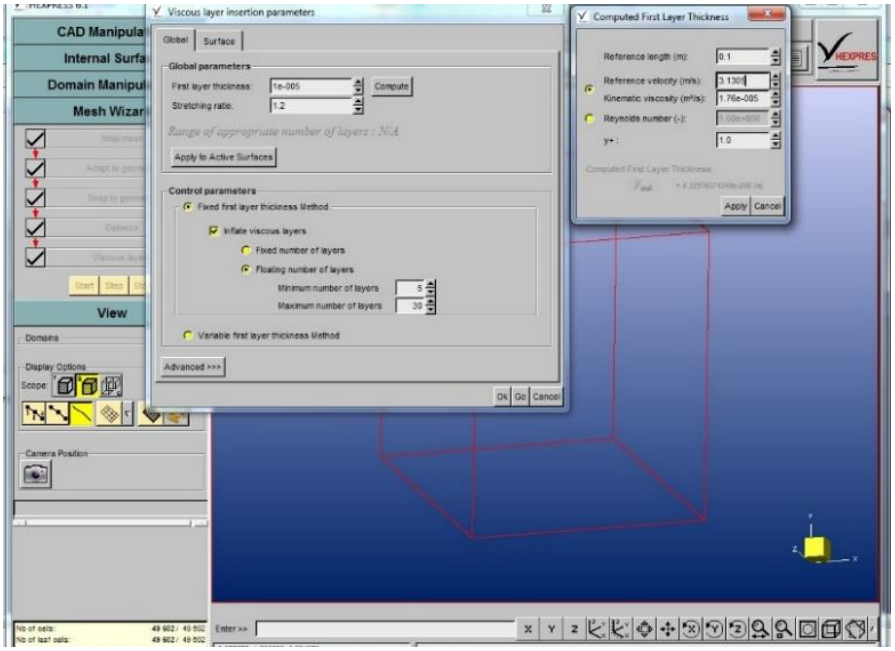

Figure 4. 13 Parameter of Meshing Optimization

4.2.2. The setting and Simulation Model

The next process after meshing and geometry definition is a process flow simulation parameter settings. Here are some parameters that should be defined at this stage:

a. Flow Conditions
   Flow conditions are divided into 2 types where the steady flow fixed flow rate and unsteady flow in which the genre has a speed changing. The explanation of the flow that is used in this study was unsteady flow.

b. Type of Fluid
   Fluid used is water fluid.

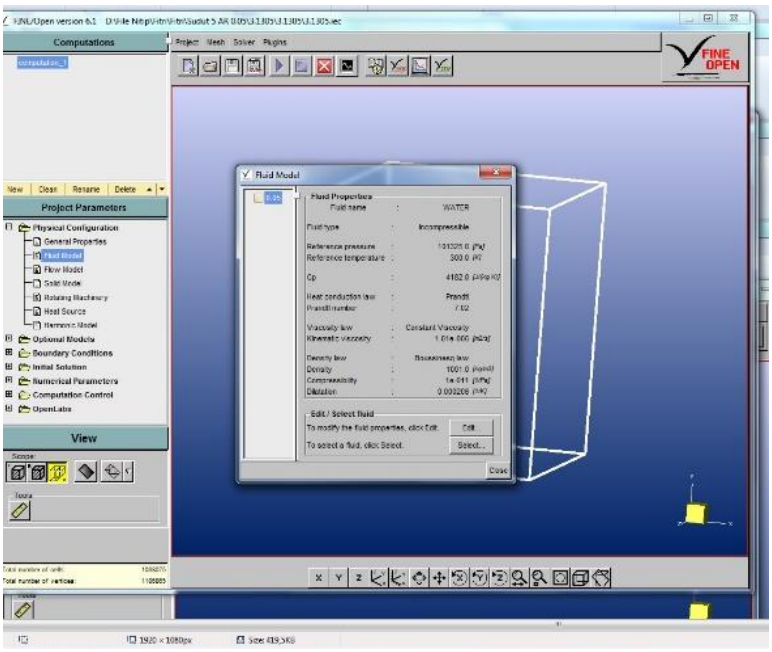

Figure 4. 14 Parameter of Fluid Type

c. Flow Types
   The most common of flow turbulence model used in this fluida flow analysis is model of k-epsilon (Launder-Sharma). Parameter size and speed of the vessel is required to obtain a value Reynolds Number and Froude Number.

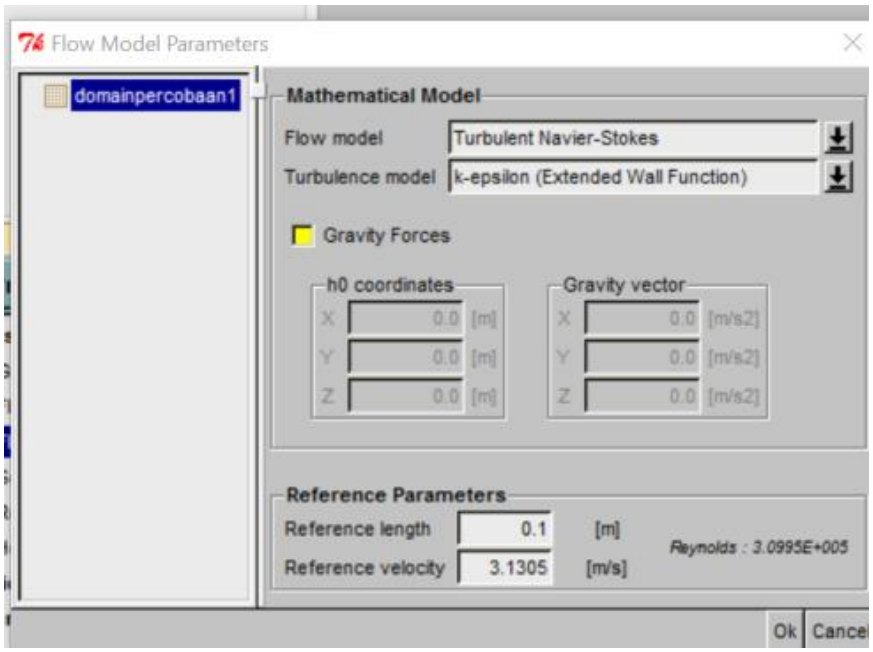

Figure 4. 15 Parameter of Flow Type

d. Geometry Boundary Condition

Domain boundaries need to be defined to distinguish the types of boundaries. The boundary conditions can be a function of the wall that has a definition of friction value or limit without slip / friction.

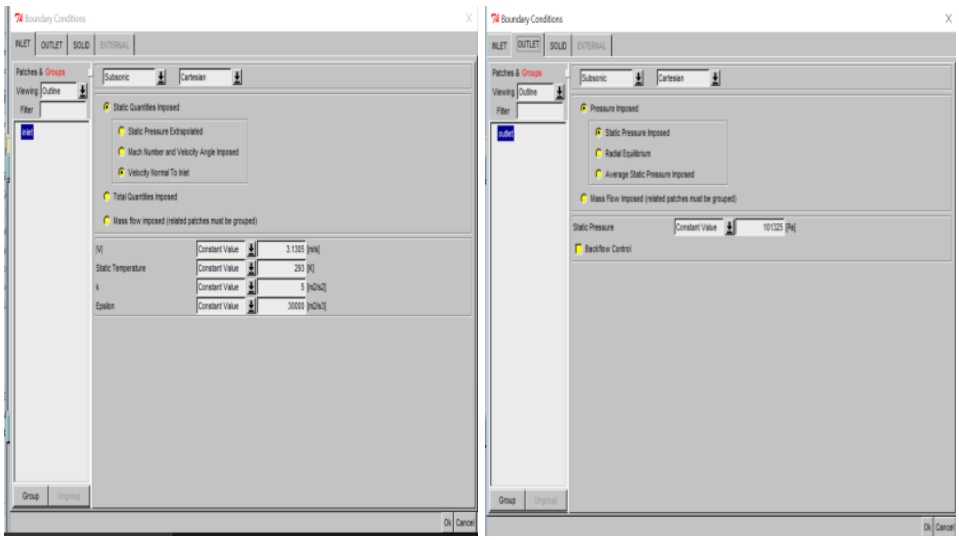

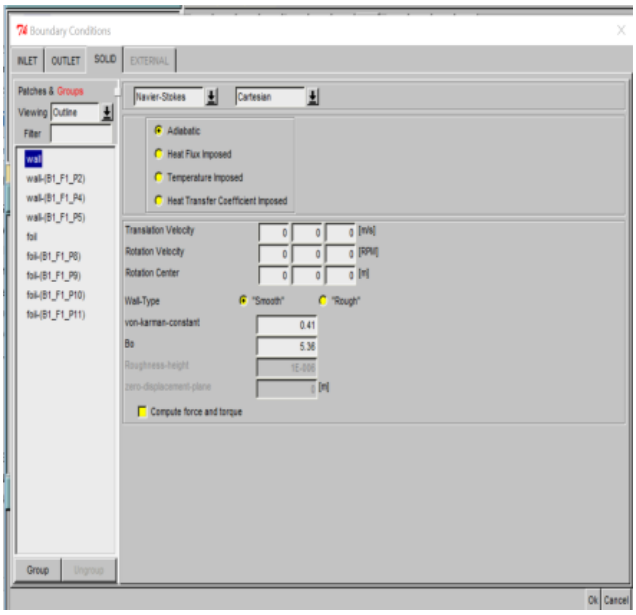

Figure 4. 16 Parameter of Boundary Condition

e. Other Parameters
Variable Control and Analysis Report defines the number of time step and period foil movement used. After all the parameters are defined, then we can do the next process, running simulation process. The process of running the simulation is computationally data calculation process by the computer (this software has a relatively heavy load so that the computer used must also have adequate specification in order the solver process can be executed).

4.3. Result of Model Simulation

Simulated models will produce data such as pressure distribution value at the lift of foil and Coeffision friction value at the drag of foil. There are five models of Aspect ratio of NACA 23021, five variations of angle of attack and five velocity variations are analyzed. Here are the results to the model AR 0.05 with angle of attack 5° and will be attachement for each model variations.

Table 4. 2 **Picture of Simulation results for each variation**

Aspect Ratio	Angle of Attack	Froude Number	Picture of Analysis Result
0.05	5°	0.1	*Pressure Distribution* 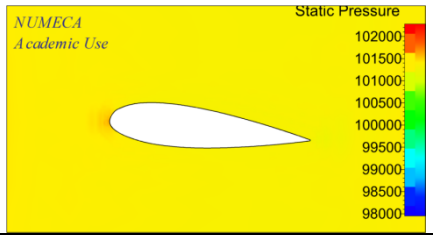
		0.2	*Pressure Distribution* 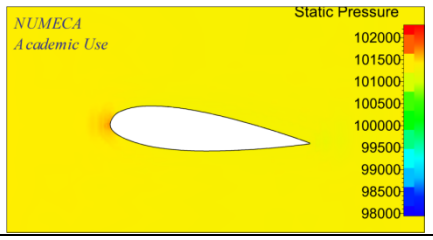
		0.3	*Pressure Distribution* 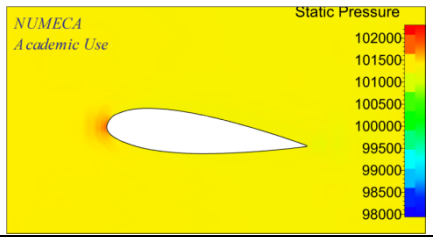
		0.4	*Pressure Distribution* 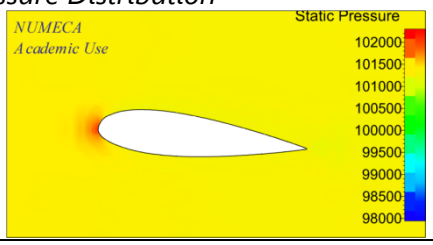
		0.5	*Pressure Distribution* 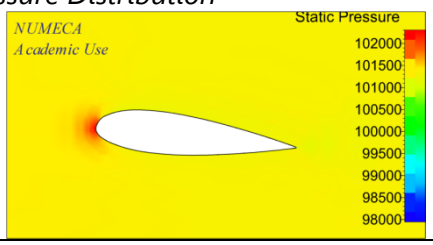

4.3.1. Discussion

The result of simulation is conducted by the 5 variation of angle of attack, the 5 variation of aspect ratio, and the 5 variation of velocity produces data value analysis

foil geometry. Existing data produced include pressure distribution, lift, drag. And then, The data is plotted become a graph for the review to know the characteristics from each model which are attachment.

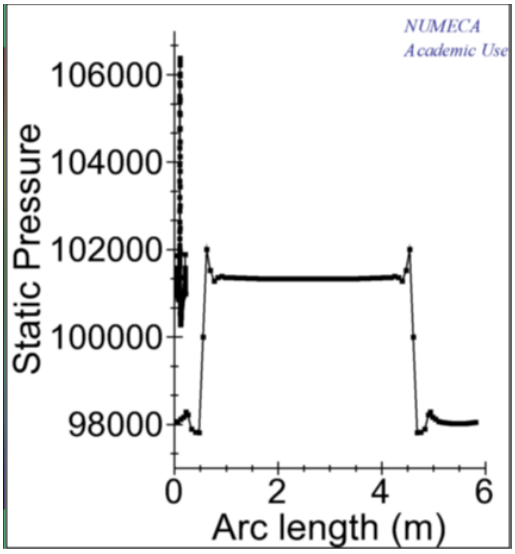

Figure 4.17 The graphic of cartesian pressure

After the graph of cartesian pressure is obtained from all models, then the lift force on the front of hydrofoil and behind of hydrofoil are calculated. The formula that used is Bernoulli equiblirium.

$$P^1-P^2 = (F^1-F^2)\ A$$

Where :

P1 : Pressure under the Foil (Pa)
P2 : Pressure on the Foil (Pa)
F1 : Lift force under the Foil (Newton)
F2 : Lift force on the Foil (Newton)
A : Surface area of Foil (m^2)

The lift force is get from the graph, then the CL value is determined for each model and to get the CD value is from the simultion result graph. The formula that used to determine the CL value is:

$$L = 1/2\ \rho V^2\ ApCL$$

Where,

L : lift force
CL : lift coefficient
ρ : fluid density
V : velocity
Ap : plan area (S), area maximum : *chord* × *span*

4.3.2. Grafik CL pada AR 0.05

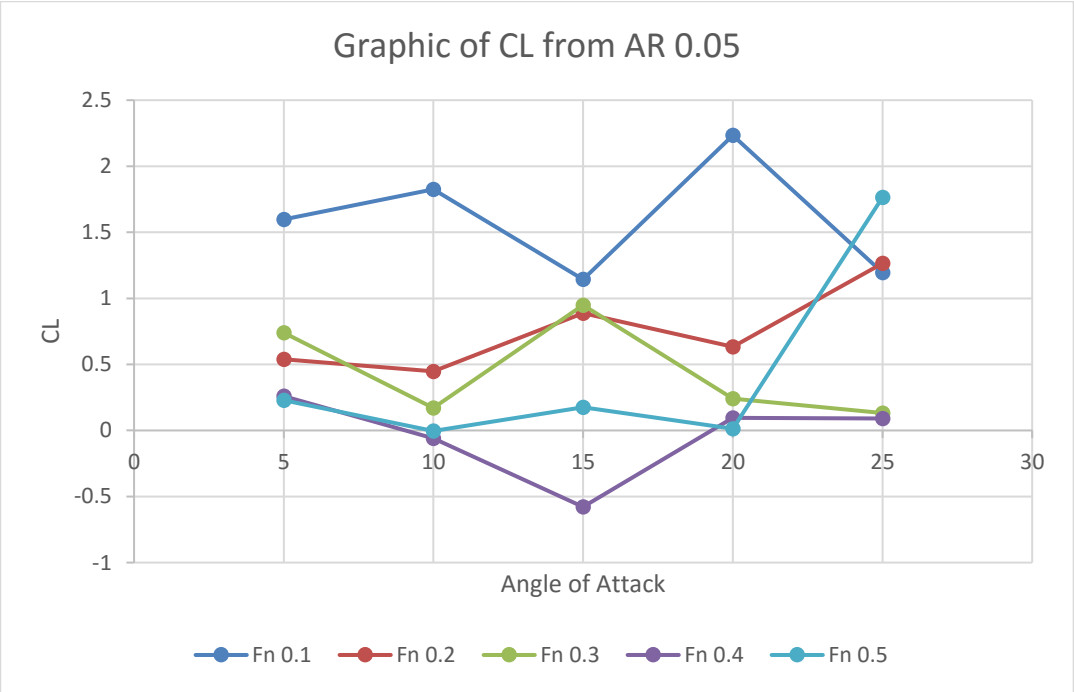

In the graph 4.3.2. Can be seen on the angle of attack 20 ° with Fn 0,1 has the largest CL ratio with other variation angle, that is equal to 2,233. And it just goes down by a huge variation. Can be concluded with the largest optimal ratio of CL is at an attack angle of 15 ° with Fn 0.1.

4.3.3. Grafik CD pada AR 0.05

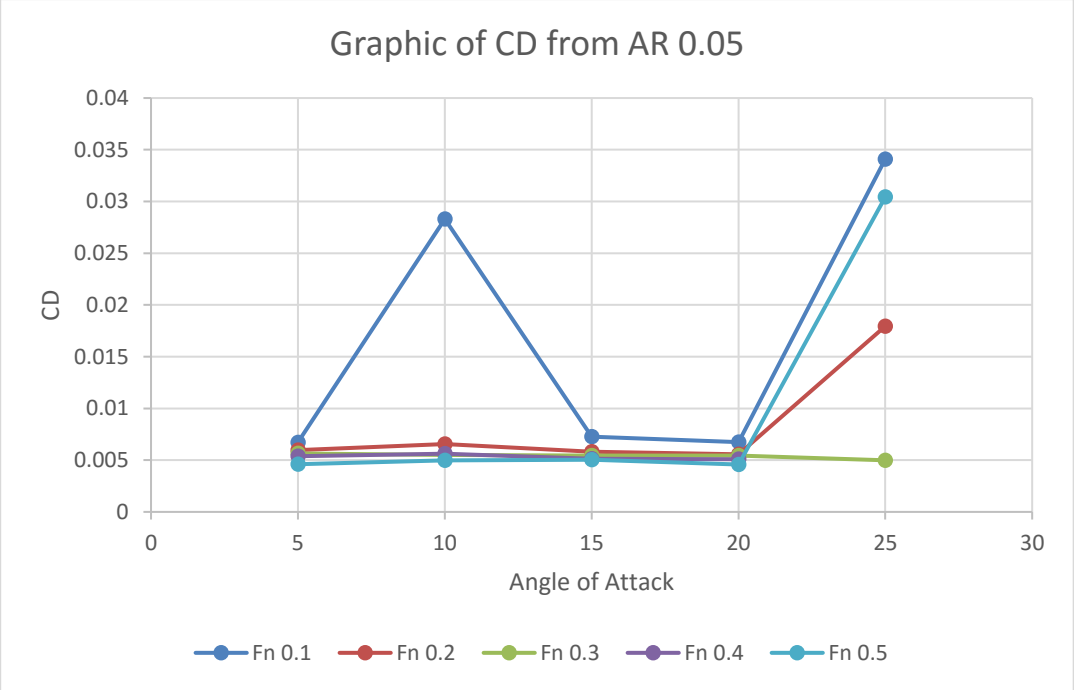

In graph 4.3.3 2 can be seen that at the angle of attack 10 ° with Fn 0.1 there is an increase of CD ratio with other Fn variation, that is equal to 0.0283. And the value immediately decreases at an angle of 15 ° and then rises again at the next corner. It can be concluded that at fn 0.1 has a high drag coefficient of other fn variations

4.3.4. Grafik CL/CD pada AR 0.05

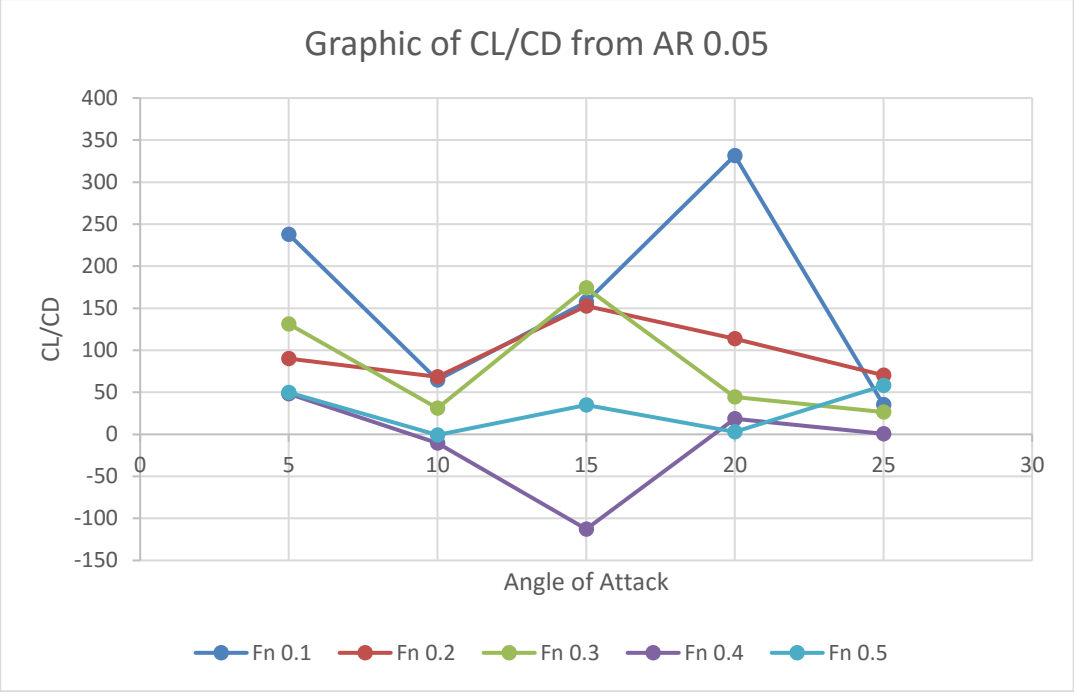

In the graph 4.3.4 it can be seen that at an angle of attack 20 ° with Fn 0.1 there is an increase in CL / CD ratio with another Fn variation, that is equal to 331. and the value is directly decreased at an angle of 25 °. At an attack angle of 15 ° with Fn 0.4 there is a decrease in CL / CD ratio with another Fn variation, that is -112 and the value rises directly as the angular variation increases.

4.3.5. Grafik CL pada AR 0.25

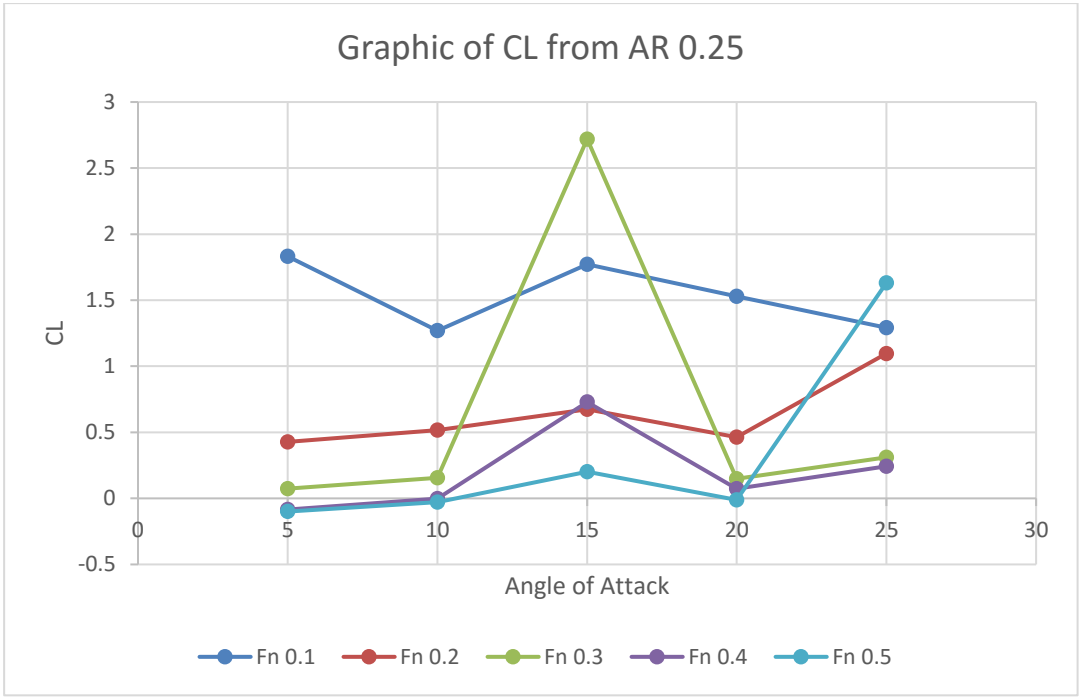

In graph 4.3.5 it can be seen that at the angle of attack 15 ° with Fn 0.3 has the largest CL ratio with other variation angle, that is equal to 2,719. And the value decreases as the angular variation increases. So it can be concluded that the largest CL is at an attack angle of 15 ° with Fn 0.3.

4.3.6. Grafik CD pada AR 0.25

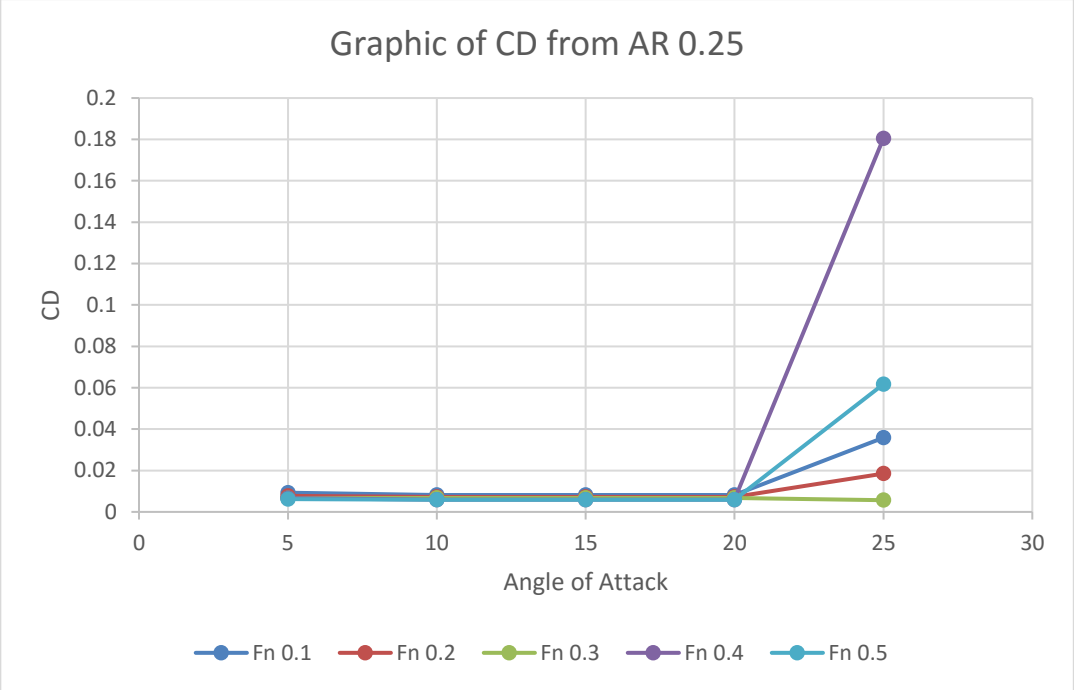

In graph 4.3.6 it can be seen that at the angle of attack 25 ° with Fn 0.4 has the largest CD ratio with other Fn variation, that is equal to 0.1805. So it can be concluded that the largest CD is at an attack angle of 25 ° with Fn 0.4.

4.3.7. Grafik CL/CD pada AR 0.25

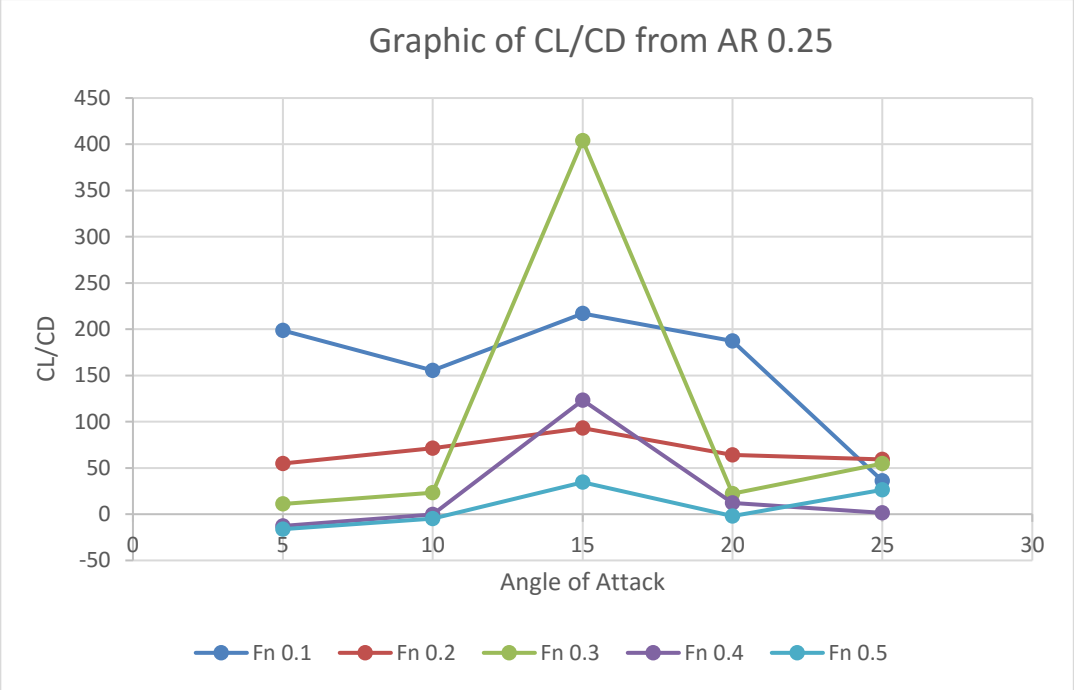

In graph 4.3.7 can be seen that at the angle of attack 15 ° with Fn 0.3 incremented ratio CL / CD with other Fn variation, that is equal to 403. and and the value decrease with variation of angle with big cave. It can be concluded that the largest CL / CD is at an attack angle of 15 ° with Fn 0.3.

4.3.8. Grafik CL pada AR 0.45

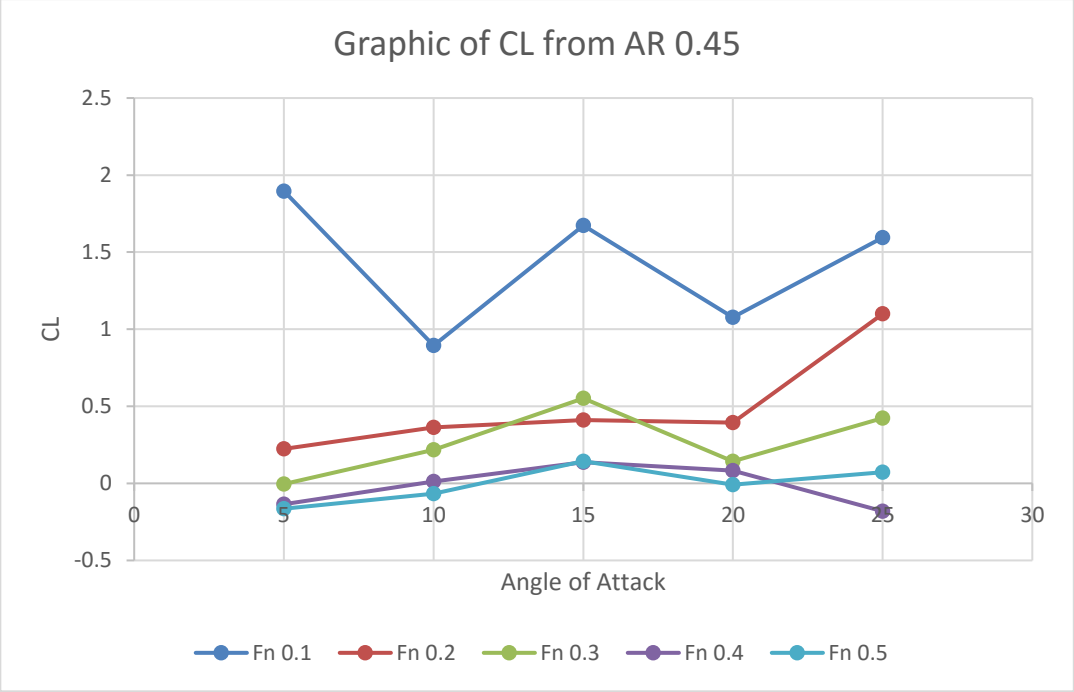

In graph 4.3.8 can be seen that at the angle of attack 5 ° with Fn 0.1 has the largest CL ratio with other angle variation, that is equal to 1.89. And the value decreases as the angular variation increases. It can be concluded that the largest CL is at an angle of 5 ° with Fn 0.1.

4.3.9. Grafik CD pada AR 0.45

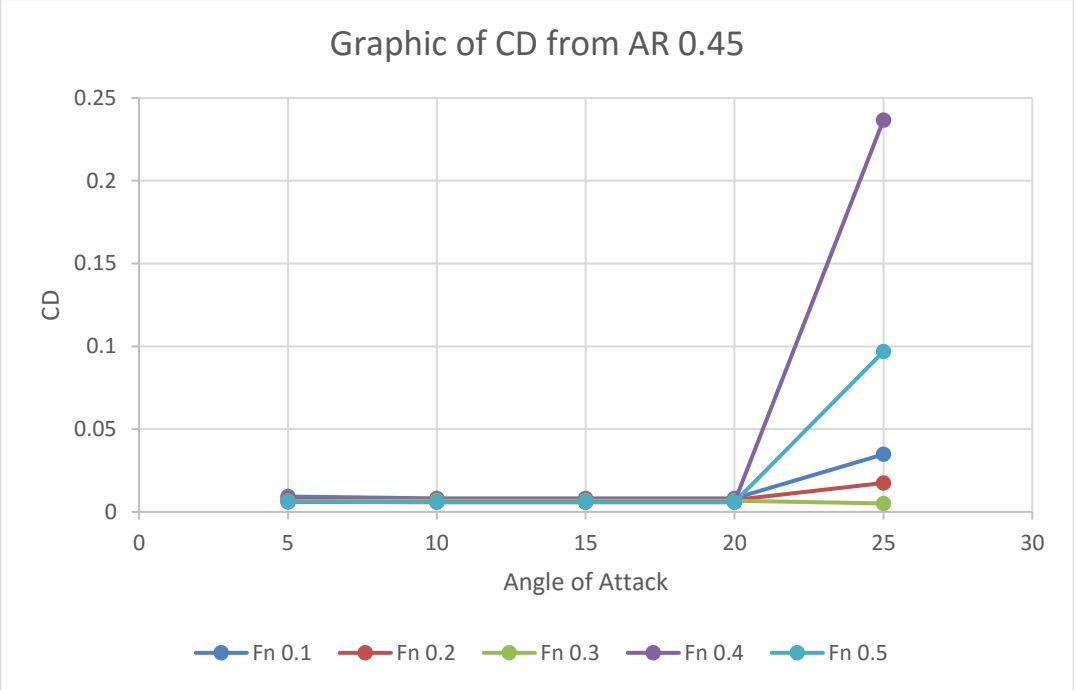

In graph 4.3.9 can be seen that at the angle of attack 25 ° with Fn 0.4 has the biggest CD ratio with other variation of angle, that is equal to 0.23. So it can be concluded that the largest CD is at an attack angle of 25 ° with Fn 0.4.

4.3.10. Grafik CL/CD pada AR 0.45

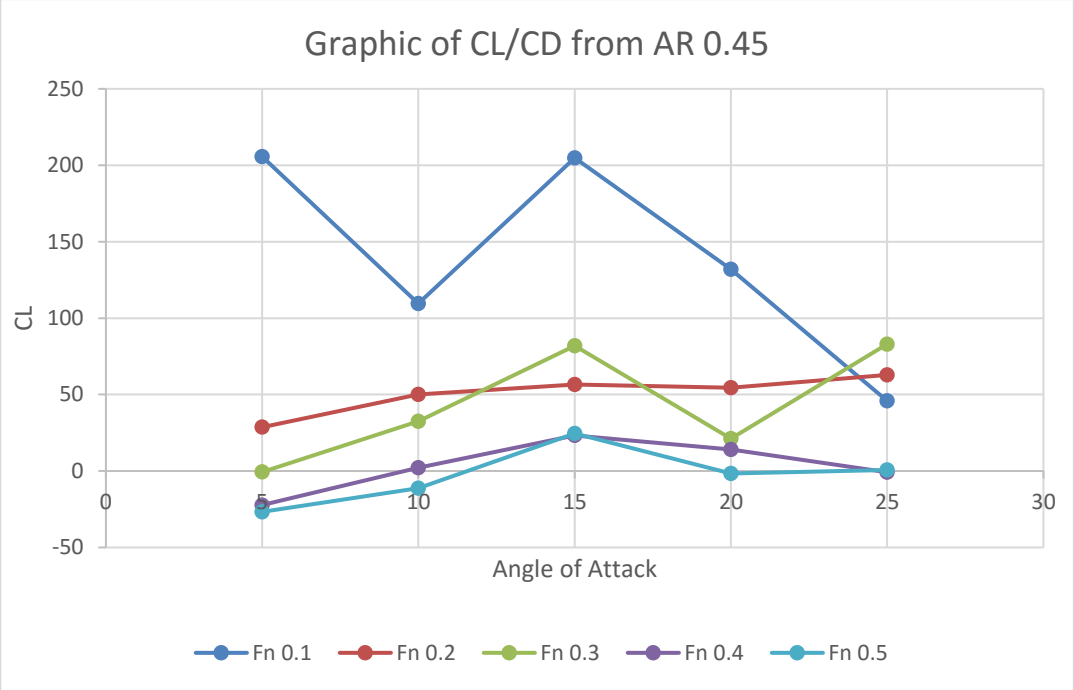

In graph 4.3.10 it can be seen that at the angle of attack 5 ° with Fn 0.1 has the biggest CL / CD ratio with other angle variation, which is 205. and the value decreases with increasing angle variation. At Fn 0.1 it also has the largest CL / CD value of any other Fn value. It can be concluded that the largest CL / CD is at an angle of 5 ° with Fn 0.1.

4.3.11. Grafik CL pada AR 0.65

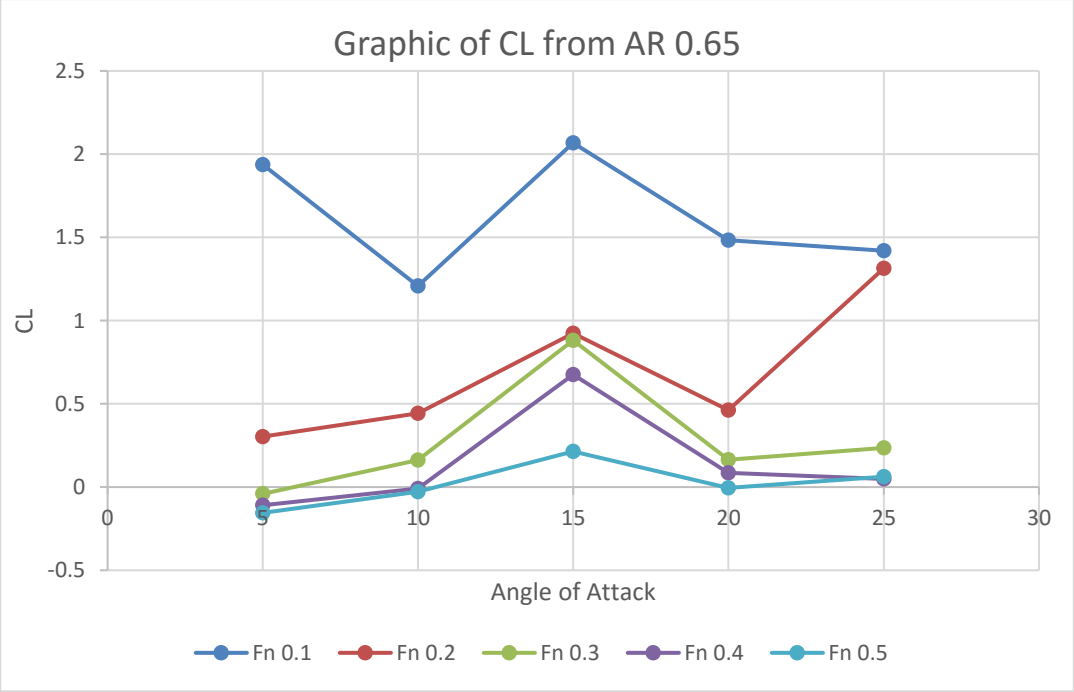

In graph 4.3.11 can be seen that the Fn 0.1 has the largest CL ratio with other Fn variations and the largest value occurs at an angle of 15 ° that is equal to 2.06. And the value increases as the angular variation increases. It can be concluded that the largest CL is at an attack angle of 15 ° with Fn 0.1.

4.3.12. Grafik CD pada AR 0.65

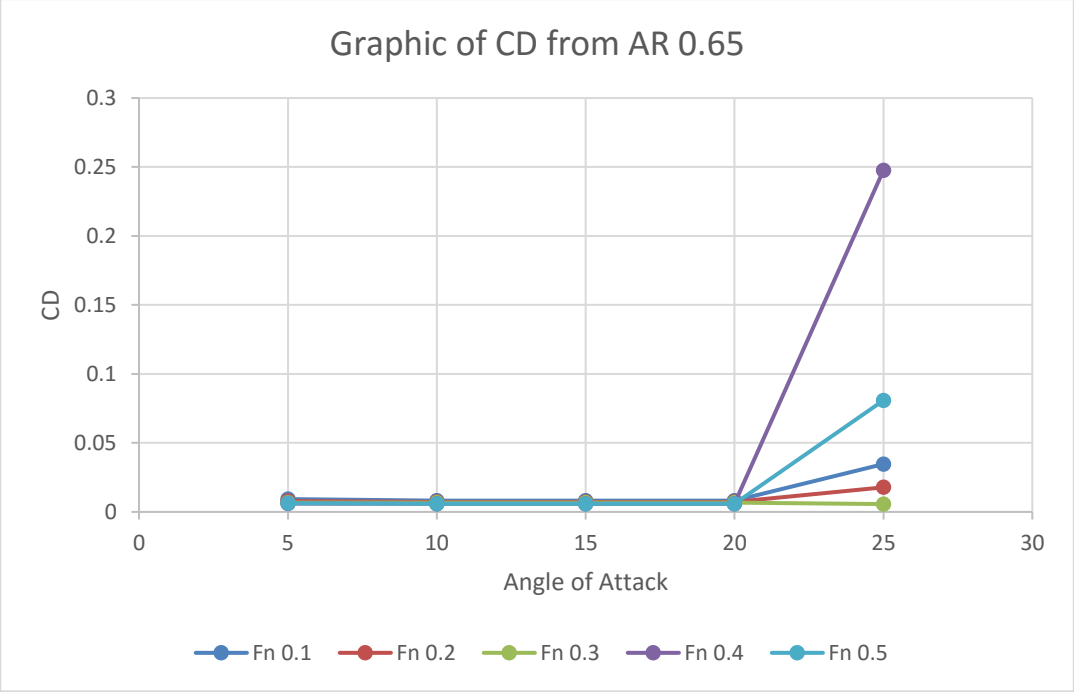

In graph 4.3.12 it can be seen that at the angle of attack 25 ° with Fn 0.4 has the largest CD ratio with other variation of angle, that is equal to 0.247. So it can be concluded that the largest CD is at an attack angle of 25 ° with Fn 0.4.

4.3.13. Grafik CL/CD pada AR 0.65

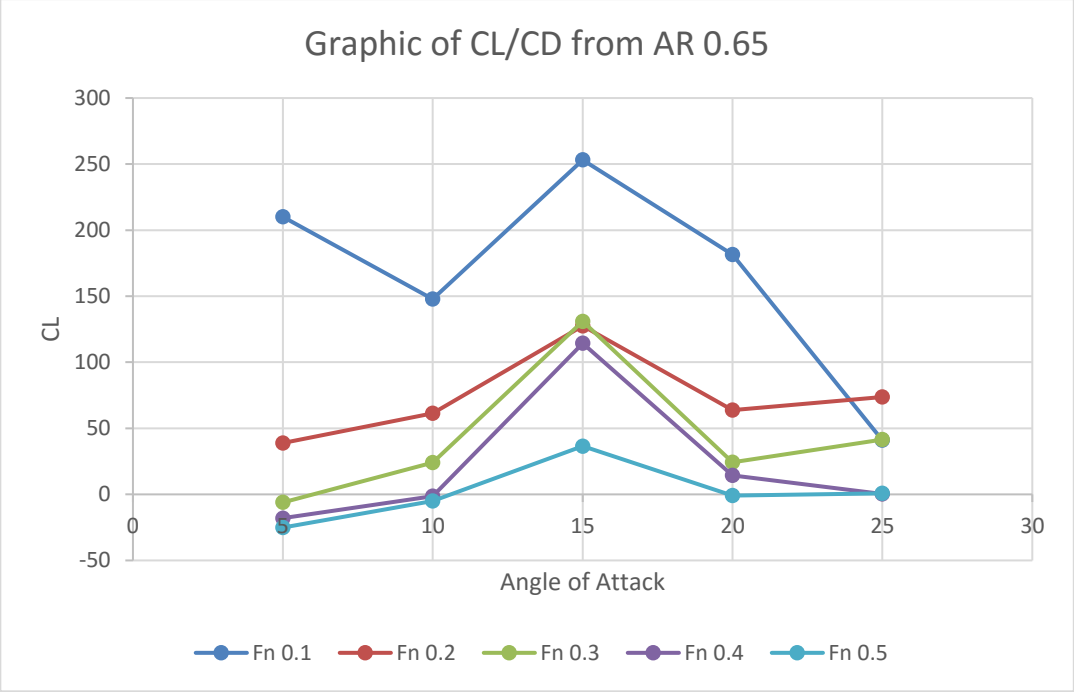

In graph 4.3.13 it can be seen that at an angle of attack 15 ° with Fn 0.1 has the largest CL ratio with other angle variations, which is 253. and the value decreases as the angle variation increases. It can be concluded that the largest CL / CD is at an attack angle of 15 ° with Fn 0.1.

4.3.14. Grafik CL pada AR 0.85

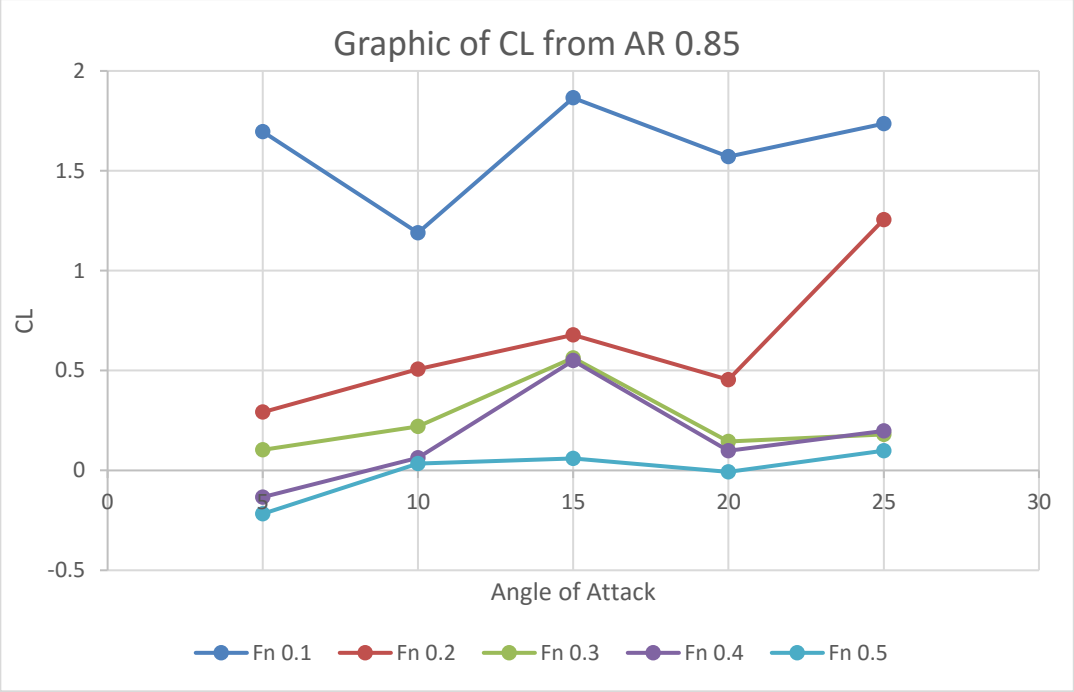

In graph 4.3.14 it can be seen that at an angle of attack 15 ° with Fn 0.1 has the largest CL ratio with other angle variation, which is equal to 1.864. And the value decreases as the angular variation increases. So it can be concluded that the largest CL is at an attack angle of 15 ° with Fn 0.1.

4.3.15. Grafik CD pada AR 0.85

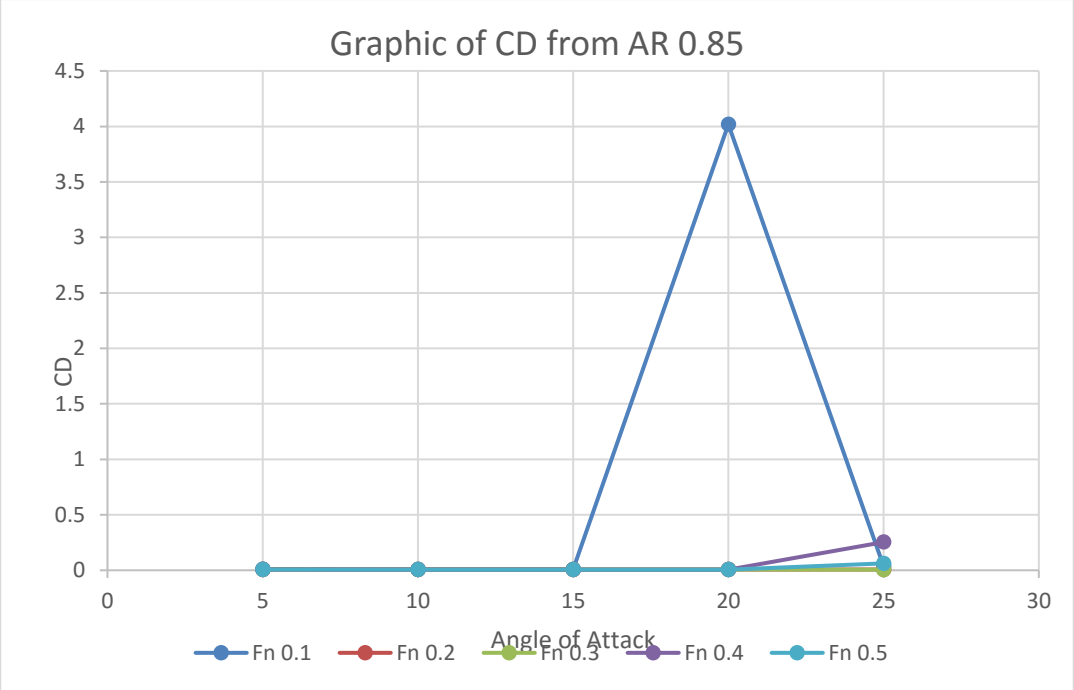

In graph 4.3.1.15 dapat dilihat bahwa pada sudut serang 20° dengan Fn 0.1 memiliki rasio CD yang paling besar dengan variasi sudut lainnya, yaitu sebesar 2.018. dan nilai tersebut semakin menurun seiring variasi sudut yang bertambah besar. Sehingga dapat disimpulkan bahwa CD terbesar berada pada sudut serang 20° dengna Fn 0.1.

4.3.16. Grafik CL/CD pada AR 0.85

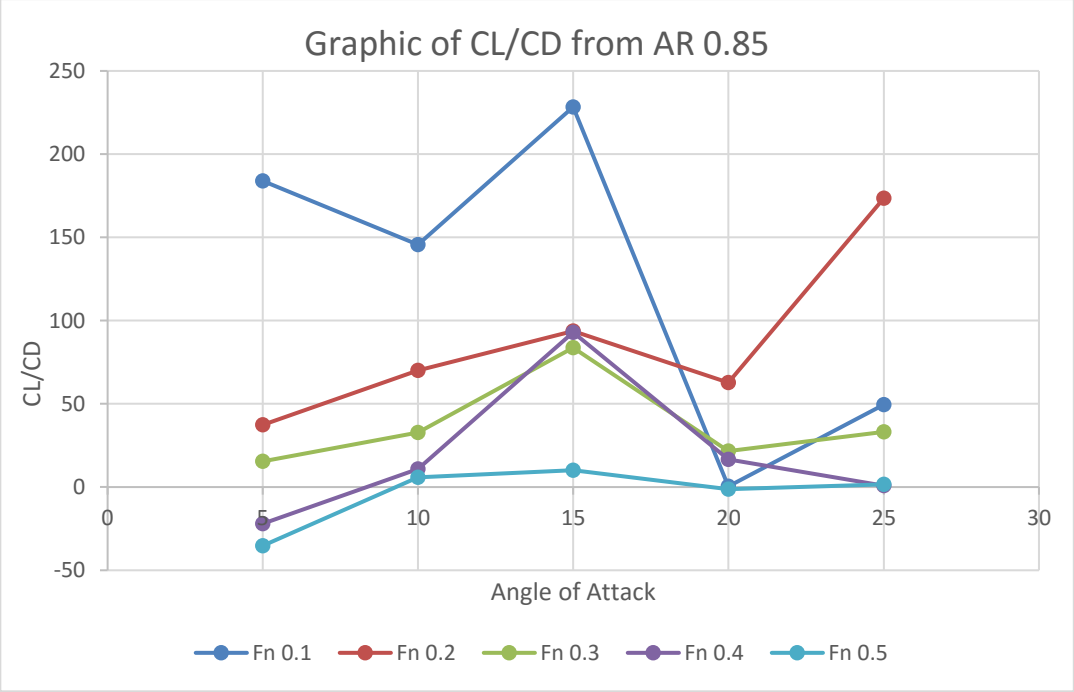

In graph 4.3.1.15 it can be seen that at an angle of attack 15 ° with Fn 0.1 has the largest CL / CD ratio with other angle variations, that is equal to 228. and the value decreases as the angle variation increases. So it can be concluded that the largest CL / CD is 1 angle of attack 15 ° with Fn 0.3.

"This page is intentionally left blank"

CHAPTER V
CONCLUSION

5.1. Conclusion

According data analysis, the discussion, and simulation result, so it can be concluded that.

1. At AR 0.05 has a maximum value of CL/CD at angle of attack 20 with fn 0.1
2. At AR 0.25 has a maximum value of CL/CD at angle of attack 15 with fn 0.3
3. At AR 0.45 has a maximum value of CL/CD at angle of attack 15 with fn 0.1
4. At AR 0.65 has a maximum value of CL/CD at angle of attack 15 with fn 0.1
5. At AR 0.85 has a maximum value of CL/CD at angle of attack 15 with fn 0.1

5.2. Recomendation

Recommendation that can be given by the author for further research are :

1. It is needed to get the comparision data by using different software.
2. The addition of analysis by using hydrofoil ship.
3. The different NACA foil analysis to be made as the comparison.
4. Analyze until the stall is reached for comparison by adding variations to the angle of attack.
5. Meshing should be done more specifically according to guidance from Numeca to produce more accurate results.

BIBLIOGRAPHY

[1] Wonggiawan, F., Budiarto, U. & Rindo, G., 2015. Studi Perancangan Hydrofoil Kapal Penumpang Untuk Perairan Kepulauan Seribu. digilib ITS.

[2] Hidayat, Syahroni. Sawarno, & Hantoro, Ridho. 2009. Studi Eksperimental Pengaruh Gaya Gelombang Laut Terhadap Pembangkitan Gaya Thrust Hydrofoil Seri Naca 0012 Dan Naca 0018. Digilib ITS

[3] A.S. Slamet, Suastika Ketut. 2012. Kajian Eksperimental Pengaruh Posisi Perletakan Hydrofoil Pendukung Terhadap Hambatan Kapal. Surabaya. Jurnal Teknik Perkapalan

[4] Suryadi, Aji. 2016. Analisa Pengaruh Sudut Serang Hidrofoil Terhadap Gaya Angkat Kapal Trimaran Hidrofoil. Jurusan Teknik Sistem Perkapalan. Institut Teknologi Sepuluh Nopember. Surabaya

[5] Chang Cai, Zhigang Zuo, Shuhong Liu and Yulin Wu. 2015. Numerical investigations of hydrodynamic performance of hydrofoils with leading-edge protuberances. International Journal Mechanical Engineering.

[6] https://en.wikipedia.org/wiki/Froude_number. Acces at 06 Februari 2017

[7] http://www.kitegeneration.com/kite-surf-fly/wing-geometry-definitions/#main. Acces at 06 Februari 2017

[8] Hamid Reza Kabarsian, Kyung Chun Kim. 2016. Numerical investigations on flow structure and behaviour of vortices in the dynamic stall of an oscillating pitching hydrofoil. International Journal Mechanical Engineering

[9] Ira H. Abbott, Albert E. Von Doenhoff. 1959. Theory of Wing Sections. New York. USA

"This page is intentionally left blank"

ATTACHMENT

Distribution of pressure to lift force with AR 0.05

No	Angle of Attack	Froude Number	Static Pressure (Pa)		Plan area Foil (m^2)	Lift (Newton)
			Down	Upper		
1	5	0.1	101128.1626	101080	0.003934	0.189471655
2		0.2	101144.85	101080	0.003934	0.2551199
3		0.3	101280.7	101080	0.003934	0.7895538
4		0.4	101205.2	101080	0.003934	0.4925368
5		0.5	101251.9	101080	0.003934	0.6762546
6	10	0.1	101265	101210	0.003934	0.21637
7		0.2	101263.95	101210	0.003934	0.2122393
8		0.3	101256.35	101210	0.003934	0.1823409
9		0.4	101181.7	101210	0.003934	-0.1113322
10		0.5	101207.15	101210	0.003934	-0.0112119
11	15	0.1	101284.45	101250	0.003934	0.1355263
12		0.2	102157	102050	0.003934	0.420938
13		0.3	101907.35	101650	0.003934	1.0124149
14		0.4	101471.1	101750	0.003934	-1.0971926
15		0.5	101382.95	101250	0.003934	0.5230253
16	20	0.1	101267.3	101200	0.003934	0.2647582
17		0.2	101276.25	101200	0.003934	0.2999675
18		0.3	101265.6	101200	0.003934	0.2580704
19		0.4	101245.55	101200	0.003934	0.1791937
20		0.5	101209.6	101200	0.003934	0.0377664
21	25	0.1	102136.05	102100	0.003934	0.1418207
22		0.2	101952.45	101800	0.003934	0.5997383
23		0.3	97335.8	97300	0.003934	0.1408372
24		0.4	90543.6	90500	0.003934	0.1715224
25		0.5	102408.8	101080	0.003934	5.2274992

Distribution of pressure to lift force with AR 0.25

No	Angle of Attack	Froude Number	Static Pressure (Pa)		Plan area Foil (m^2)	Lift (Newton)
			Down	Upper		
1	5	0.1	101275.2	101010	0.814455	44.957916
2		0.2	101271.55	101949.8	0.814455	41.98515525
3		0.3	101240	92333.2	0.814455	16.2891
4		0.4	101179.25	96533.2	0.814455	-33.18904125
5		0.5	101144.9	76666.4	0.814455	-61.1655705
6	10	0.1	101258.25	101060	0.814455	31.15290375
7		0.2	101282.4	101400	0.814455	50.821992
8		0.3	101262.5	102240	0.814455	34.6143375
9		0.4	101218.75	96260	0.814455	-1.01806875
10		0.5	101198.25	100720	0.814455	-17.71439625
11	15	0.1	101273.4	100240	0.814455	43.491897
12		0.2	102081.2	98060	0.814455	66.133746
13		0.3	101957.65	94720	0.814455	600.7827307
14		0.4	101571.35	91740	0.814455	286.1587643
15		0.5	101372.25	82720	0.814455	124.0007738
16	20	0.1	101266.1	99420	0.814455	37.5463755
17		0.2	101275.85	95140	0.814455	45.48731175
18		0.3	101260.3	87740	0.814455	32.8225365
19		0.4	105754.85	78560	0.814455	28.38375675
20		0.5	101211.5	60260	0.814455	-6.9228675
21	25	0.1	102138.95	98520	0.814455	31.72302225
22		0.2	101952.2	89360	0.814455	107.670951
23		0.3	102204	72000	0.814455	68.41422
24		0.4	86617.5	39660	0.814455	95.6984625
25		0.5	102448.6	36680	0.814455	1000.639413

Distribution of pressure to lift force with AR 0.45

No	angle of attack	Froude Number	Static Pressure (Pa)		Plan area Foil (m^2)	Lift (Newton)
			Down	Upper		
1	5	0.1	101287.15	101230	1.235511	70.60945365
2		0.2	101256.95	101230	1.235511	33.29702145
3		0.3	101228.8	101230	1.235511	-1.4826132
4		0.4	101164.85	101230	1.235511	-80.49354165
5		0.5	101106.05	101230	1.235511	-153.1415884
6	10	0.1	101256.95	101230	1.235511	33.29702145
7		0.2	101273.65	101230	1.235511	53.93005515
8		0.3	101289.3	101230	1.235511	73.2658023
9		0.4	101236.05	101230	1.235511	7.47484155
10		0.5	101180.1	101230	1.235511	-61.6519989
11	15	0.1	101280.4	101230	1.235511	62.2697544
12		0.2	102149.4	102100	1.235511	61.0342434
13		0.3	101979.65	101830	1.235511	184.8942211
14		0.4	105996.25	105930	1.235511	81.85260375
15		0.5	101338.4	101230	1.235511	133.9293924
16	20	0.1	101262.45	101230	1.235511	40.09233195
17		0.2	101277.6	101230	1.235511	58.8103236
18		0.3	101268.55	101230	1.235511	47.62894905
19		0.4	101270.35	101230	1.235511	49.85286885
20		0.5	101223.25	101230	1.235511	-8.33969925
21	25	0.1	102148.05	102100	1.235511	59.36630355
22		0.2	101962.5	101830	1.235511	163.7052075
23		0.3	97714.95	97600	1.235511	142.0219894
24		0.4	90412.85	-1760	1.235511	-107.6747836
25		0.5	104053.8	-27600	1.235511	66.4704918

Distribution of pressure to lift force with AR 0.65

No	Angle of attack	Froude Number	Static pressure (Pa)		Plan area Foil (m^2)	Lift (Newton)
			Down	Up		
1	5	0.1	101278.35	101220	1.656567	96.66068445
2		0.2	101256.55	101220	1.656567	60.54752385
3		0.3	101209	101220	1.656567	-18.222237
4		0.4	101167.3	101220	1.656567	-87.3010809
5		0.5	101103.35	101220	1.656567	-193.2385405
6	10	0.1	101256.4	101220	1.656567	60.2990388
7		0.2	101273.5	101220	1.656567	88.6263345
8		0.3	101263.75	101220	1.656567	72.47480625
9		0.4	101215.85	101220	1.656567	-6.87475305
10		0.5	101198.35	101220	1.656567	-35.86467555
11	15	0.1	101282.3	101220	1.656567	103.2041241
12		0.2	102151.3	102040	1.656567	184.3759071
13		0.3	102019.15	101780	1.656567	396.167998
14		0.4	101545.8	101220	1.656567	539.7095286
15		0.5	101381.15	101220	1.656567	266.955772
16	20	0.1	101264.7	101220	1.656567	74.0485449
17		0.2	101275.65	101220	1.656567	92.18795355
18		0.3	101264.4	101220	1.656567	73.5515748
19		0.4	101261.15	101220	1.656567	68.16773205
20		0.5	101215.5	101220	1.656567	-7.4545515
21	25	0.1	102152.8	102110	1.656567	70.9010676
22		0.2	101938.35	101780	1.656567	262.3173845
23		0.3	97463.75	97400	1.656567	105.6061463
24		0.4	90423.35	33060	1.656567	146672.4422
25		0.5	103837.05	11528	1.656567	208515.4014

Distribution of pressure to lift force with AR 0.85

No	Angle of attack	Froude Number	Static pressure (Pa)		Plan area Foil (m^2)	Lift (Newton)
			Down	Upper		
1	5	0.1	101271.1	101220	2.077622	106.1664842
2		0.2	101255.15	101220	2.077622	73.0284133
3		0.3	101247.95	101220	2.077622	58.0695349
4		0.4	101155.6	101220	2.077622	-133.7988568
5		0.5	101056.35	101220	2.077622	-340.0028403
6	10	0.1	101255.85	101220	2.077622	74.4827487
7		0.2	101281.2	101220	2.077622	127.1504664
8		0.3	101279.7	101220	2.077622	124.0340334
9		0.4	101250.75	101220	2.077622	63.8868765
10		0.5	101245.4	101220	2.077622	52.7715988
11	15	0.1	101286.2	101230	2.077622	116.7623564
12		0.2	102181.85	102100	2.077622	170.0533607
13		0.3	102032.85	101880	2.077622	317.5645227
14		0.4	101494.95	101230	2.077622	550.4659489
15		0.5	101274.7	101230	2.077622	92.8697034
16	20	0.1	101267.35	101220	2.077622	98.3754017
17		0.2	101274.7	101220	2.077622	113.6459234
18		0.3	101259.4	101220	2.077622	81.8583068
19		0.4	101267.1	101220	2.077622	97.8559962
20		0.5	101214.2	101220	2.077622	-12.0502076
21	25	0.1	102182.3	102130	2.077622	108.6596306
22		0.2	101971.4	101820	2.077622	314.5519708
23		0.3	99948.95	99900	2.077622	101.6995969
24		0.4	90495.5	90400	2.077622	198.412901
25		0.5	103294.45	103220	2.077622	154.6789579

CL CD CL/CD foil With AR 0.05

No	Angle of Attack	Froude Number	CL	CD	CL/CD
1	5	0.1	1.831757093	0.00922	198.6721359
2		0.2	0.427658868	0.0078	54.82806005
3		0.3	0.073742234	0.006665	11.06410113
4		0.4	-0.084515514	0.006665	-12.68049715
5		0.5	-0.099684752	0.006165	-16.16946504
6	10	0.1	1.269288203	0.008167	155.4167017
7		0.2	0.517670483	0.00724	71.5014479
8		0.3	0.156702247	0.0067325	23.27549161
9		0.4	-0.0025925	0.00591125	-0.438570592
10		0.5	-0.028870085	0.0058575	-4.928738305
11	15	0.1	1.772025884	0.008167	216.9739052
12		0.2	0.673635308	0.00724	93.0435508
13		0.3	2.719797946	0.0067325	403.9803856
14		0.4	0.728700017	0.00591125	123.2734221
15		0.5	0.202090592	0.0058575	34.50116813
16	20	0.1	1.529782645	0.008167	187.3126784
17		0.2	0.463331674	0.00724	63.99608759
18		0.3	0.148590602	0.0067325	22.07064264
19		0.4	0.072278912	0.00591125	12.22734812
20		0.5	-0.011282562	0.0058575	-1.92617359
21	25	0.1	1.292517007	0.03584	36.06353256
22		0.2	1.096731375	0.018515	59.23474888
23		0.3	0.309717383	0.0056615	54.70588764
24		0.4	0.243695039	0.1805	1.350111019
25		0.5	1.630794757	0.0617345	26.41626249

CL CD CL/CD foil with AR 0.25

No	Angle of Attack	Froude Number	CL	CD	CL/CD
1	5	0.1	1.831757093	0.00922	198.6721359
2		0.2	0.427658868	0.0078	54.82806005
3		0.3	0.073742234	0.006665	11.06410113
4		0.4	-0.084515514	0.006665	-12.68049715
5		0.5	-0.099684752	0.006165	-16.16946504
6	10	0.1	1.269288203	0.008167	155.4167017
7		0.2	0.517670483	0.00724	71.5014479
8		0.3	0.156702247	0.0067325	23.27549161
9		0.4	-0.0025925	0.00591125	-0.438570592
10		0.5	-0.028870085	0.0058575	-4.928738305
11	15	0.1	1.772025884	0.008167	216.9739052
12		0.2	0.673635308	0.00724	93.0435508
13		0.3	2.719797946	0.0067325	403.9803856
14		0.4	0.728700017	0.00591125	123.2734221
15		0.5	0.202090592	0.0058575	34.50116813
16	20	0.1	1.529782645	0.008167	187.3126784
17		0.2	0.463331674	0.00724	63.99608759
18		0.3	0.148590602	0.0067325	22.07064264
19		0.4	0.072278912	0.00591125	12.22734812
20		0.5	-0.011282562	0.0058575	-1.92617359
21	25	0.1	1.292517007	0.03584	36.06353256
22		0.2	1.096731375	0.018515	59.23474888
23		0.3	0.309717383	0.0056615	54.70588764
24		0.4	0.243695039	0.1805	1.350111019
25		0.5	1.630794757	0.0617345	26.41626249

CL CD CL/CD foil with AR 0.45

No	Angle of Attack	Froude Number	CL	CD	CL/CD
1	5	0.1	1.896465903	0.00922	205.6904451
2		0.2	0.223577236	0.0078	28.66374818
3		0.3	-0.004424534	0.006665	-0.663846068
4		0.4	-0.135121122	0.006075	-22.24215994
5		0.5	-0.164526298	0.006165	-26.68715301
6	10	0.1	0.894308943	0.008167	109.502748
7		0.2	0.362120458	0.00724	50.01663784
8		0.3	0.218645724	0.0067325	32.47615654
9		0.4	0.012547702	0.00591125	2.122681668
10		0.5	-0.066235275	0.0058575	-11.30777202
11	15	0.1	1.672473868	0.008167	204.7843599
12		0.2	0.409822466	0.00724	56.60531292
13		0.3	0.551776266	0.0067325	81.95711341
14		0.4	0.137402522	0.00591125	23.2442414
15		0.5	0.143885847	0.0058575	24.56437849
16	20	0.1	1.076820972	0.008167	131.8502476
17		0.2	0.394889663	0.00724	54.54277116
18		0.3	0.142138156	0.0067325	21.11224004
19		0.4	0.083685913	0.00591125	14.15705873
20		0.5	-0.008959681	0.0058575	-1.529608439
21	25	0.1	1.594491455	0.0347485	45.88662691
22		0.2	1.099220176	0.0174875	62.85747968
23		0.3	0.42383349	0.0051045	83.03134294
24		0.4	-0.180749129	0.236595	-0.763960054
25		0.5	0.071411979	0.096798	0.737742303

CL CD CL/CD foil dengan AR 0.65

No	Angle of Attack	Froude Number	CL	CD	CL/CD
1	5	0.1	1.93628671	0.00922	210.0094045
2		0.2	0.303218849	0.0078	38.87421135
3		0.3	-0.040558229	0.006665	-6.085255621
4		0.4	-0.109299817	0.006075	-17.9917395
5		0.5	-0.154836569	0.006165	-25.11542073
6	10	0.1	1.207897793	0.008167	147.8998155
7		0.2	0.443836071	0.00724	61.30332473
8		0.3	0.161311137	0.0067325	23.9600649
9		0.4	-0.008607101	0.00591125	-1.456054367
10		0.5	-0.028737349	0.0058575	-4.906077439
11	15	0.1	2.067363531	0.008167	253.1362227
12		0.2	0.923344948	0.00724	127.5338326
13		0.3	0.881772763	0.0067325	130.9725605
14		0.4	0.675709308	0.00591125	114.3090392
15		0.5	0.213904098	0.0058575	36.51798519
16	20	0.1	1.483325037	0.008167	181.624224
17		0.2	0.461672474	0.00724	63.76691628
18		0.3	0.16370776	0.0067325	24.316043
19		0.4	0.085345114	0.00591125	14.4377439
20		0.5	-0.005973121	0.0058575	-1.01973896
21	25	0.1	1.420275427	0.034665	40.97145326
22		0.2	1.31367181	0.017815	73.73964694
23		0.3	0.235053371	0.00567	41.45562098
24		0.4	0.048427908	0.24758	0.195605088
25		0.5	0.062452298	0.080842	0.772522921

CL CD CL/CD foil with AR 0.85

No	Angle of Attack	Froude Number	CL	CD	CL/CD
1	5	0.1	1.695702671	0.00922	183.915691
2		0.2	0.291604447	0.0078	37.38518547
3		0.3	0.103054772	0.006665	15.46208133
4		0.4	-0.133565621	0.006075	-21.98611051
5		0.5	-0.217222499	0.006165	-35.23479299
6	10	0.1	1.18964659	0.008167	145.6650655
7		0.2	0.507715281	0.00724	70.12642006
8		0.3	0.220120569	0.0067325	32.69521999
9		0.4	0.06377551	0.00591125	10.78883658
10		0.5	0.033714949	0.0058575	5.755859905
11	15	0.1	1.864941098	0.008167	228.3508141
12		0.2	0.679027709	0.00724	93.78835755
13		0.3	0.563575024	0.0067325	83.70962102
14		0.4	0.549506388	0.00591125	92.95942278
15		0.5	0.059333001	0.0058575	10.129407
16	20	0.1	1.571262651	4.018885	0.390969797
17		0.2	0.453791273	0.00724	62.67835257
18		0.3	0.145272201	0.0067325	21.57774987
19		0.4	0.097685416	0.00591125	16.52533992
20		0.5	-0.007698689	0.0058575	-1.314330215
21	25	0.1	1.735523478	0.035085	49.46625275
22		0.2	1.256014601	0.00724	173.4826797
23		0.3	0.180484118	0.0054337	33.21569424
24		0.4	0.198067032	0.25368	0.780775117
25		0.5	0.098821968	0.0623665	1.584536054

Attachment 1. AR 0.05 with angle of attack 5°

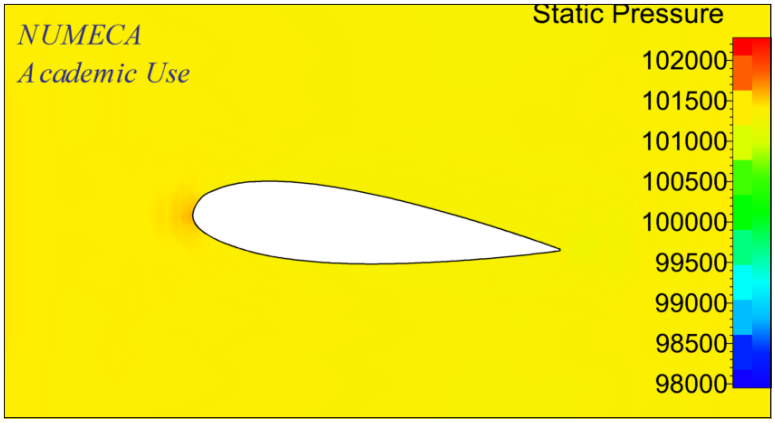

Figure 1. Distribution Static Pressure Fn 0.1

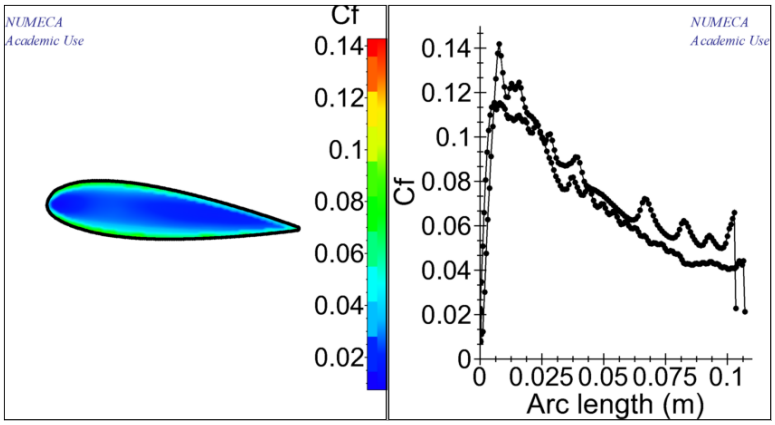

Figure 2. Coefficien Friction Fn 0.1

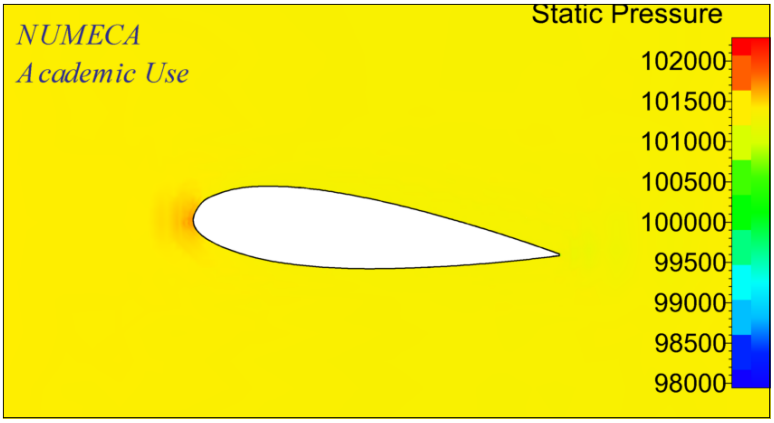

Figure 3. Distribution Static Pressure Fn 0.2

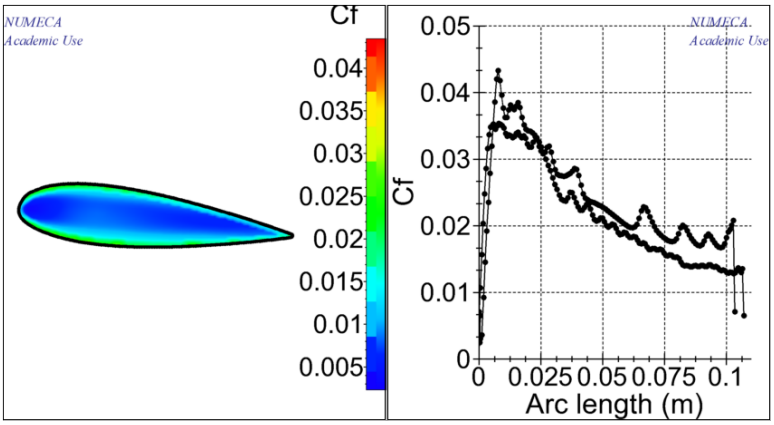

Figure 4. Coefficien Friction Fn 0.2

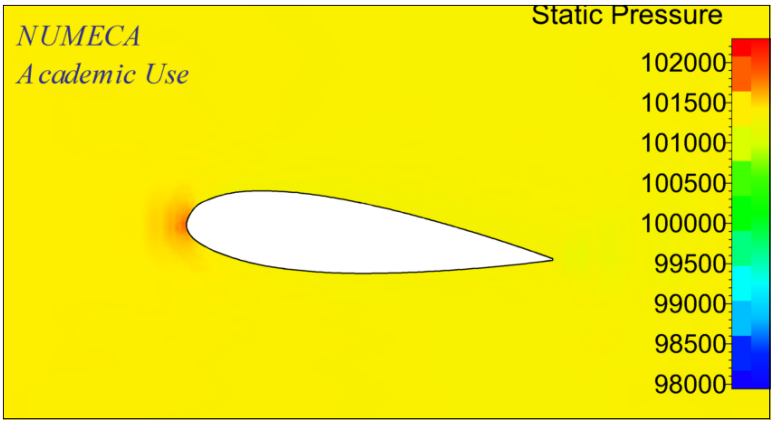

Figure 5. Distribution Static Pressure Fn 0.3

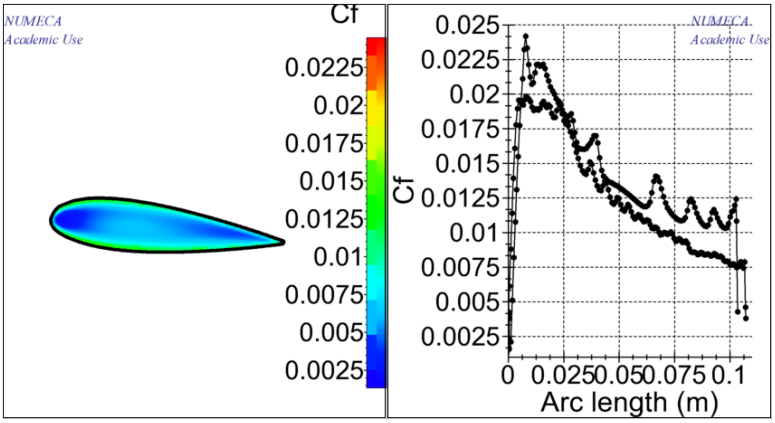

Figure 6. Coefficien Friction Fn 0.3

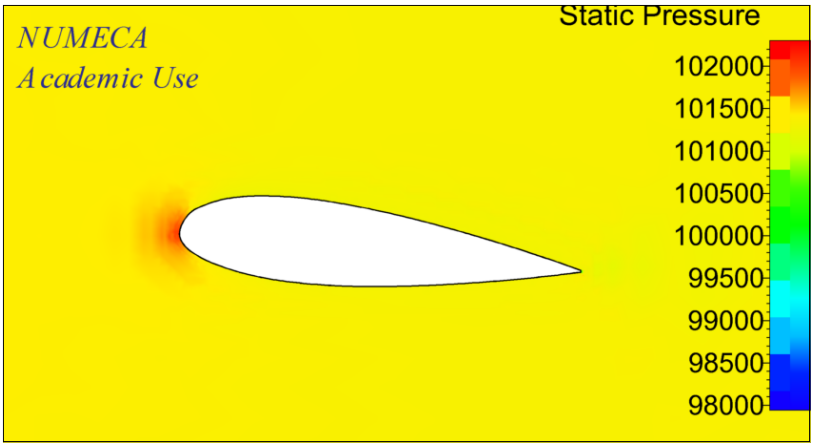

Figure 7. Distribution Static Pressure Fn 0.4

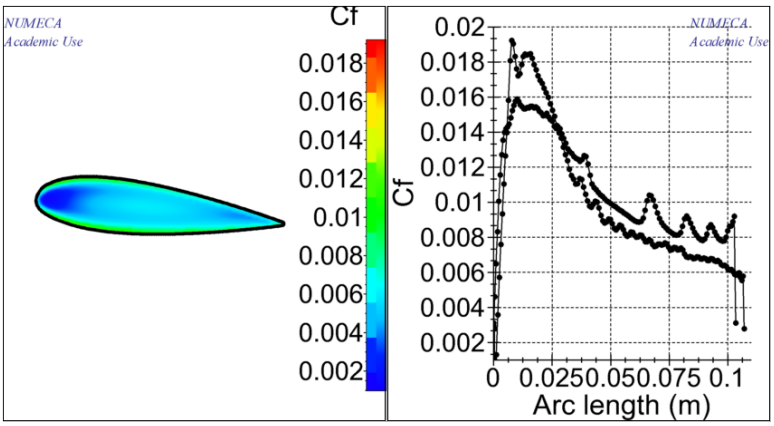

Figure 8. Coefficient Friction Fn 0.4

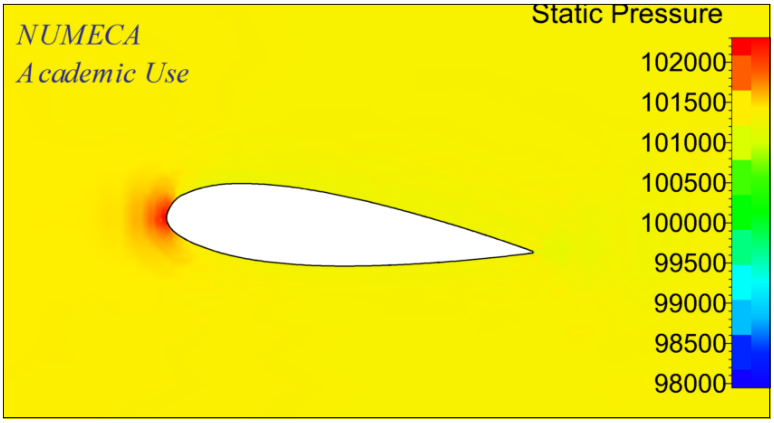

Figure 9. Distribution Static Pressure Fn 0.5

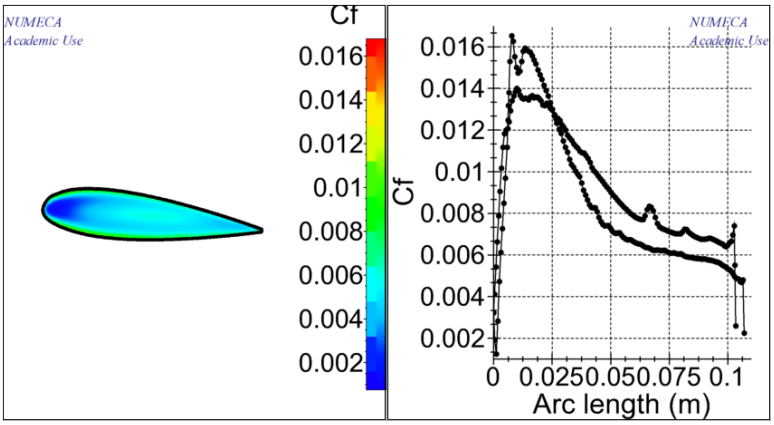

Figure 10. Coefficien Friction Fn 0.5

Attachment 2. AR 0.25 with angle of attack 5°

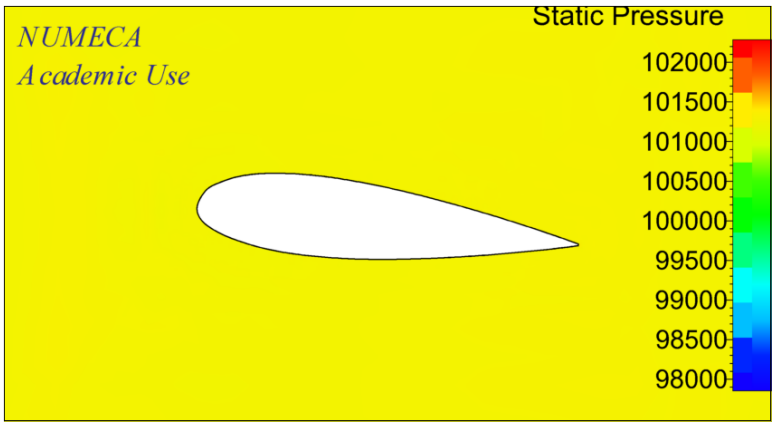

Figure 11. Distribution Static Pressure Fn 0.1

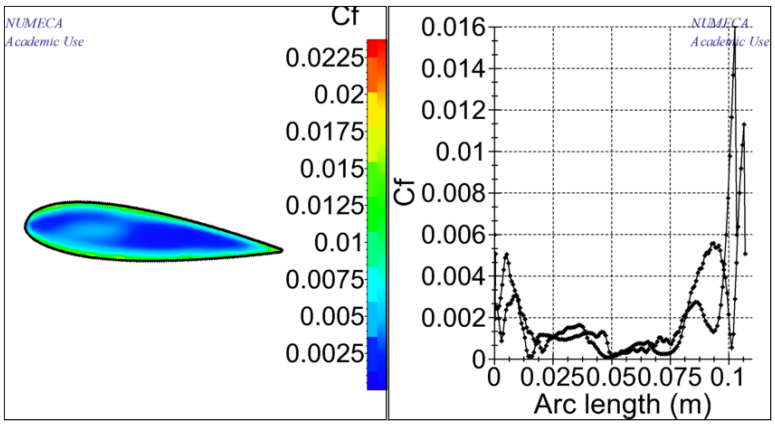

Figure 12. Coefficien Friction Fn 0.1

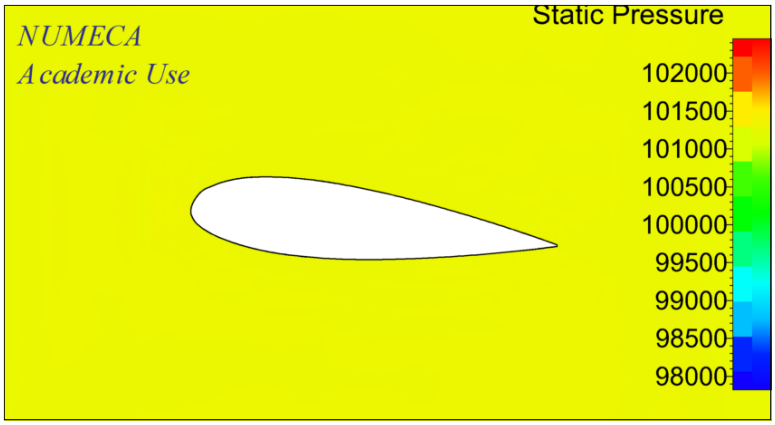

Figure 13. Distribution Static Pressure Fn 0.2

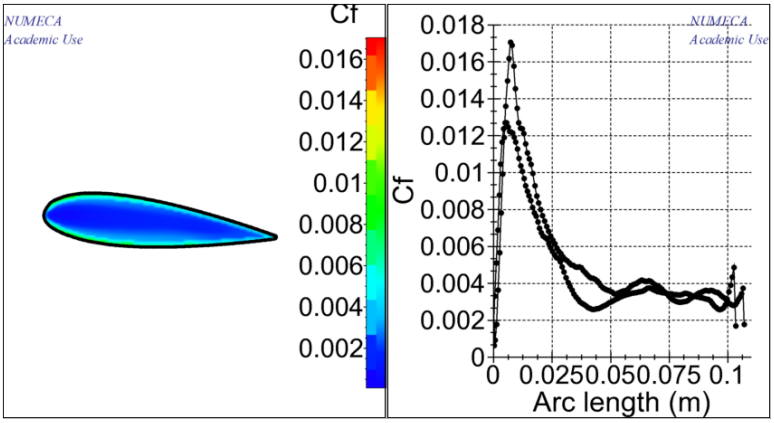

Figure 14. Coefficien Friction **Fn 0.2**

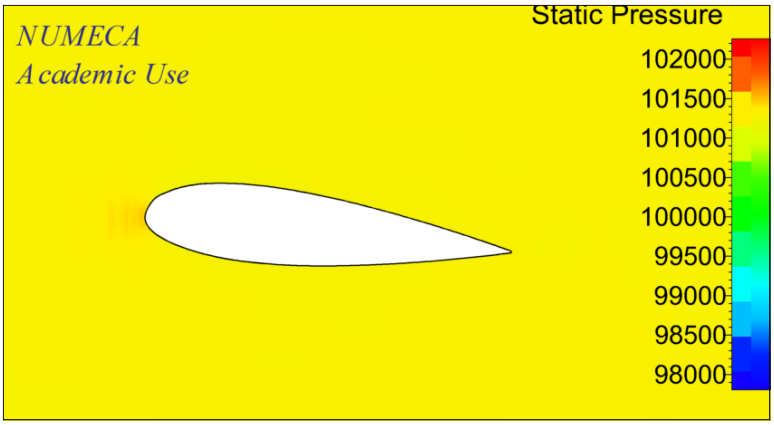

Figure 15. Distribution Static Pressure Fn 0.3

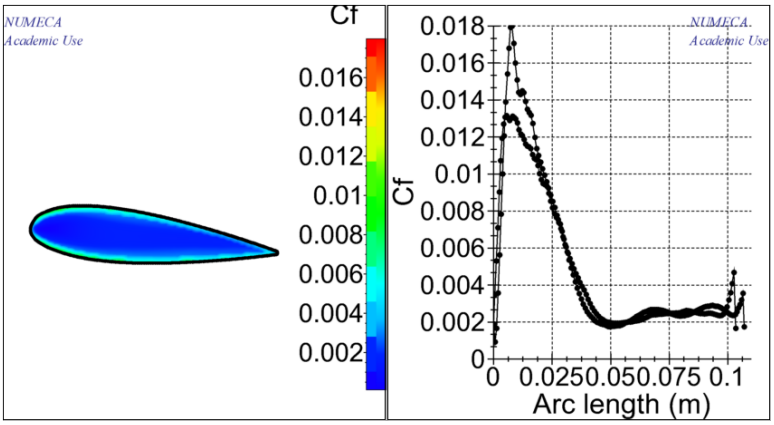

Figure 16. Coefficien Friction **Fn 0,3**

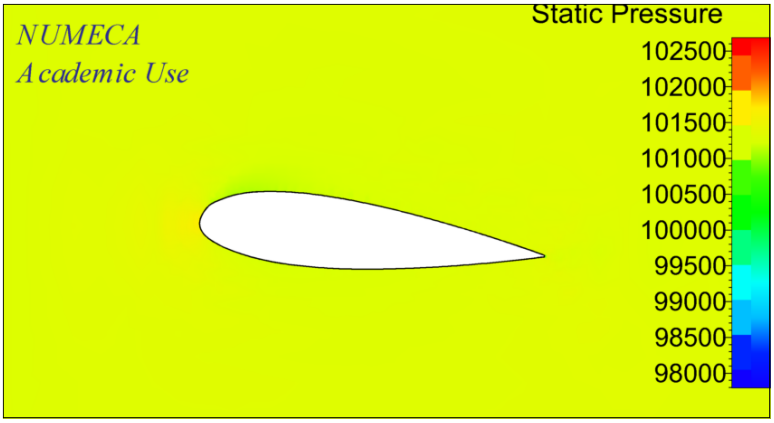

Figure 17. Distribution Static Pressure Fn 0.4

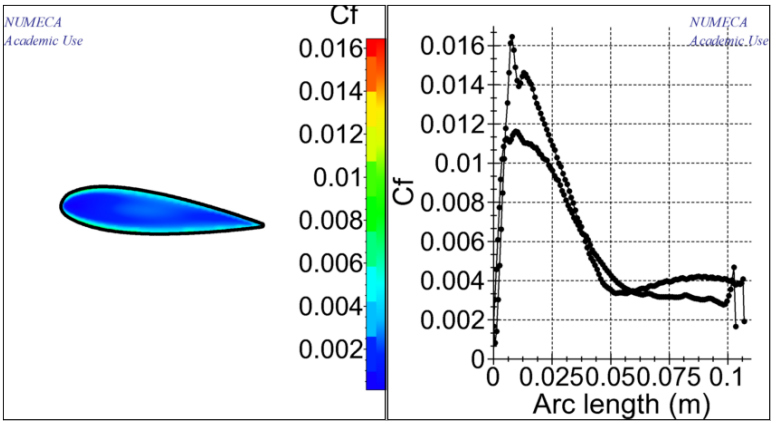

Figure 18. Coefficien Friction Fn 0.4

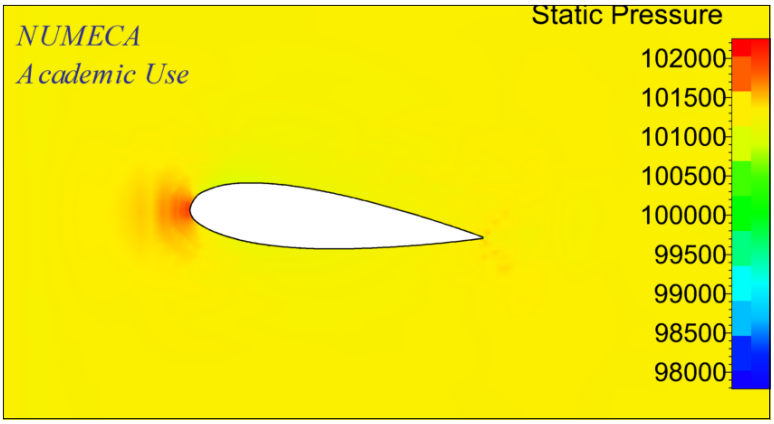

Figure 19. Distribution Static Pressure Fn 0.5

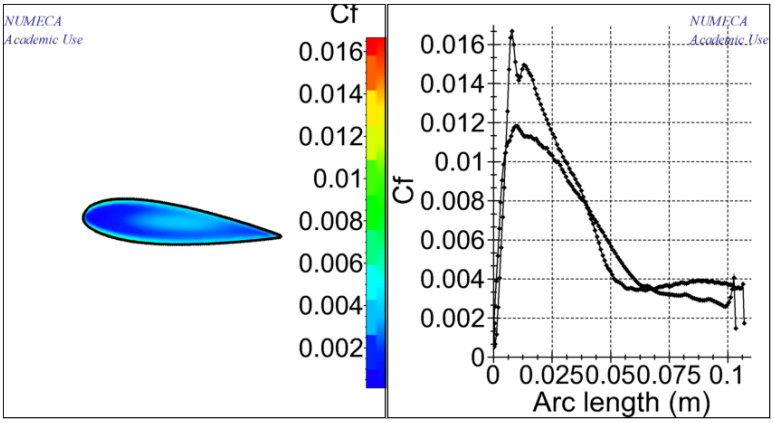

Figure 20. Coefficien Friction 0.5

Attachment 3. AR 0.45 with angle of attack 5°

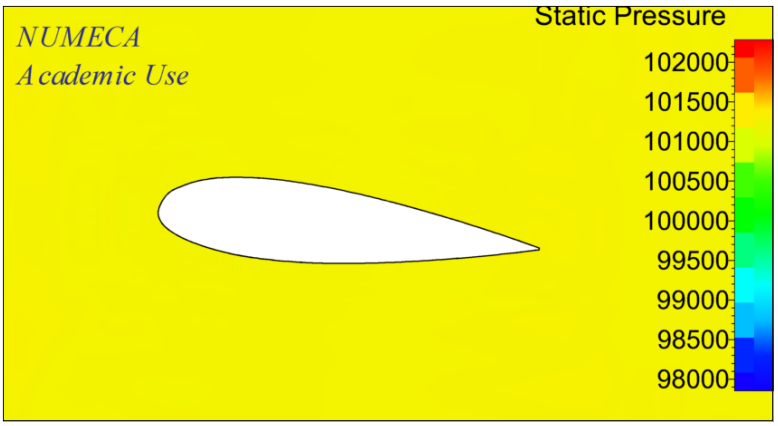

Figure 21. Distribution Static Pressure Fn 0.1

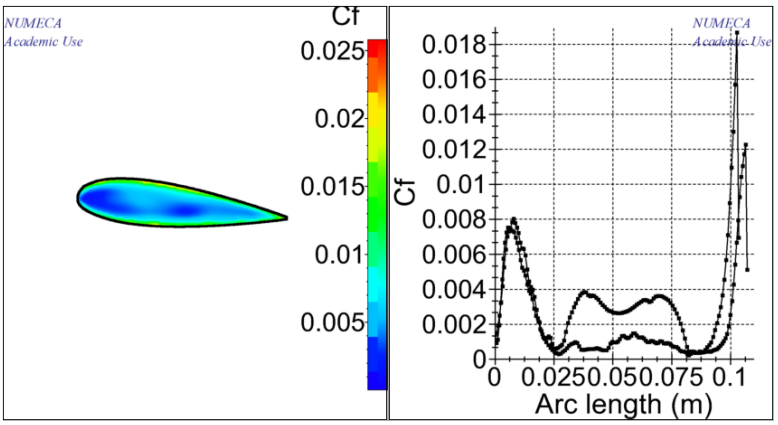

Figure 22. Coefficien Friction Fn 0.1

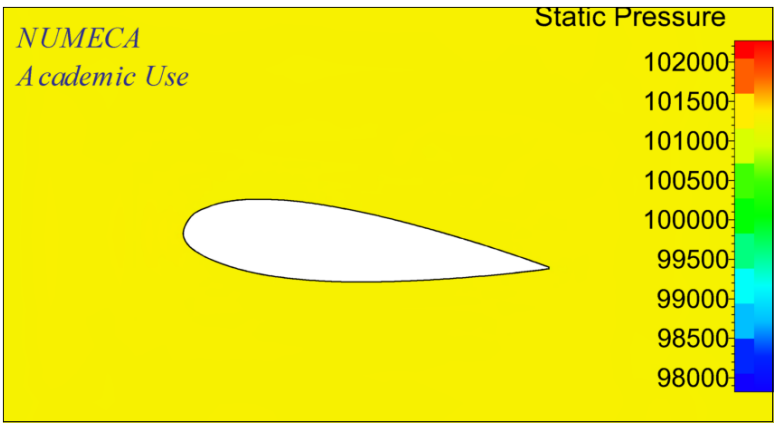

Figure 23. Distribution Static Pressure Fn 0.2

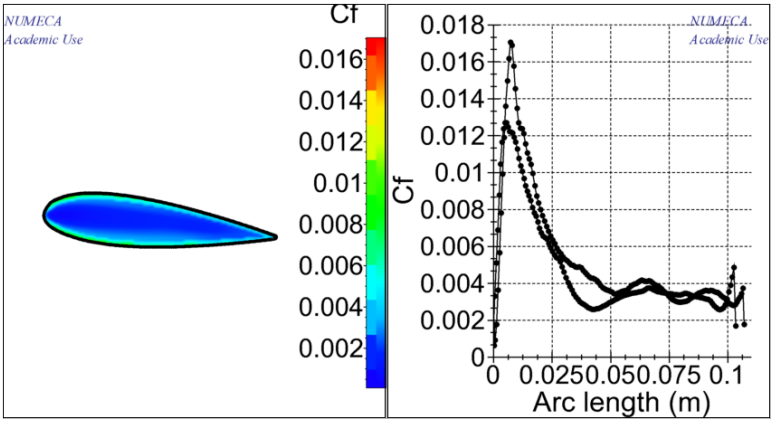

Figure 24. Coefficient Friction Fn 0.2

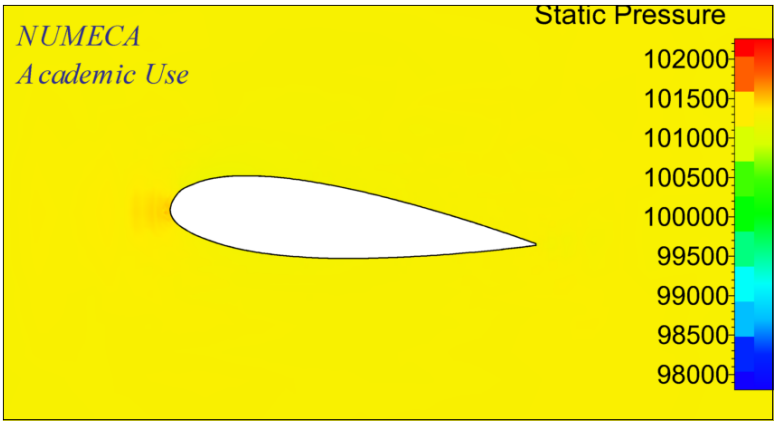

Figure 25. Distribution Static Pressure Fn 0.3

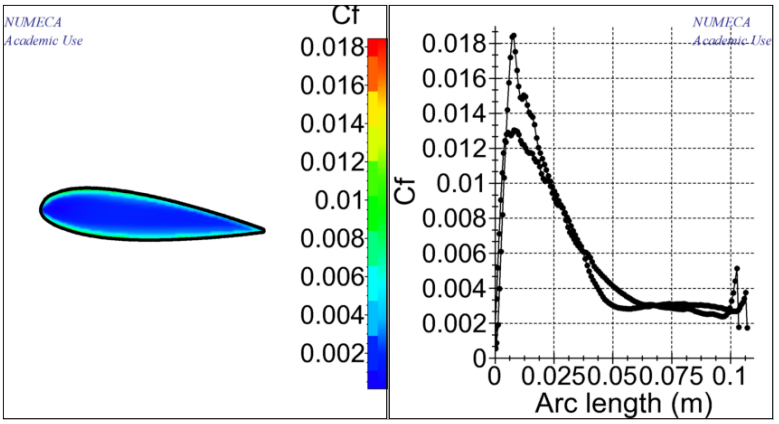

Figure 26. Coefficient Friction Fn 0,3

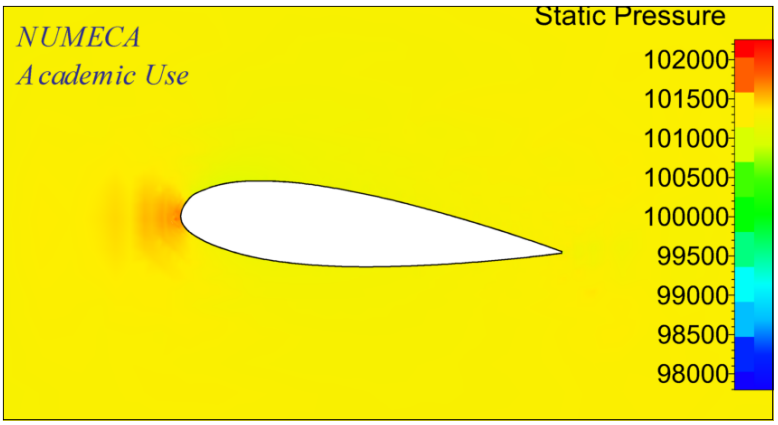

Figure 27. Distribution Static Pressure Fn 0.4

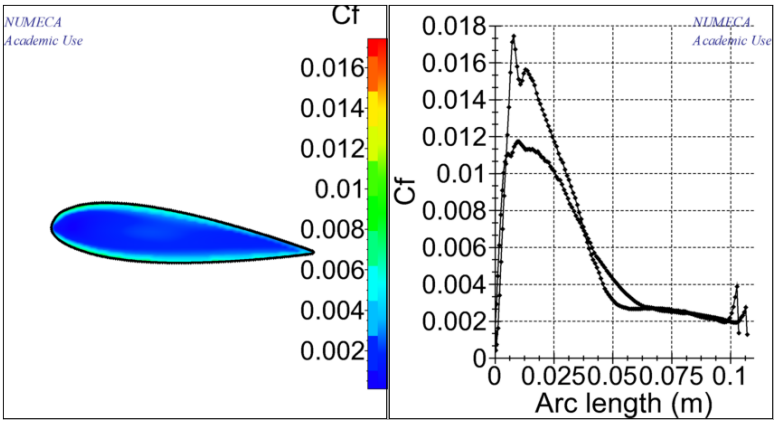

Figure 28. Coefficien Friction Fn 0.4

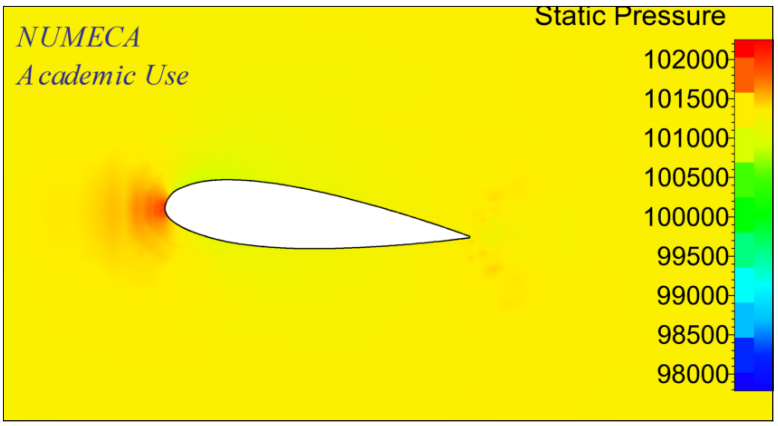

Figure 29. Distribution Static Pressure Fn 0.5

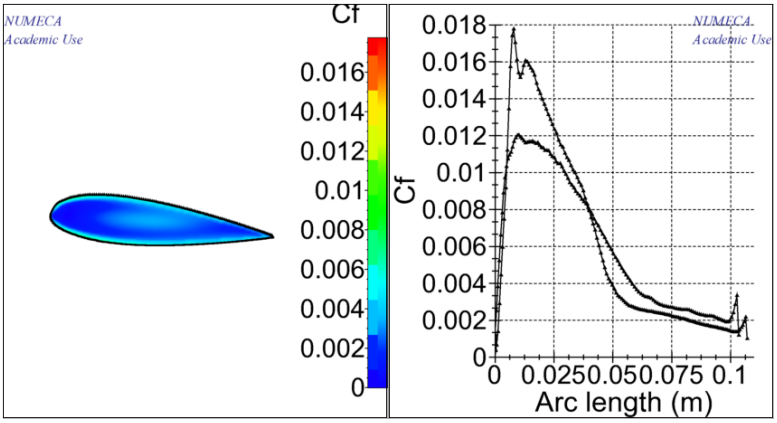

Figure 30. Coefficien Friction Fn 0.5

Attachment 4. AR 0.65 with angle of attack 5°

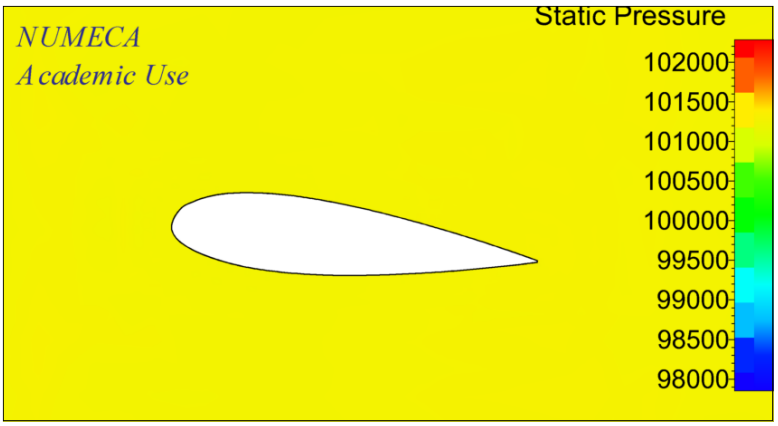

Figure 31. Distribution Static Pressure Fn 0.1

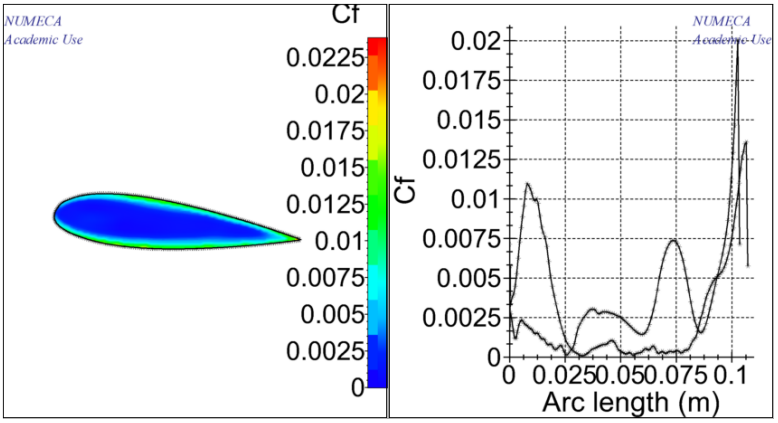

Figure 32. Coefficien Friction Fn 0.1

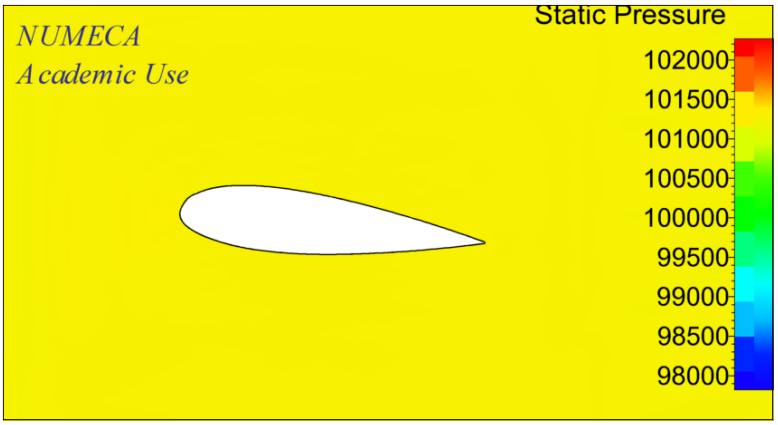

Figure 33. Distribution Static Pressure Fn 0.2

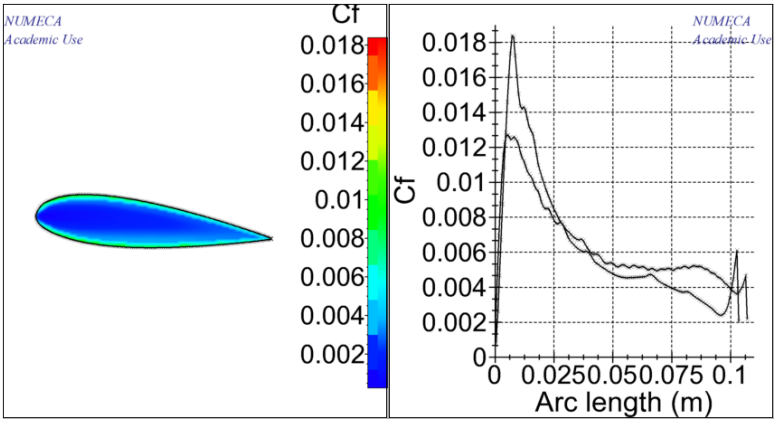

Figure 34. Coefficien Friction Fn 0.2

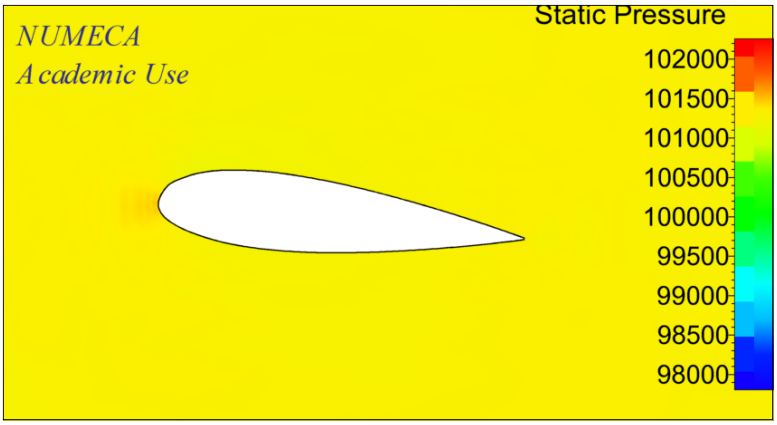

Figure 35. Distribution Static Pressure Fn 0.3

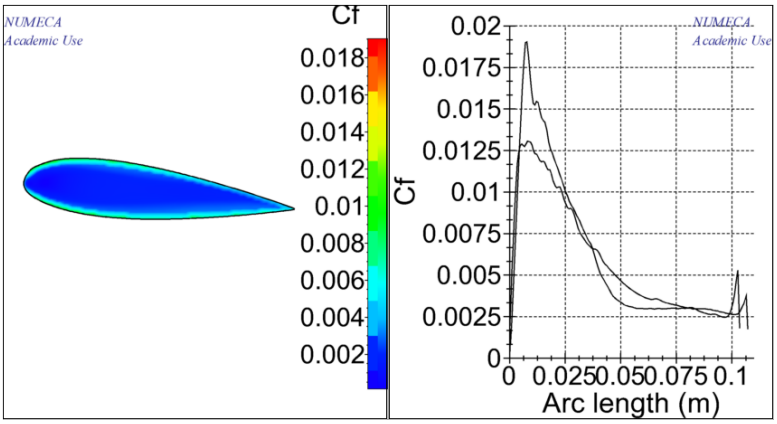

Figure 36. Coefficien Friction Fn 0.3

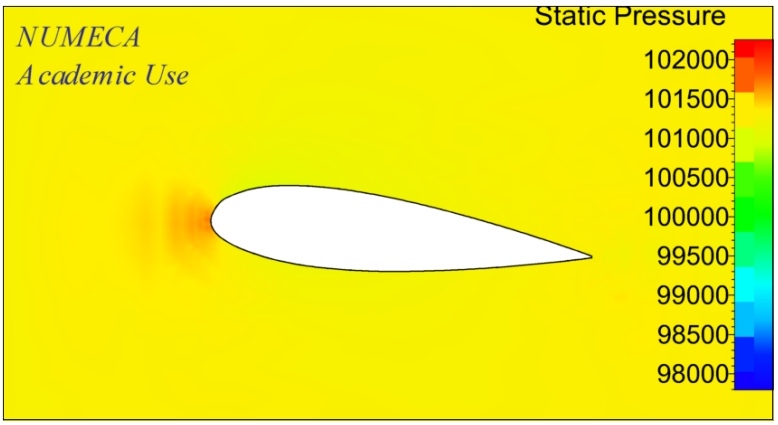

Figure 37. Distribution Static Pressure Fn 0.4

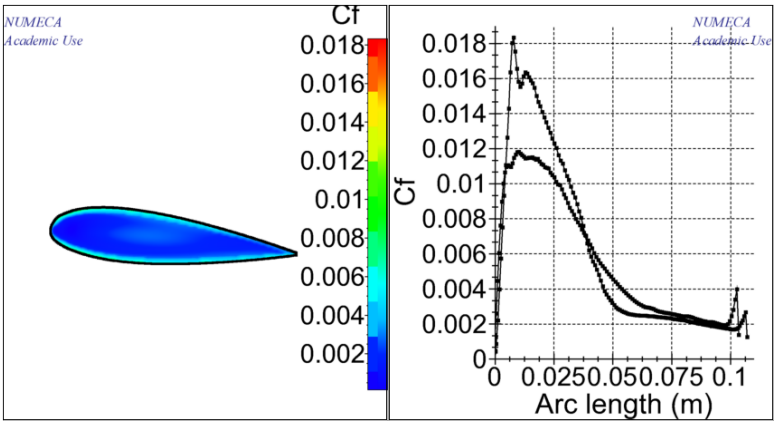

Figure 38. Coefficien Friction Fn 0.4

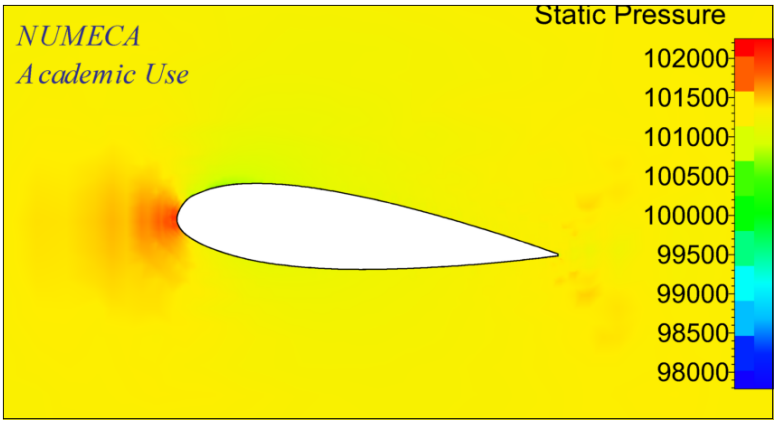

Figure 39. Distribution Static Pressure Fn 0.5

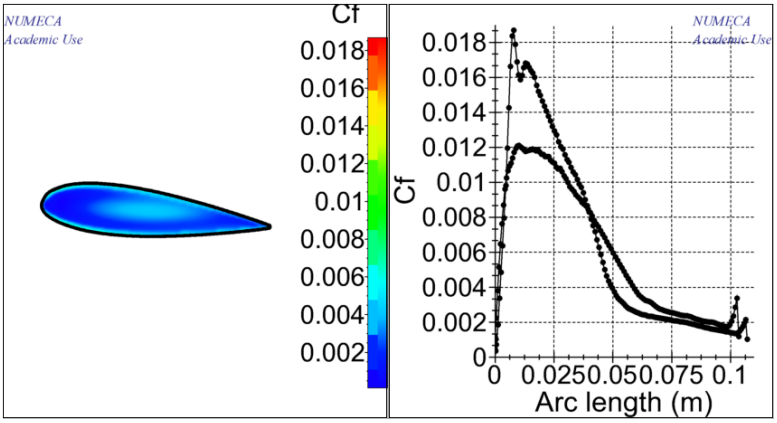

Figure 40. Coefficien Friction Fn 0.5

Attachment 5. AR 0.85 with angle of attack 5°

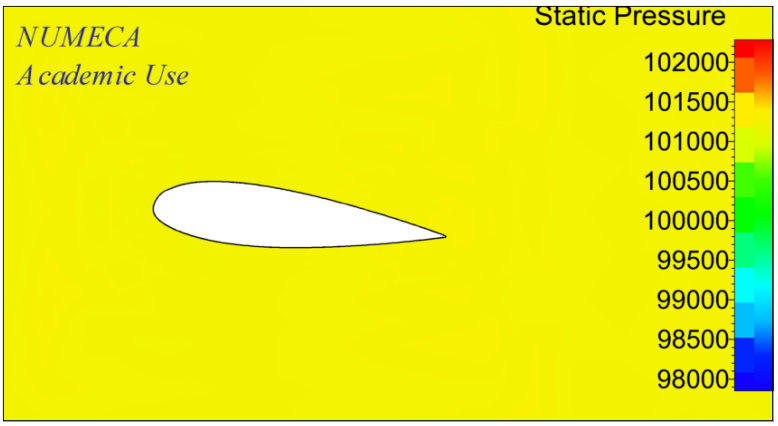

Figure 41. Distribution Static Pressure Fn 0.1

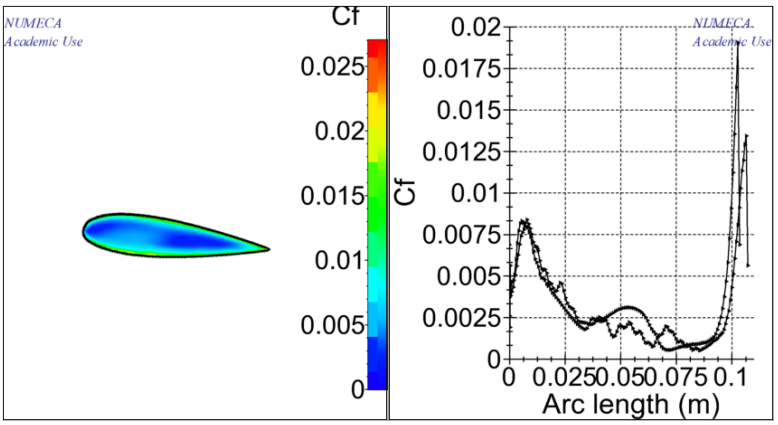

Figure 42. Coefficien Friction Fn 0.1

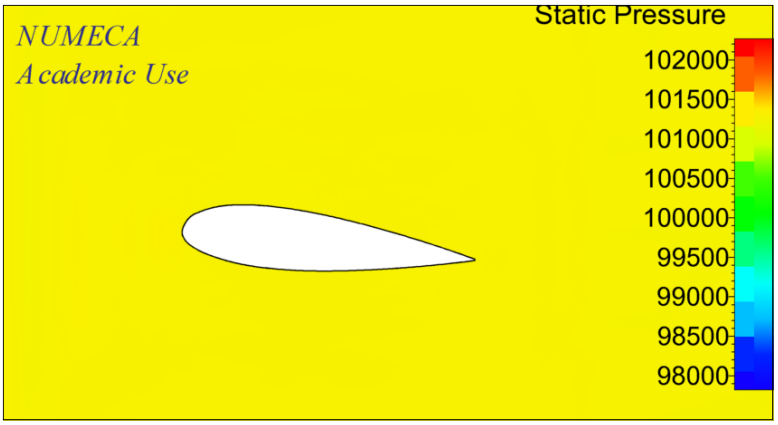

Figure 43. Distribution Static Pressure Fn 0.2

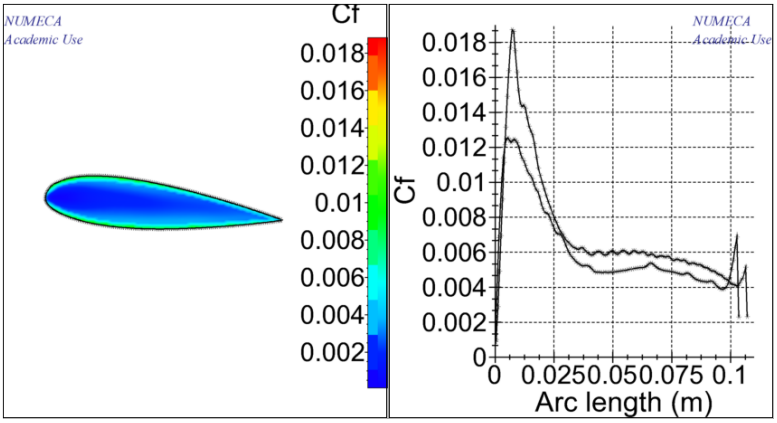

Figure 44. Coefficien Friction Fn 0.2

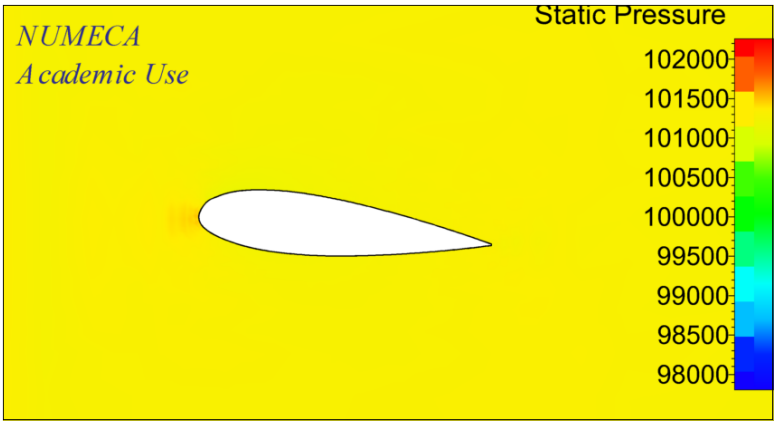

Figure 45. Distribution Static Pressure Fn 0.3

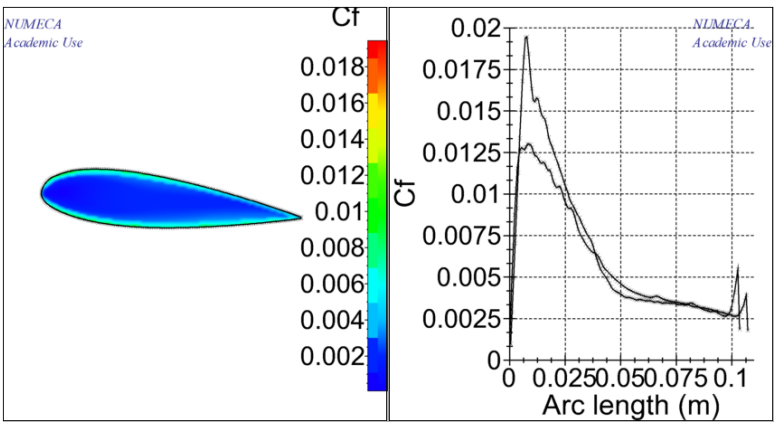

Figure 46. Coefficien Friction Fn 0.3

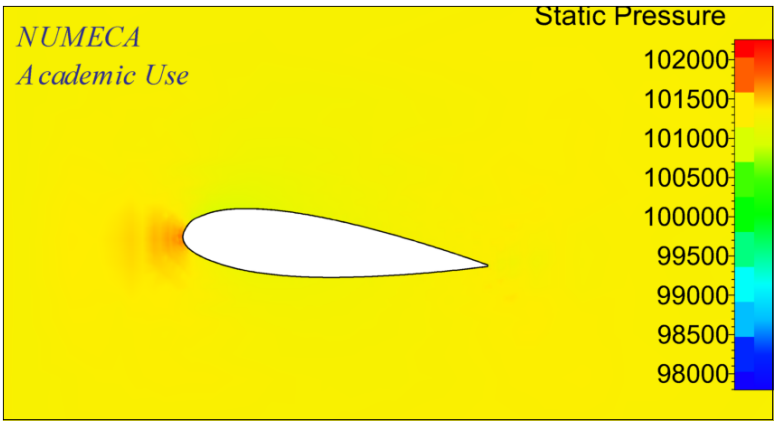

Figure 47. Distribution Static Pressure Fn 0.4

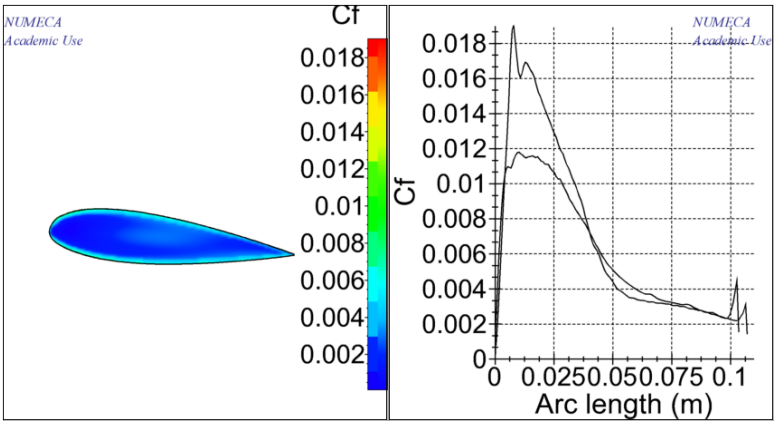

Figure 48. Coefficien Friction Fn 0.4

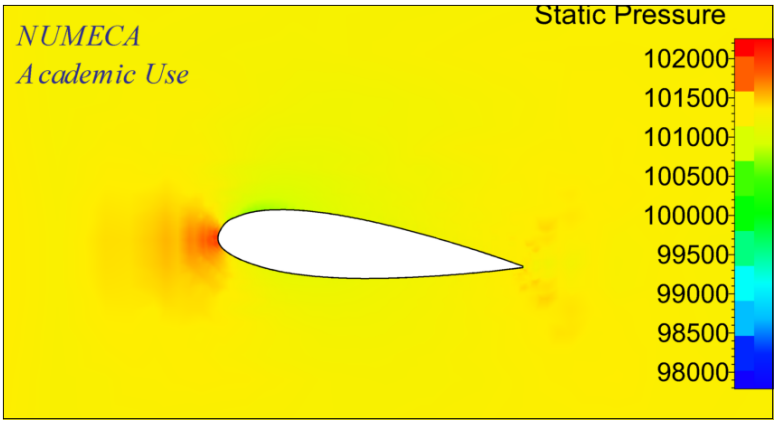

Figure 49. Distribution Static Pressure Fn 0.5

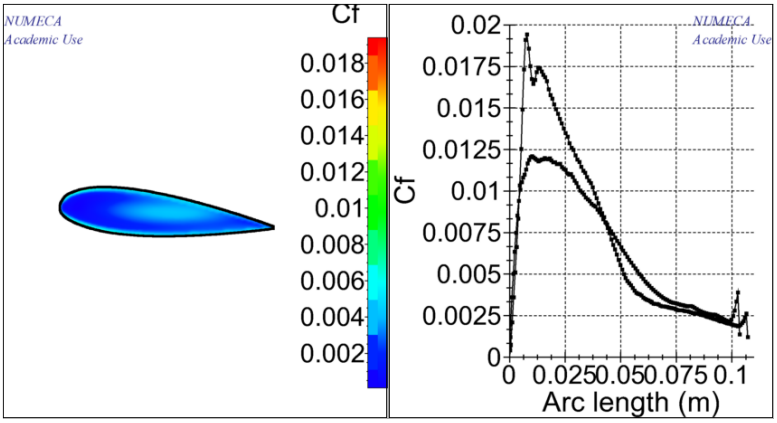

Figure 50. Coefficien Friction Fn 0.5

Attachment 6. AR 0.05 with angle of attack 10°

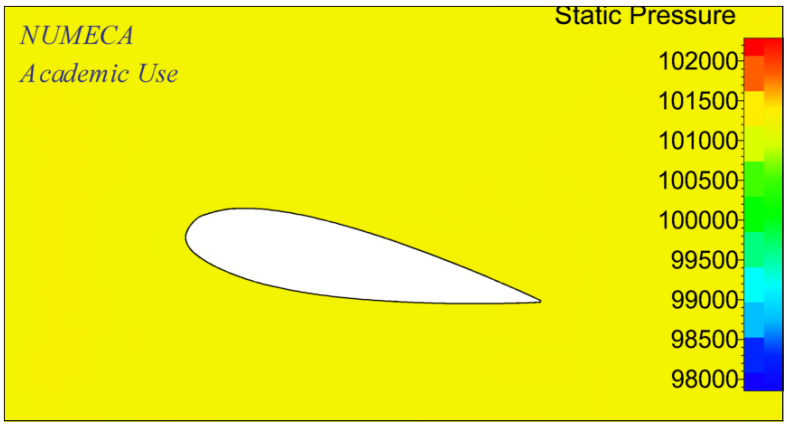

Figure 51. Distribution Static Pressure Fn 0.1

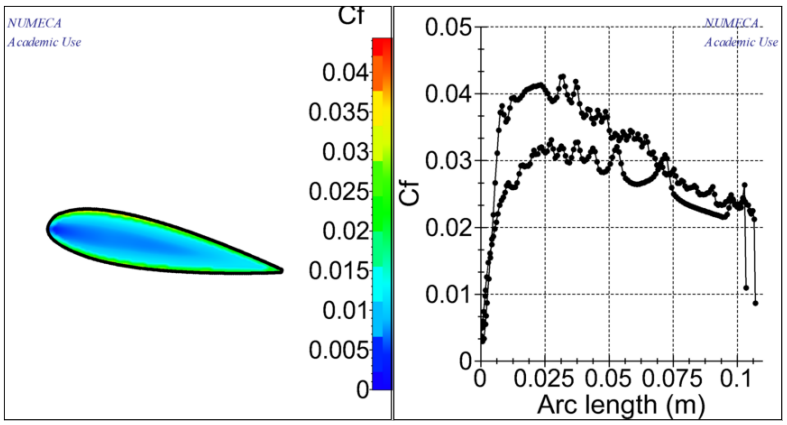

Figure 52. Coefficien Friction Fn 0.1

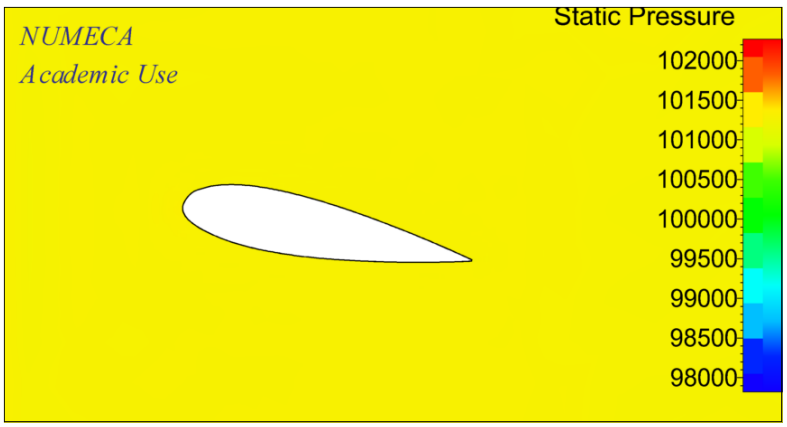

Figure 53. Distribution Static Pressure Fn 0.2

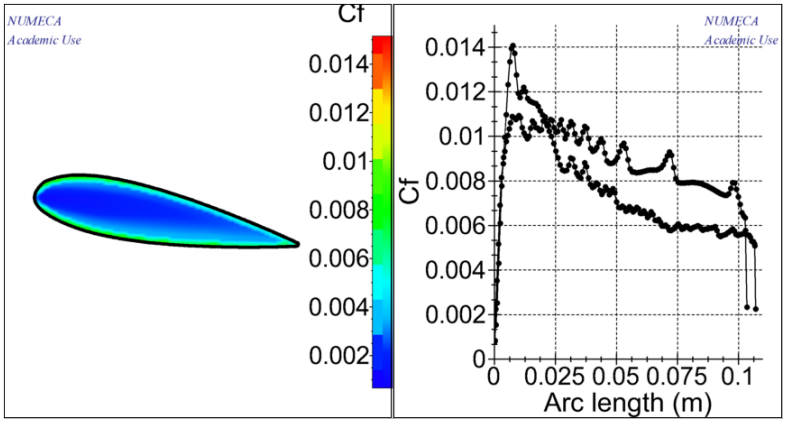

Figure 54. Coefficien Friction Fn 0.2

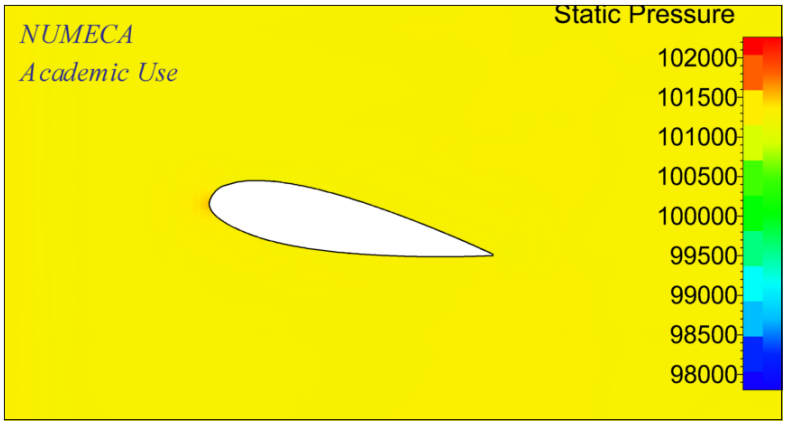

Figure 55. Distribution Static Pressure Fn 0.3

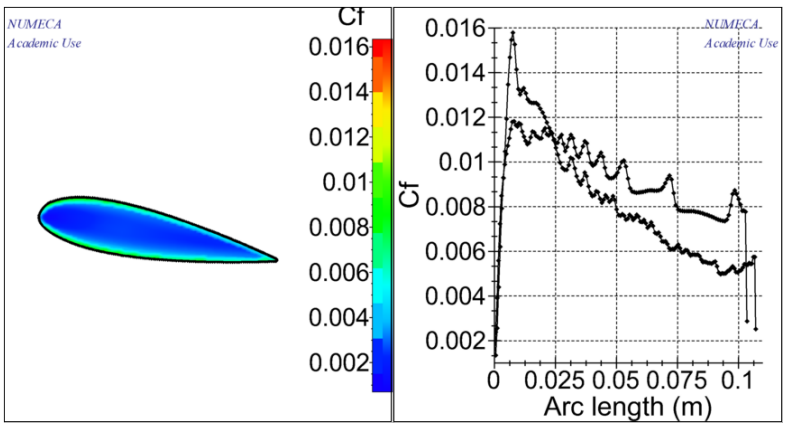

Figure 56. Coefficien Friction Fn 0.3

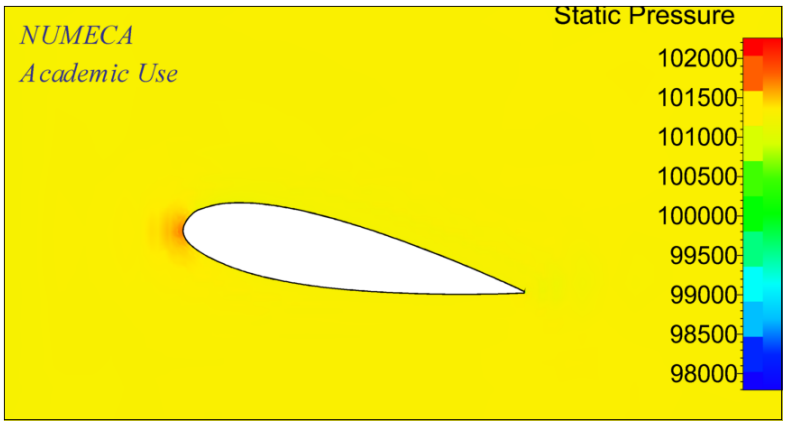

Figure 57. Distribution Static Pressure Fn 0.4

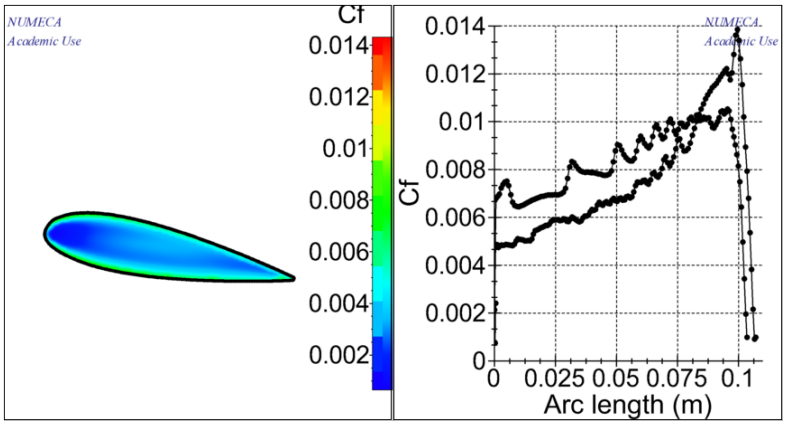

Figure 58. Coefficien Friction Fn 0.4

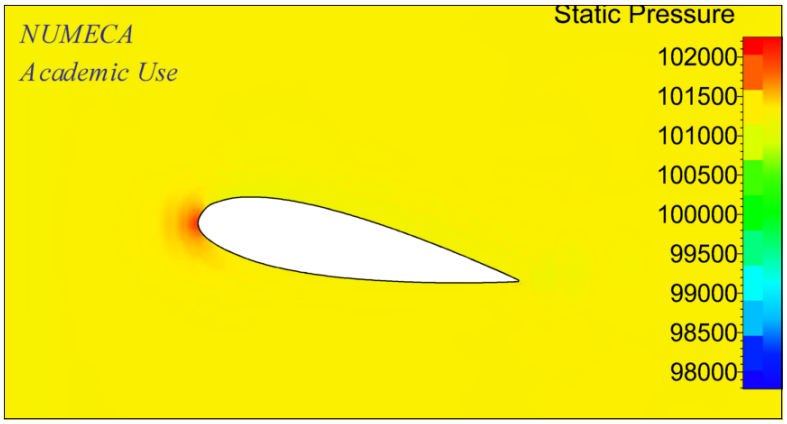

Figure 59. Distribution Static Pressure Fn 0.5

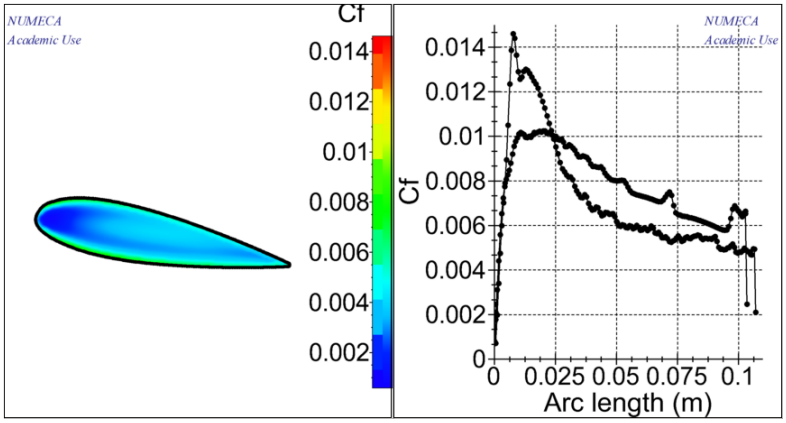

Figure 60. Coefficien Friction Fn 0.5

Attachment 7. AR 0.25 with angle of attack 10°

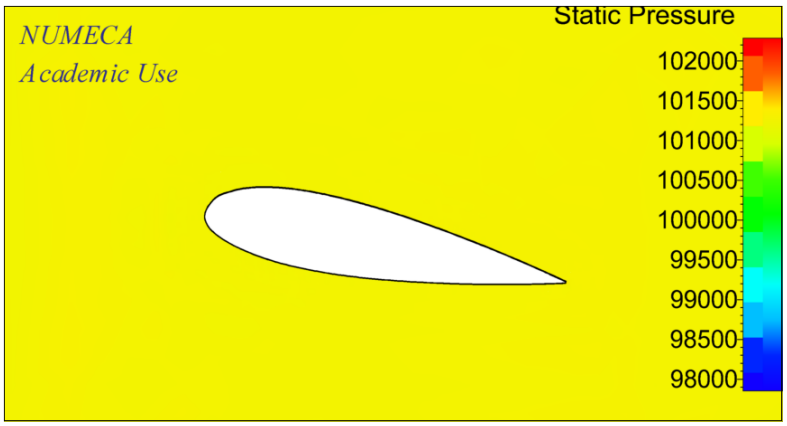

Figure 61. Distribution Static Pressure Fn 0.1

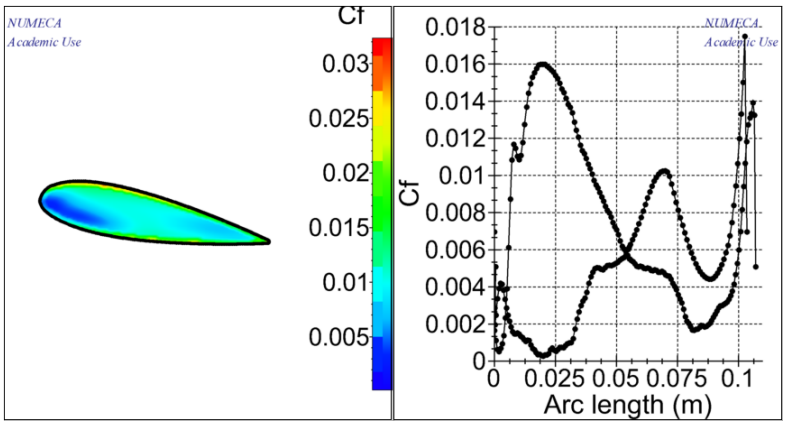

Figure 62. Coefficien Friction Fn 0.1

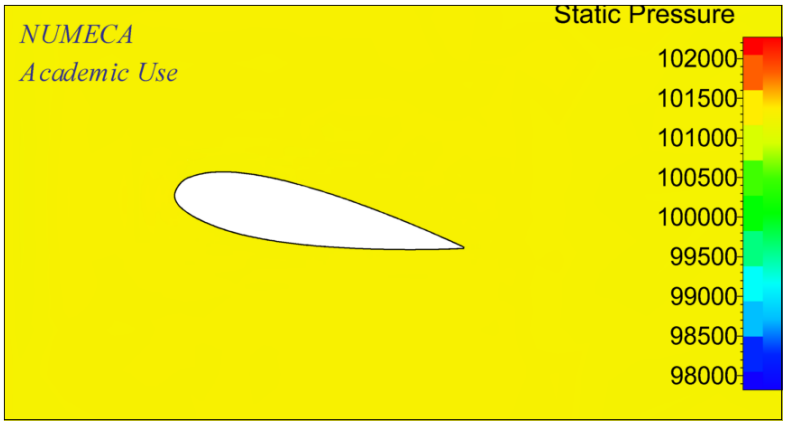

Figure 63. Distribution Static Pressure Fn 0.2

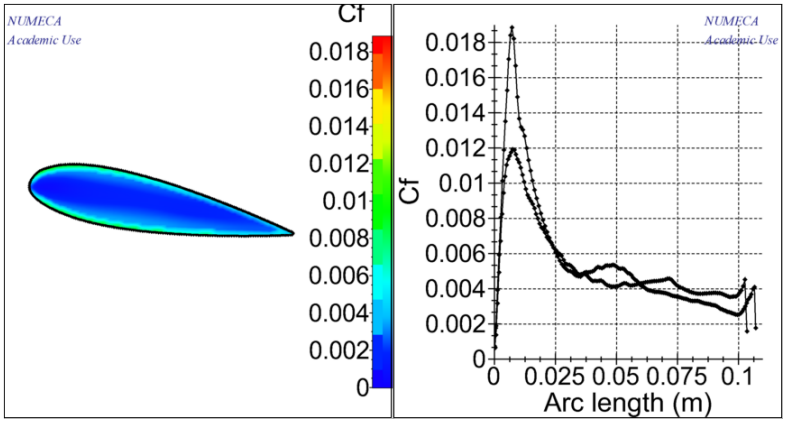

Figure 64. Coefficien Friction Fn 0.2

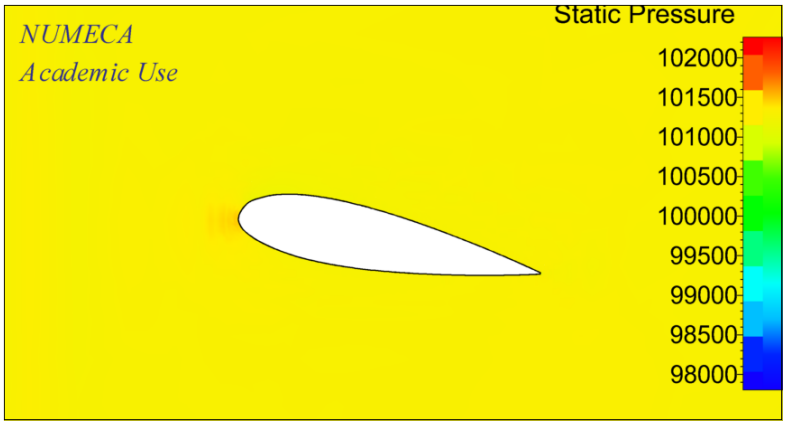

Figure 65. Distribution Static Pressure Fn 0.3

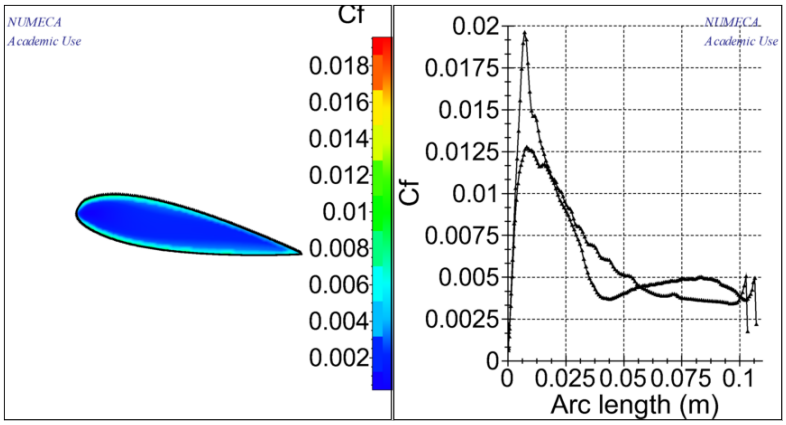

Figure 66. Coefficien Friction Fn 0.3

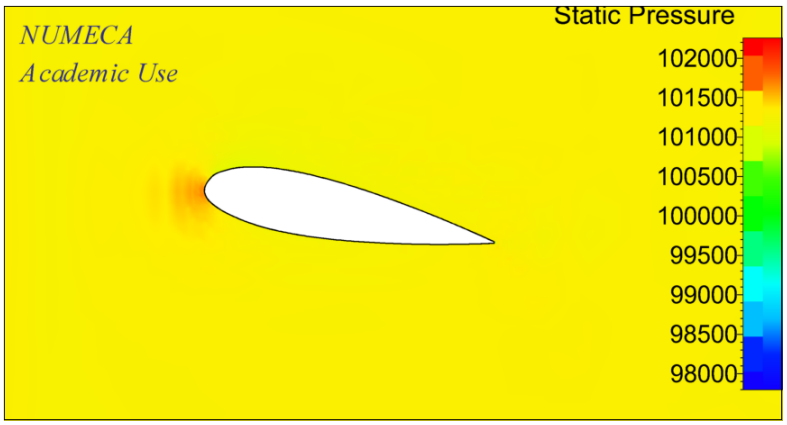

Figure 67. Distribution Static Pressure Fn 0.4

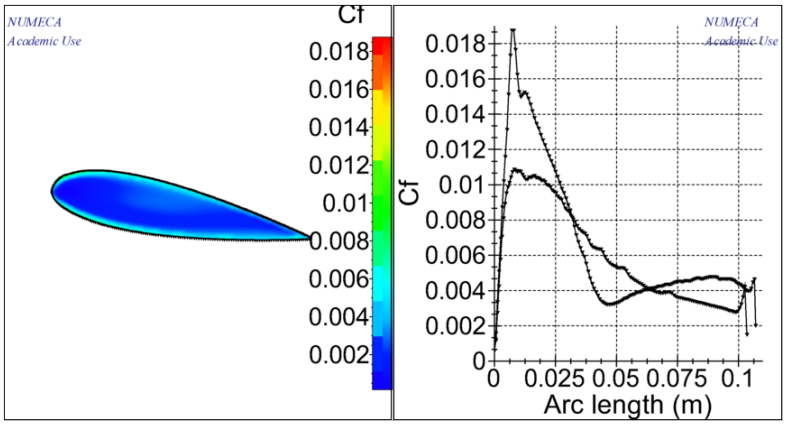

Figure 68. Coefficien Friction Fn 0.4

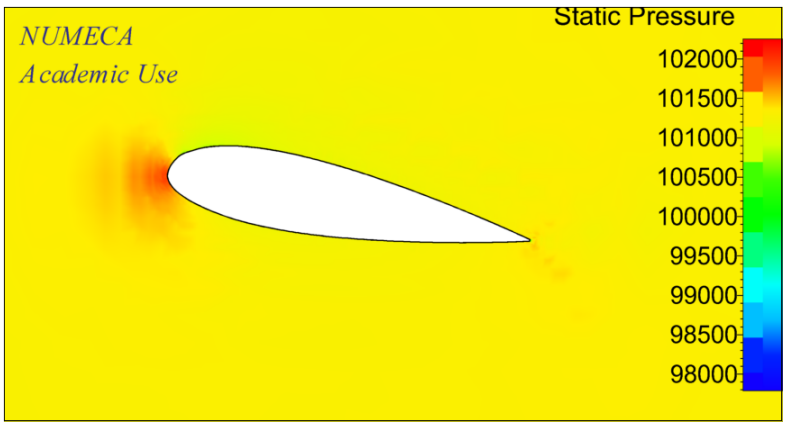

Figure 69. Distribution Static Pressure Fn 0.5

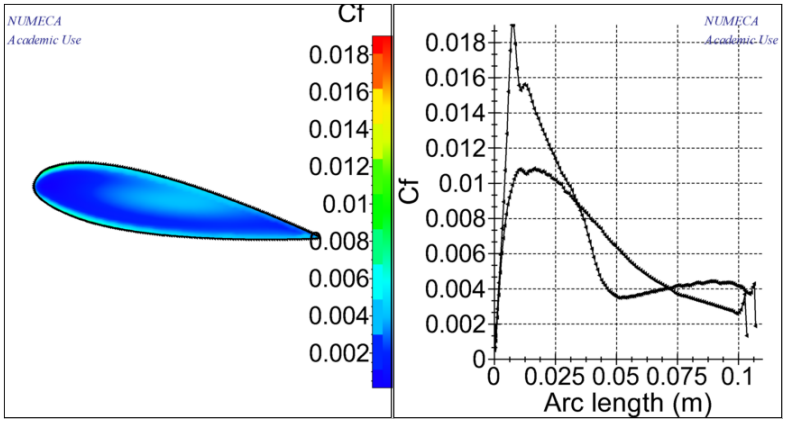

Figure 70. Coefficien Friction Fn 0.5

Attachment 8. AR 0.45 with angle of attack 10°

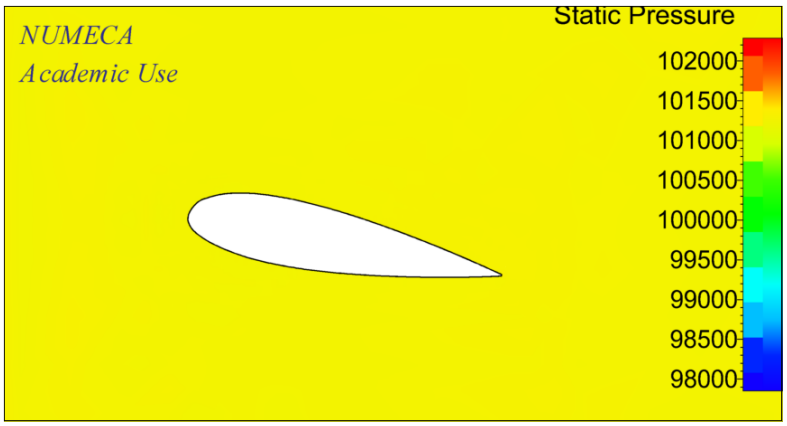

Figure 71. Distribution Static Pressure Fn 0.1

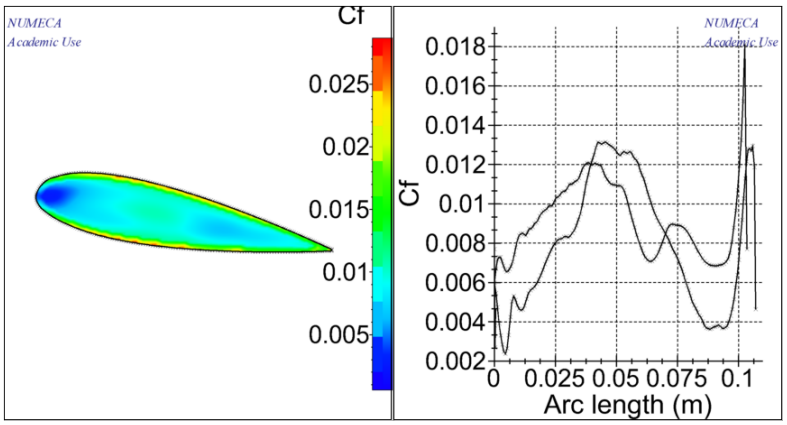

Figure 72. Coefficien Friction Fn 0.1

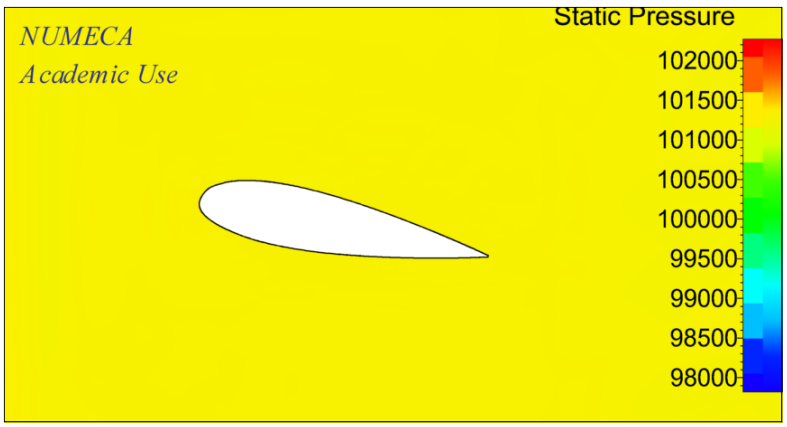

Figure 73. Distribution Static Pressure Fn 0.2

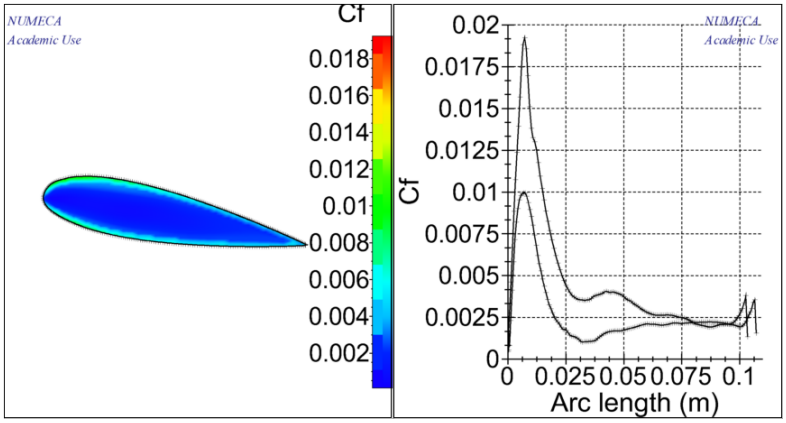

Figure 74. Coefficient Friction Fn 0,2

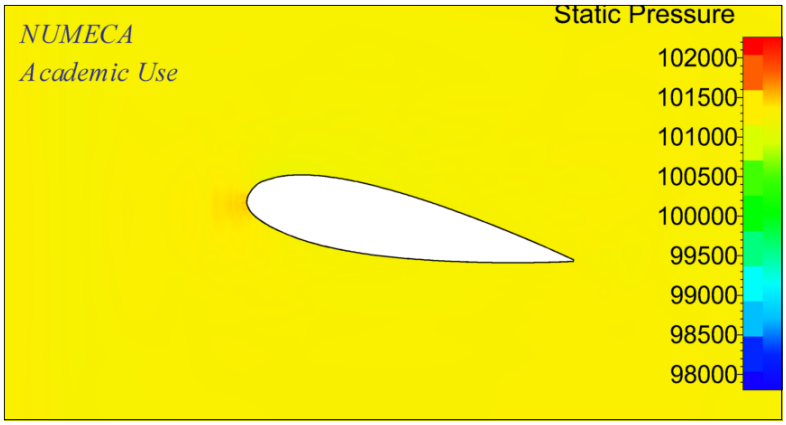

Figure 75. Distribution Static Pressure Fn 0.3

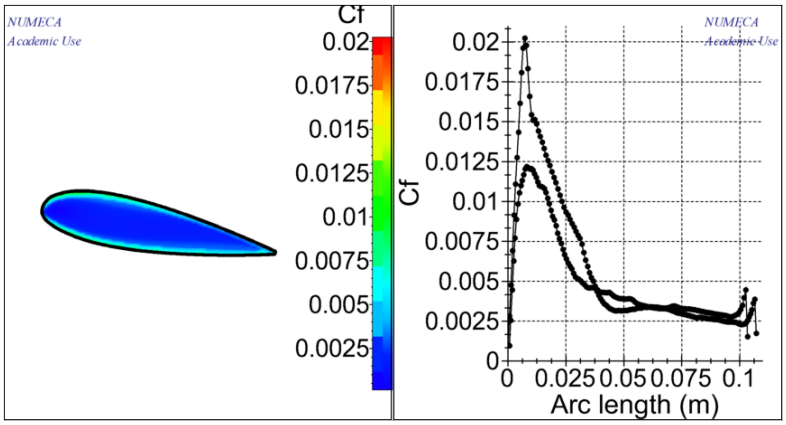

Figure 76. Coefficient Friction Fn 0.3

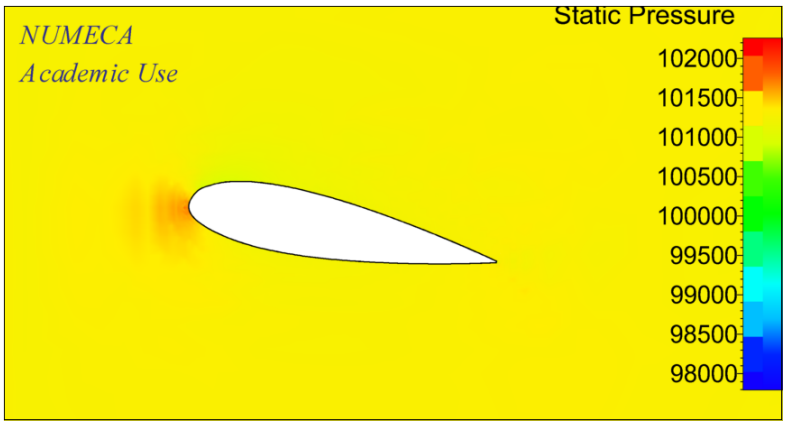

Figure 77. Distribution Static Pressure Fn 0.4

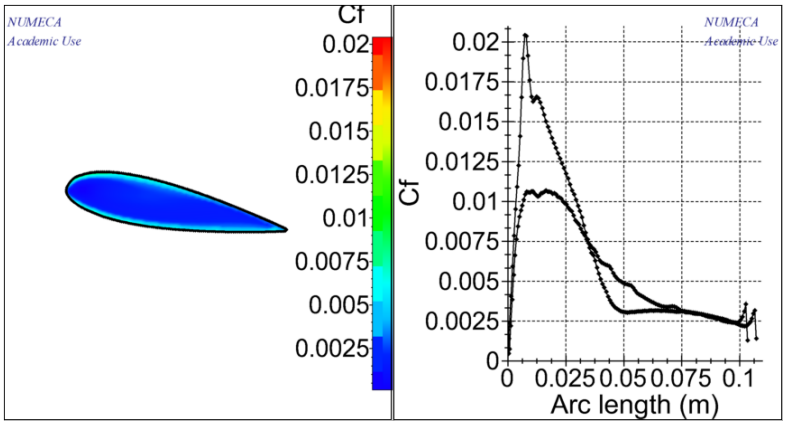

Figure 78. Coefficient Friction Fn 0.4

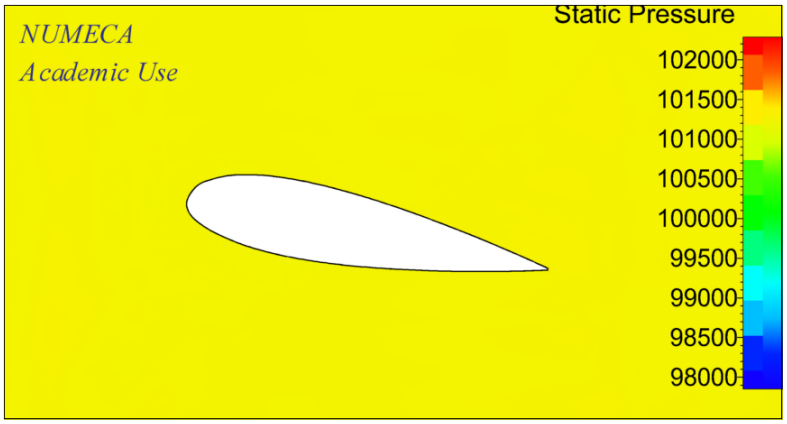

Figure 79. Distribution Static Pressure Fn 0.5

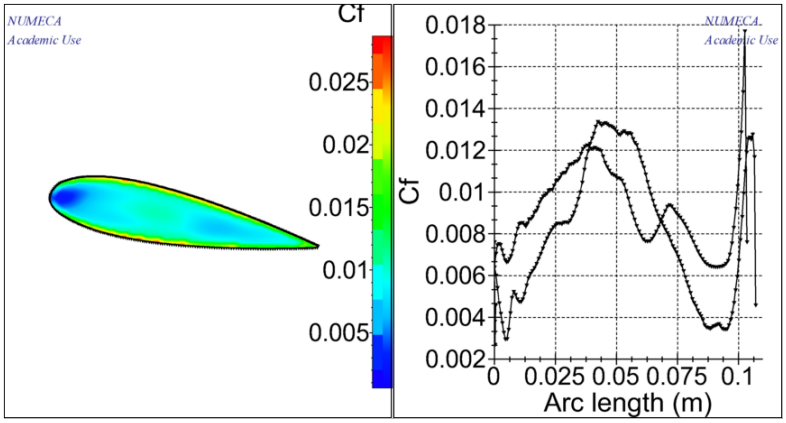

Figure 80. Coefficient Friction Fn 0.5

Attachment 9. AR 0.65 with angle of attack 10°

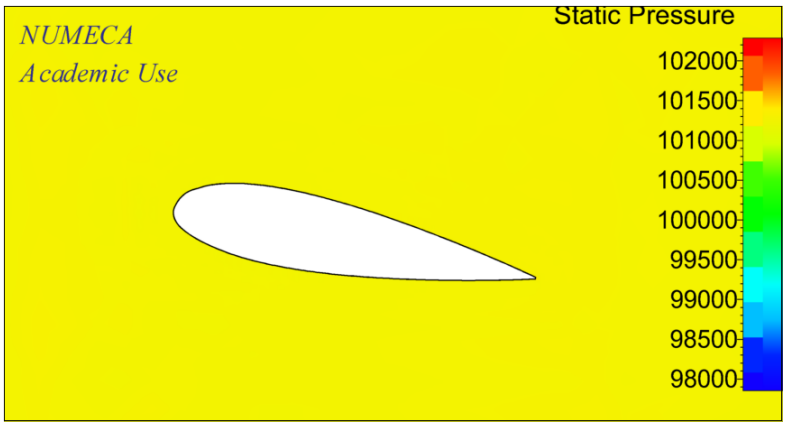

Figure 81. Distribution Static Pressure Fn 0.1

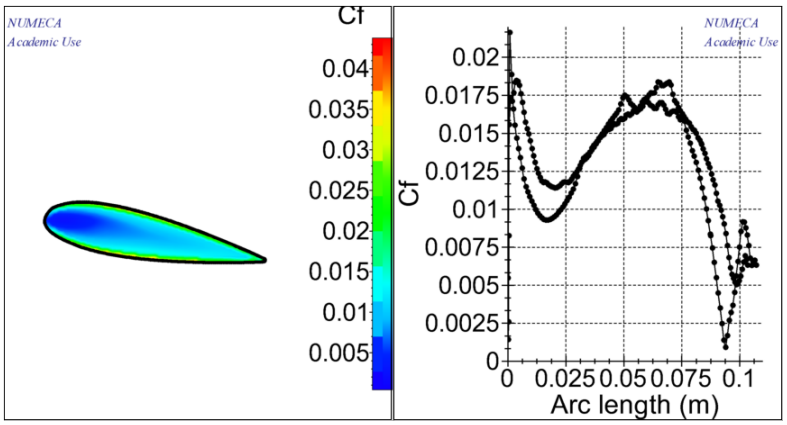

Figure 82. Coefficient Friction Fn 0.1

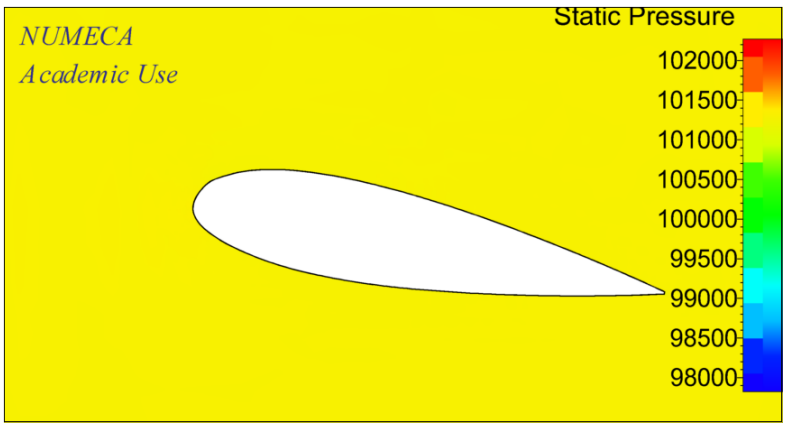

Figure 83. Distribution Static Pressure Fn 0.2

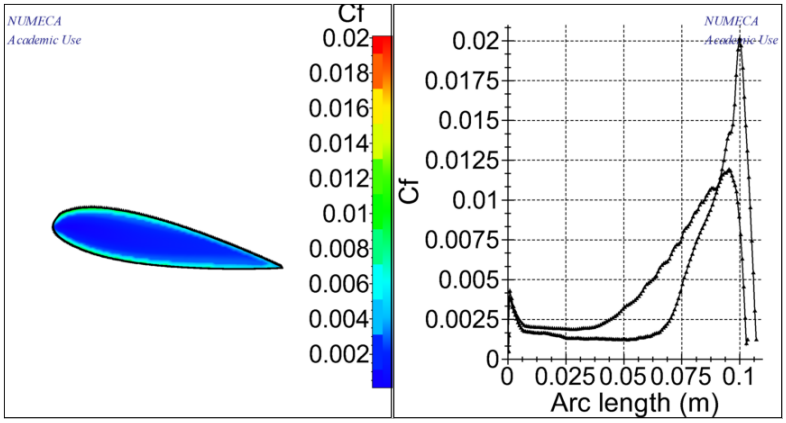

Figure 84. Coefficient Friction Fn 0.2

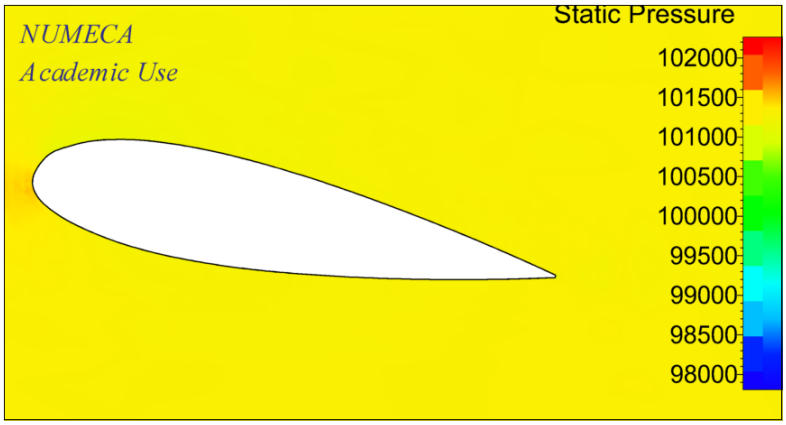

Figure 85. Distribution Static Pressure Fn 0.3

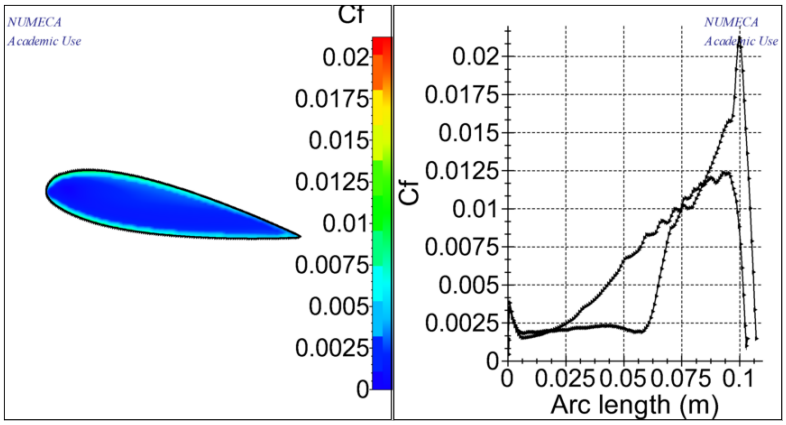

Figure 86. Coefficient Friction Fn 0.3

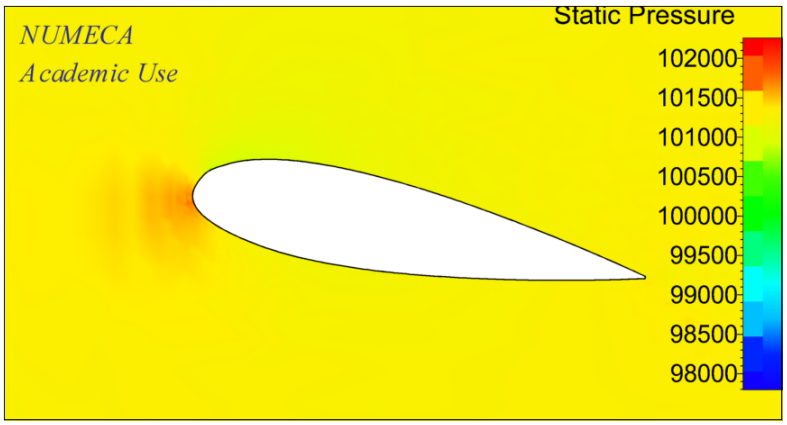

Figure 87. Distribution Static Pressure Fn 0.4

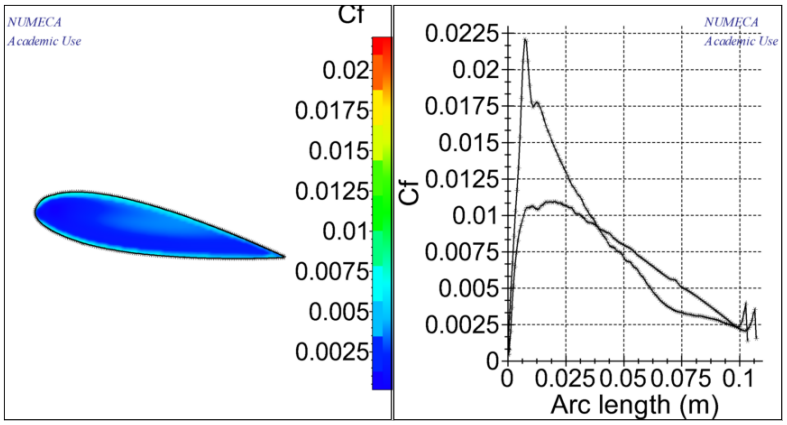

Figure 88. Coefficient Friction Fn 0.4

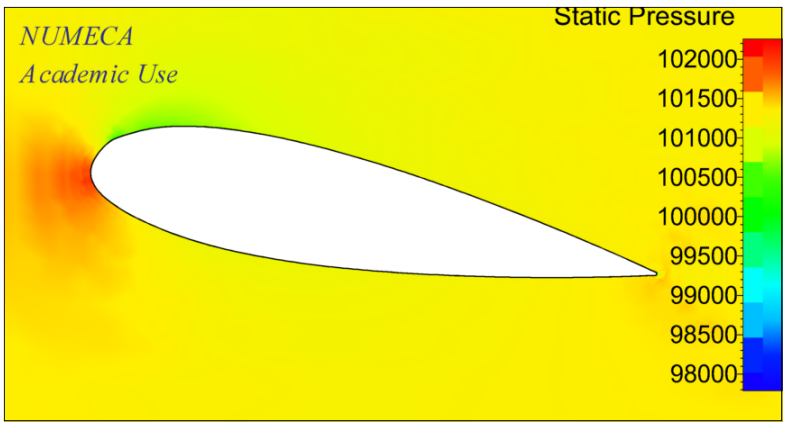

Figure 89. Distribution Static Pressure Fn 0.5

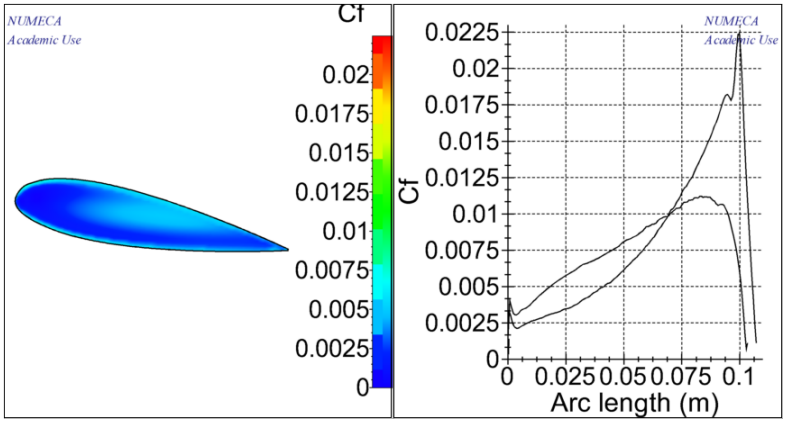

Figure 90. Coefficient Friction Fn 0.5

Lampiran 1. AR 0.85 with angle of attack 10°

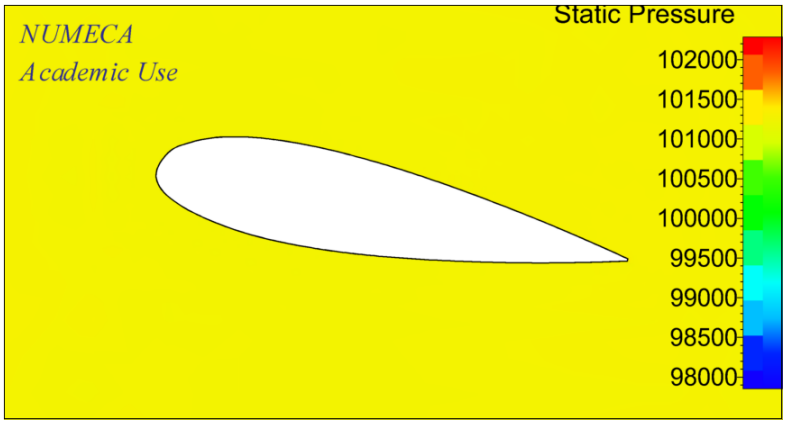

Figure 91. Distribution Static Pressure Fn 0.1

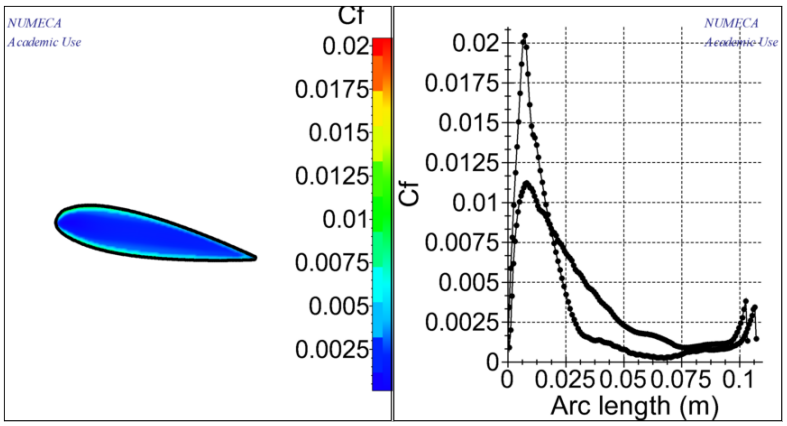

Figure 92. Coefficient Friction Fn 0.1

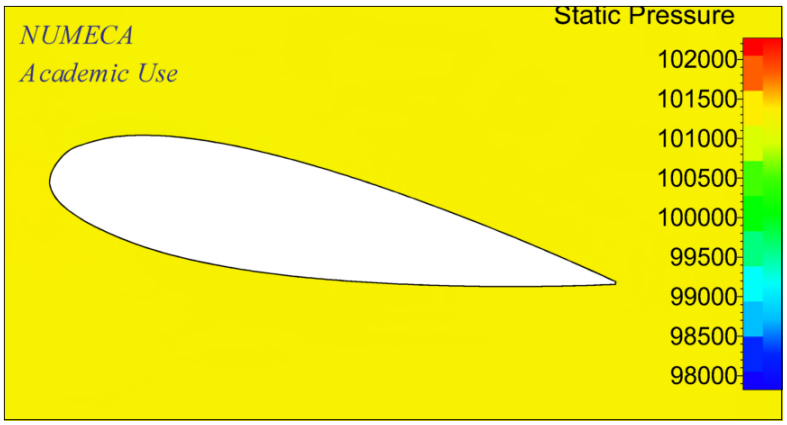

Figure 93. Distribution Static Pressure Fn 0.2

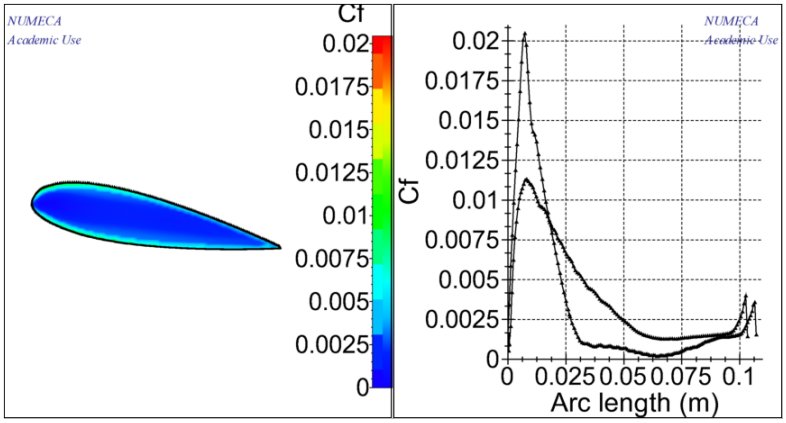

Figure 94. Coefficient Friction Fn 0.2

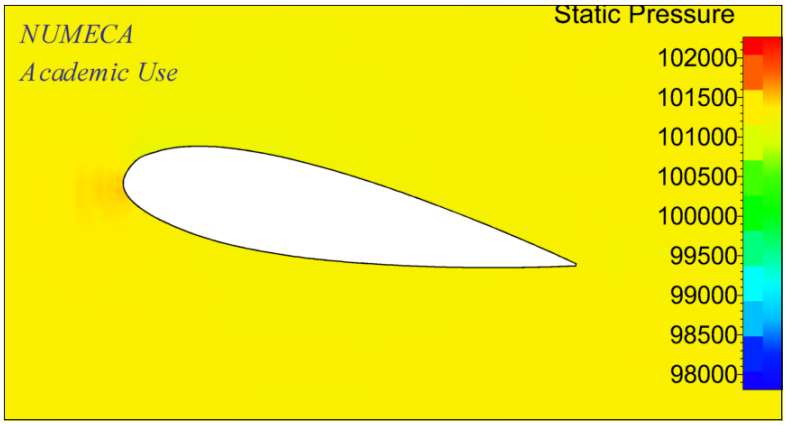

Figure 95. Distribution Static Pressure Fn 0.3

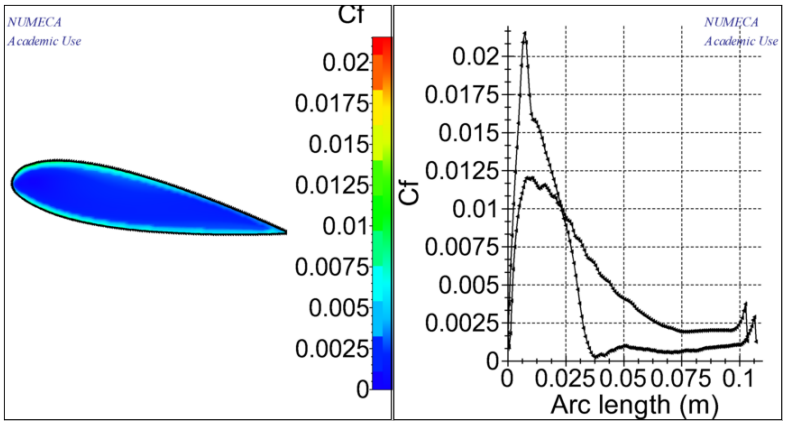

Figure 96. Coefficient Friction Fn 0.3

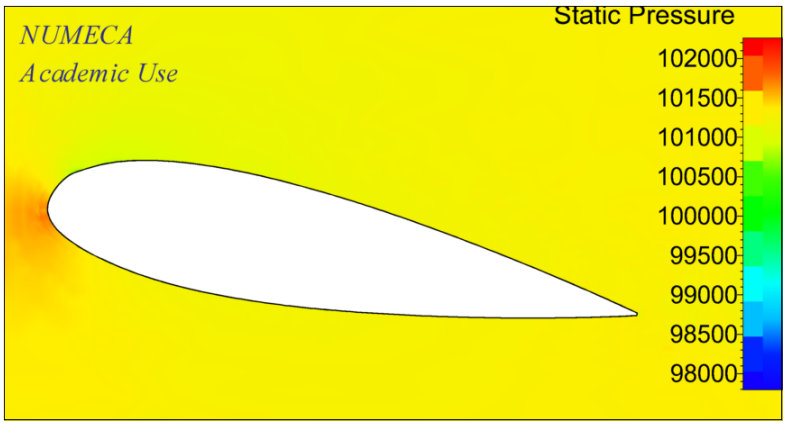

Figure 97. Distribution Static Pressure Fn 0.4

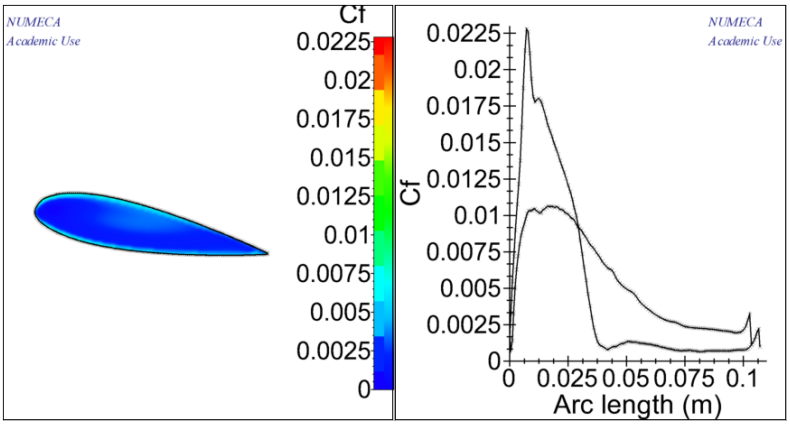

Figure 98. Coefficient Friction Fn 0.4

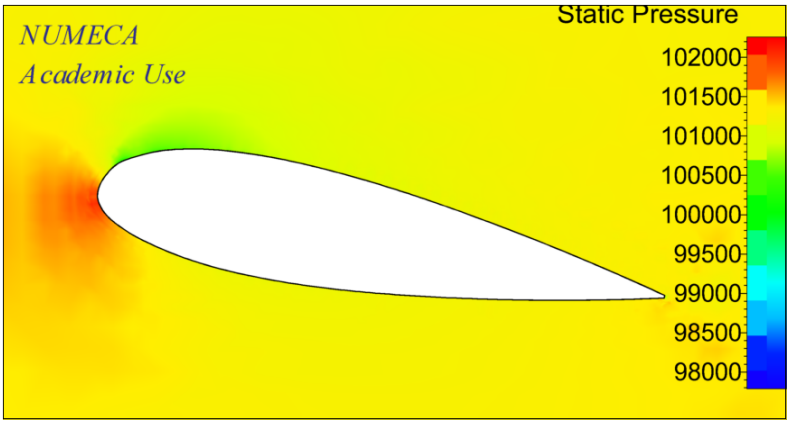

Figure 99. Distribution Static Pressure Fn 0.5

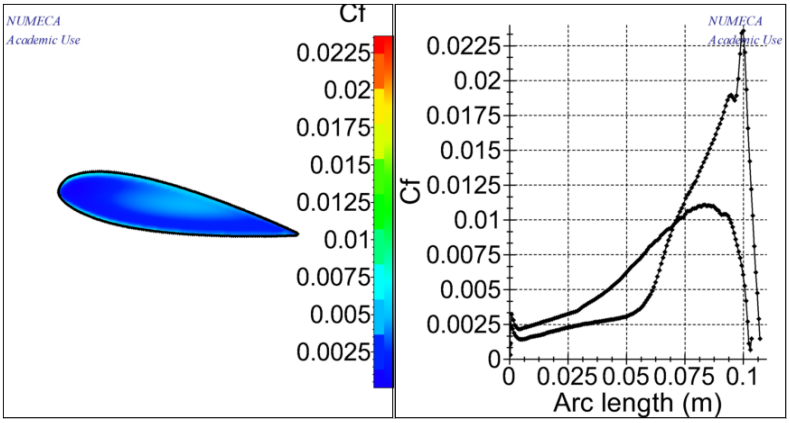

Figure 100. Coefficient Friction Fn 0.5

Lampiran 2. AR 0.05 with angle of attack 15°

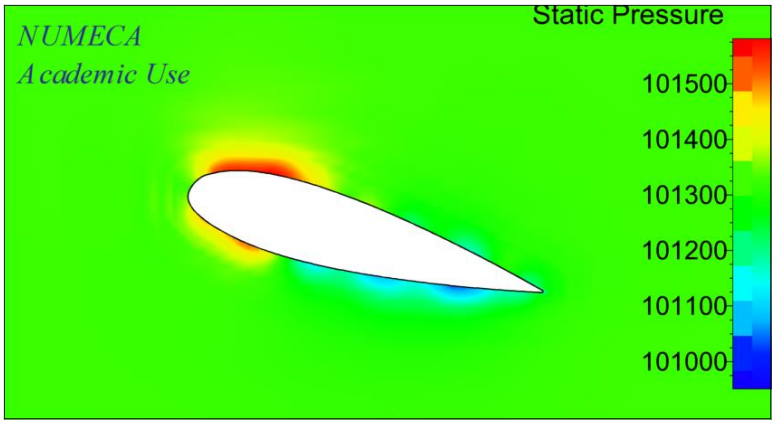

Figure 101. Distribution Static Pressure Fn 0.1

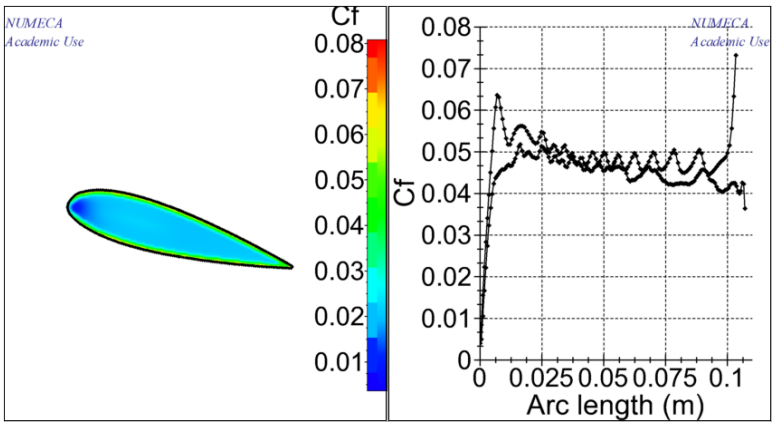

Figure 102. Coefficient Friction Fn 0.1

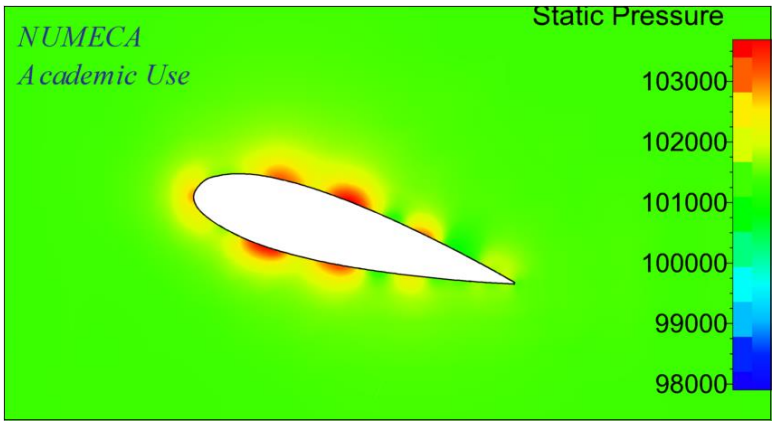

Figure 103. Distribution Static Pressure Fn 0.2

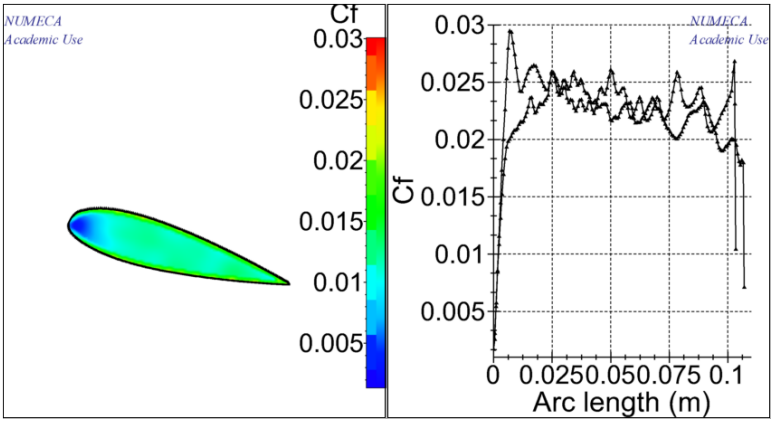

Figure 104. Coefficient Friction Fn 0.2

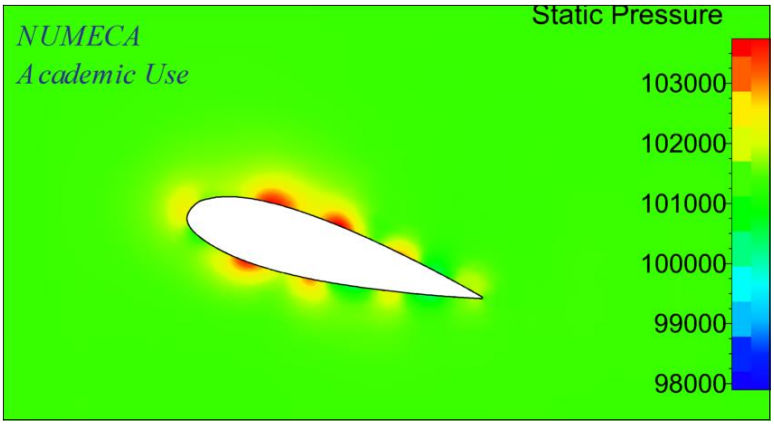

Figure 105. Distribution Static Pressure Fn 0.3

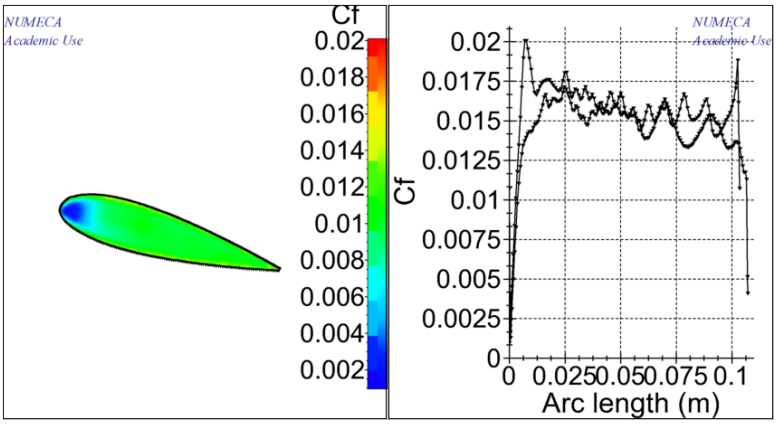

Figure 106. Coefficient Friction Fn 0.3

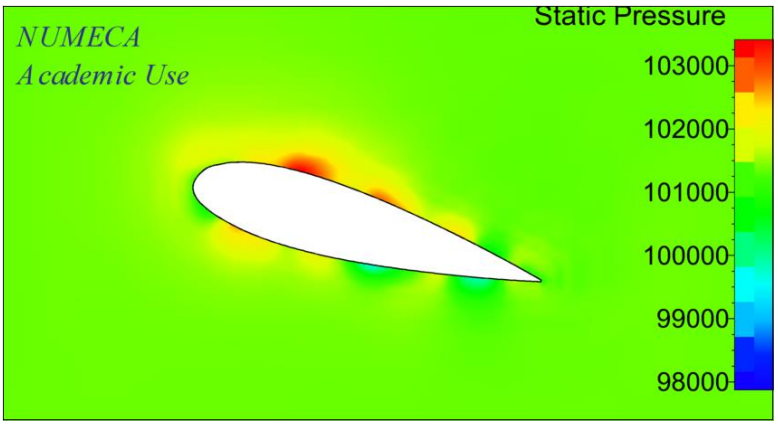

Figure 107. Distribution Static Pressure Fn 0.4

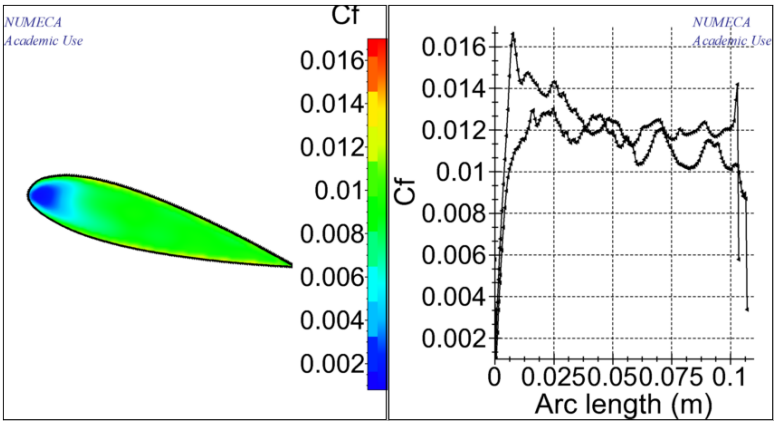

Figure 108, Coefficient Friction Fn 0.4

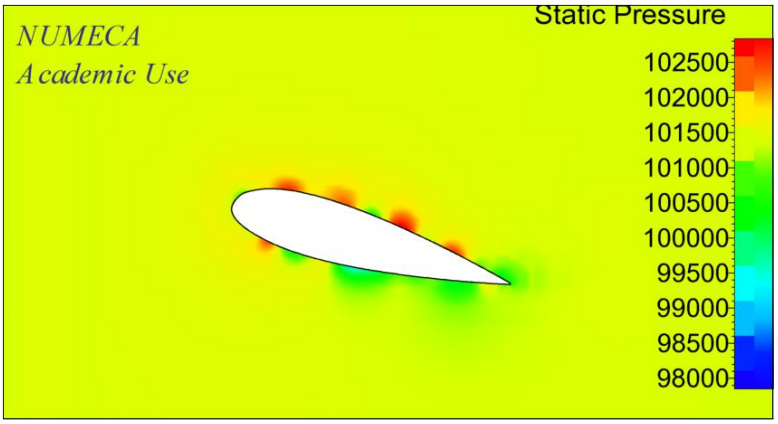

Figure 109. Distribution Static Pressure Fn 0.5

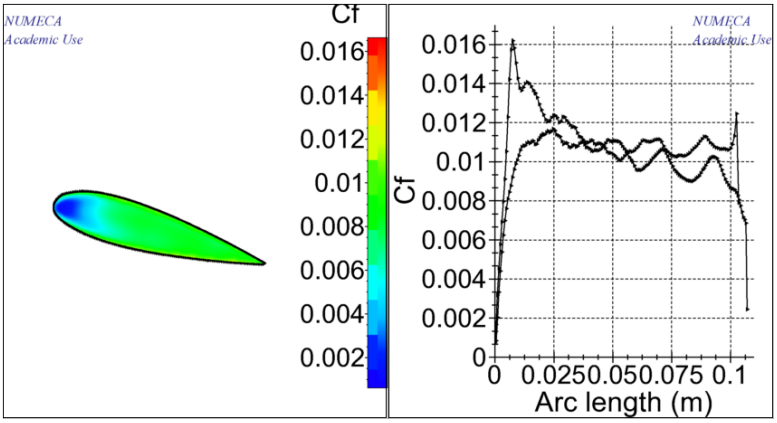

Figure 110. Coefficient Friction Fn 0.5

Lampiran 3. AR 0.25 with angle of attack 15°

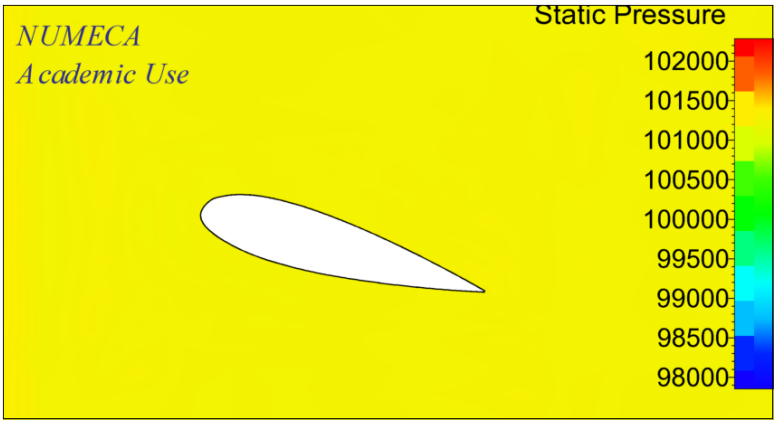

Figure 111. Distribution Static Pressure Fn 0.1

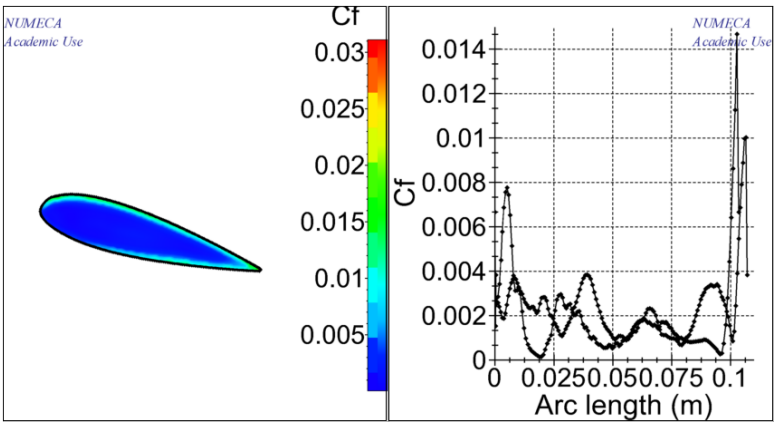

Figure 112. Coefficient Friction Fn 0.1

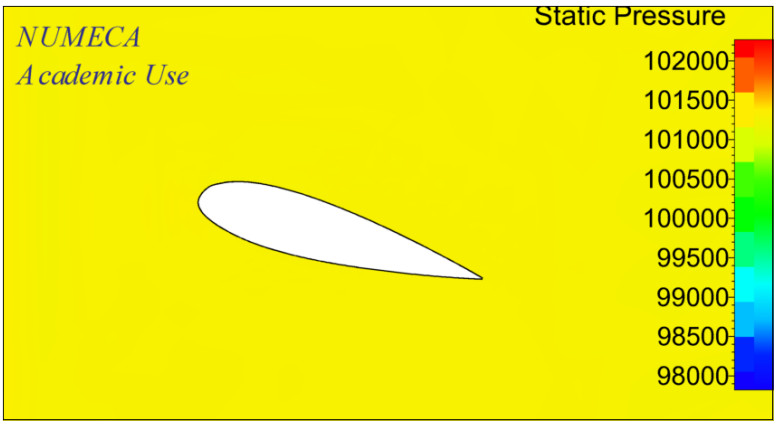

Figure 113. Distribution Static Pressure Fn 0.2

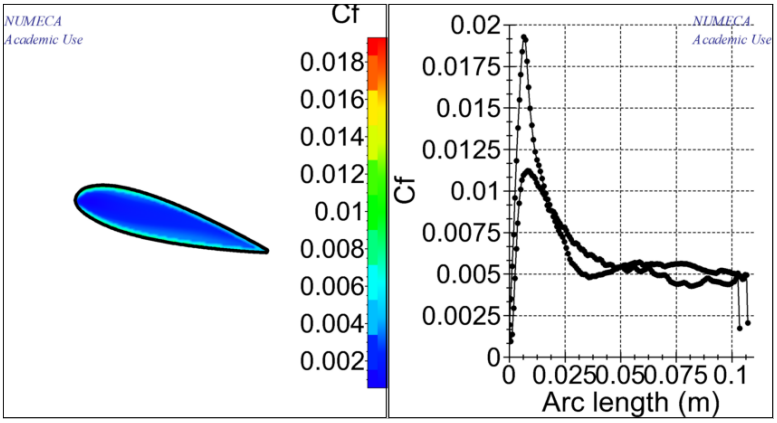

Figure 114. Coefficient Friction Fn 0.2

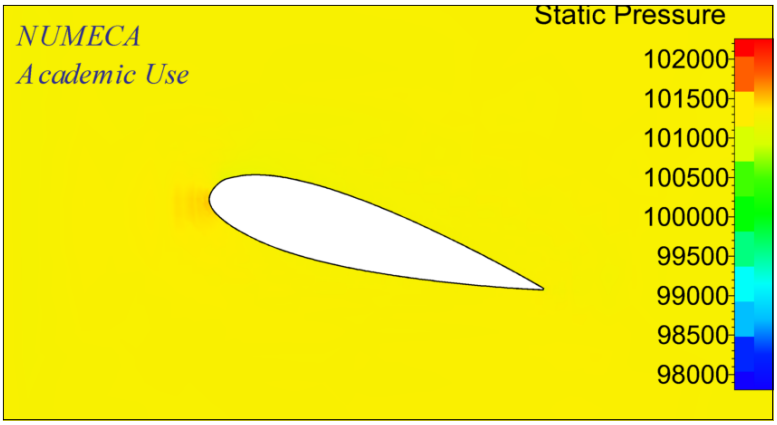

Figure 115. Distribution Static Pressure Fn 0.3

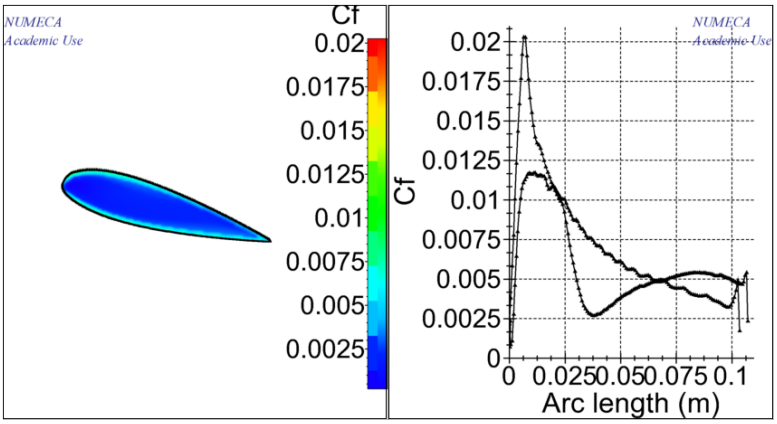

Figure 116. Coefficient Friction Fn 0.3

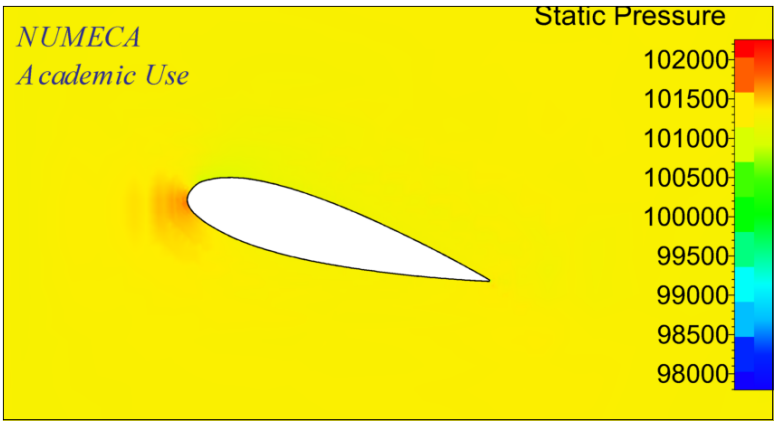

Figure 117. Distribution Static Pressure Fn 0.4

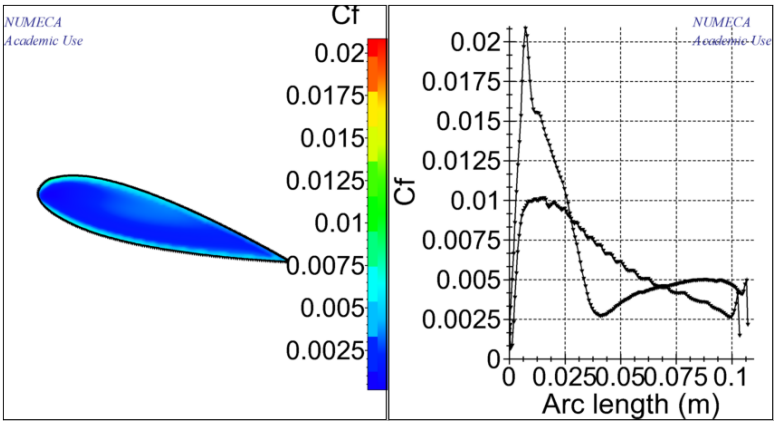

Figure 118. Coefficient Friction Fn 0.4

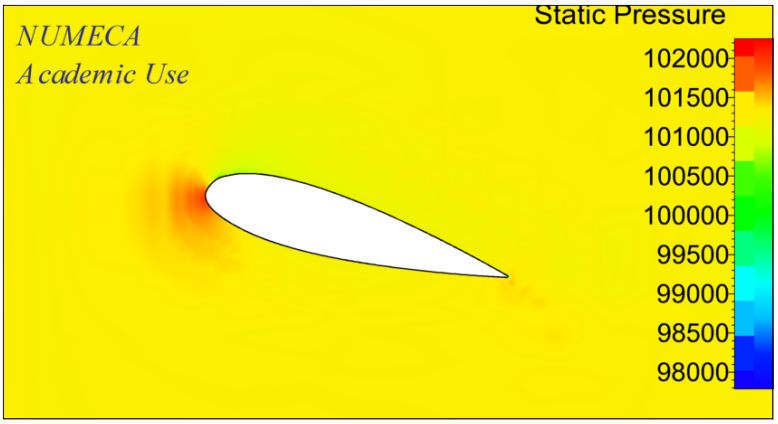

Figure 119. Distribution Static Pressure Fn 0.5

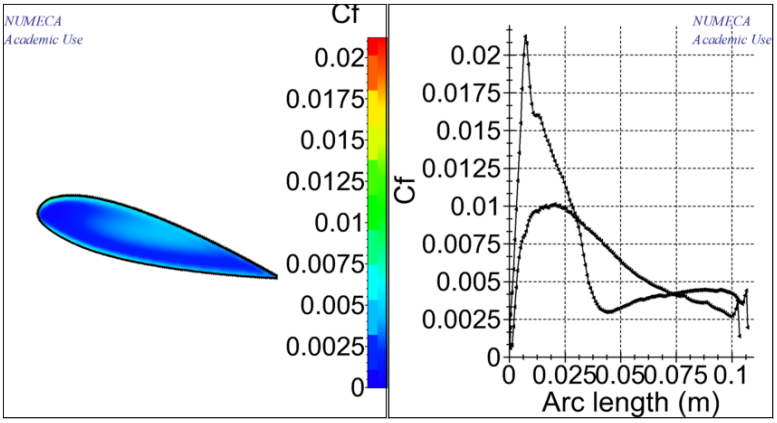

Figure 120. Coefficient Friction Fn 0.5

Lampiran 4. AR 0.45 with angle of attack 15°

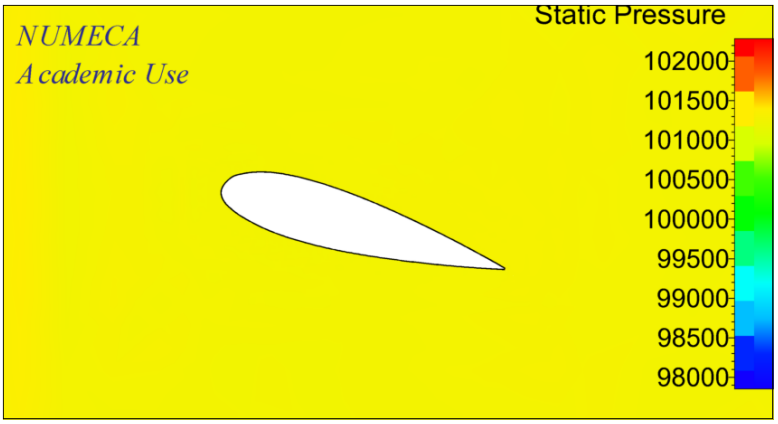

Figure 121. Distribution Static Pressure Fn 0.1

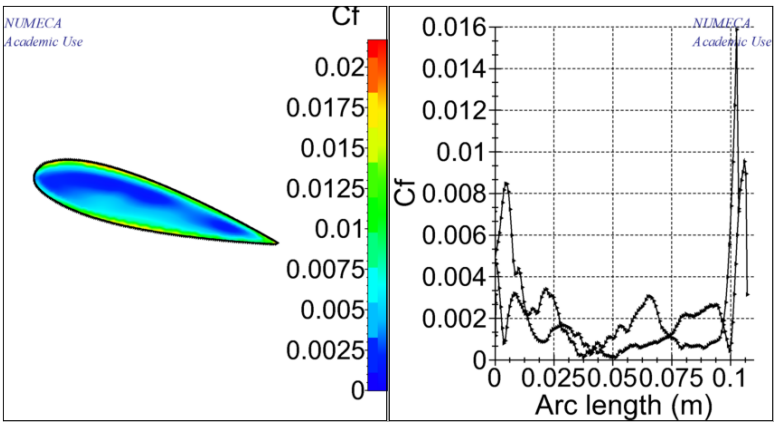

Figure 122. Coefficient Friction Fn 0.1

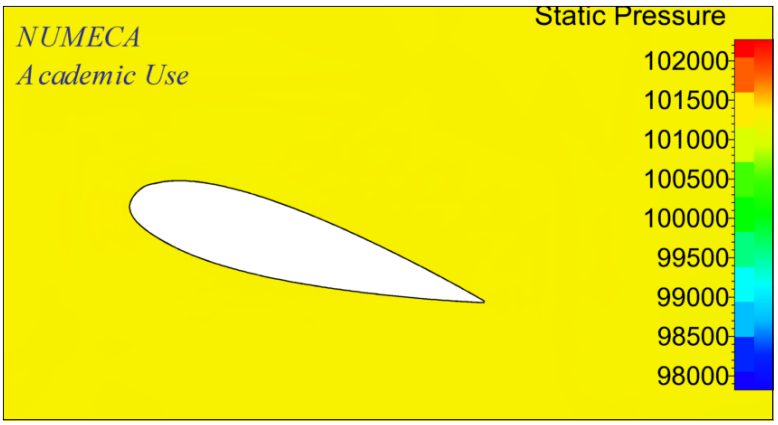

Figure 123. Distribution Static Pressure Fn 0.2

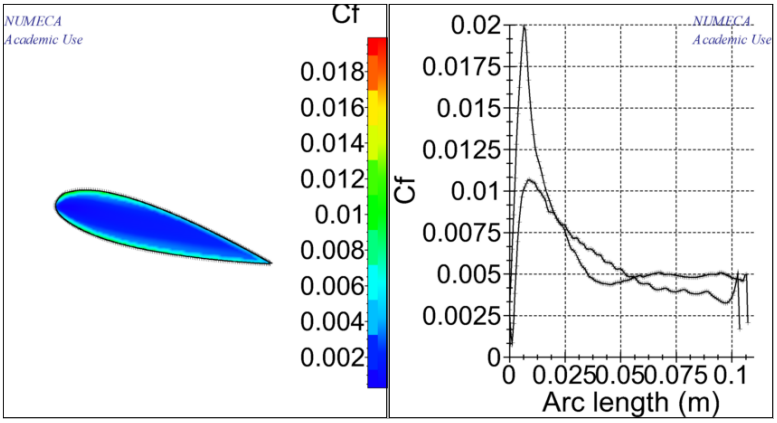

Figure 124. Coefficient Friction Fn 0.2

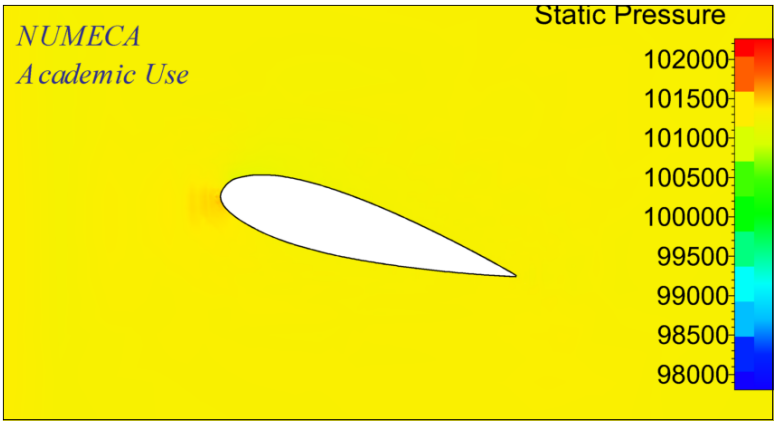

Figure 125. Distribution Static Pressure Fn 0.3

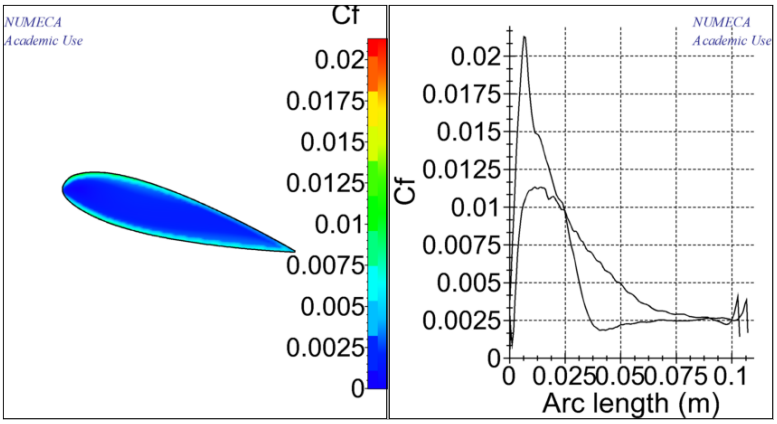

Figure 126. Coefficient Friction Fn 0.3

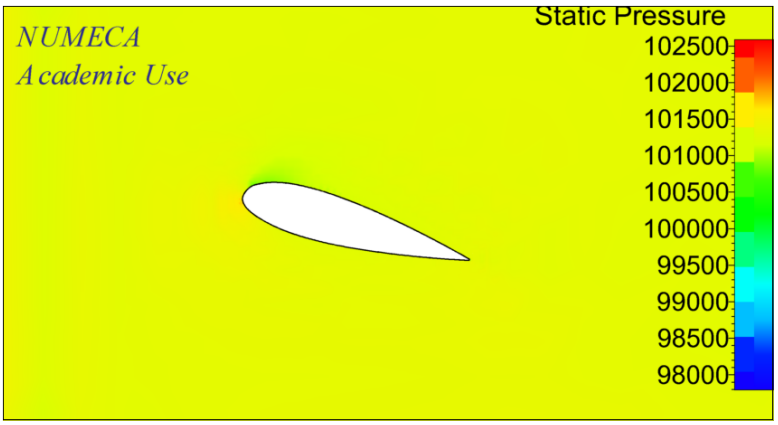

Figure 127. Distribution Static Pressure Fn 0.4

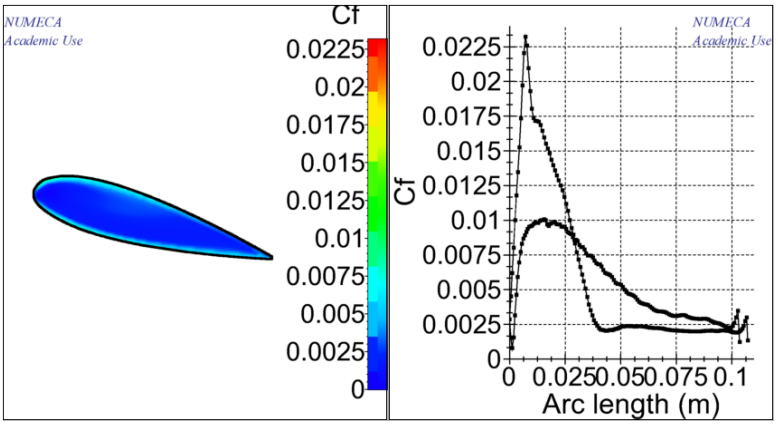

Figure 128. Coefficient Friction Fn 0.4

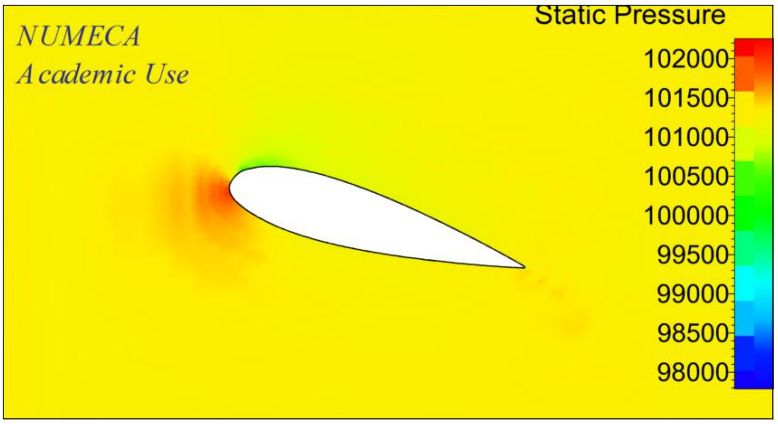

Figure 129. Distribution Static Pressure Fn 0.5

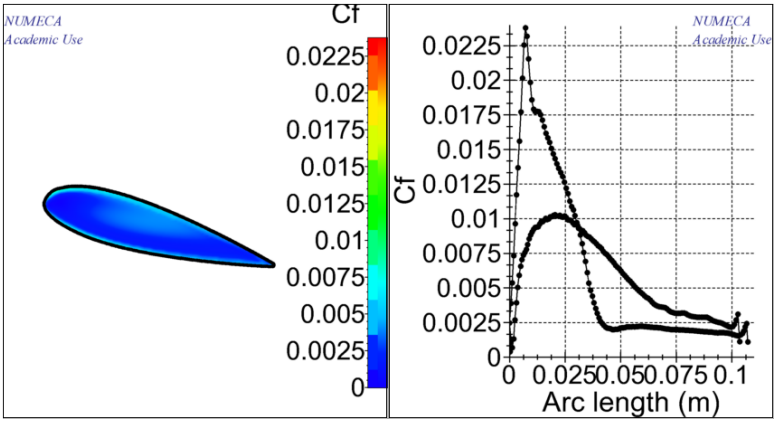

Figure 130. Coefficient Friction Fn 0.5

Lampiran 5. AR 0.65 with angle of attack 15°

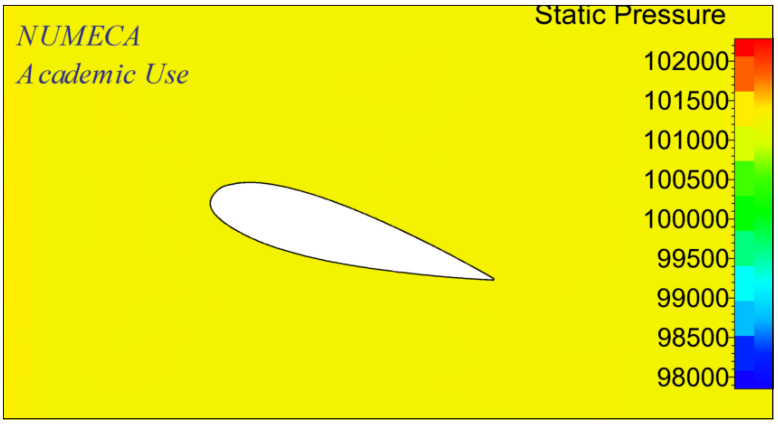

Figure 131. Distribution Static Pressure Fn 0.1

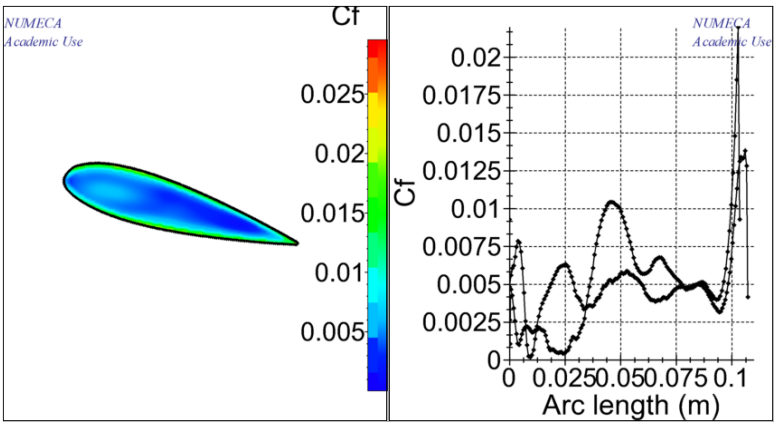

Figure 132. Coefficient Friction Fn 0.1

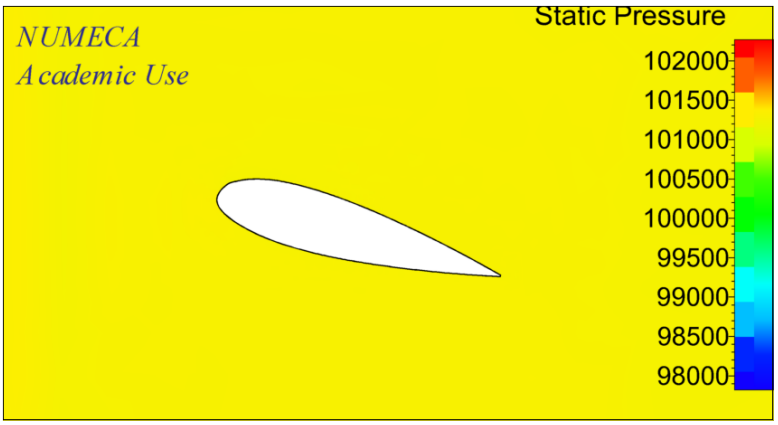

Figure 133. Distribution Static Pressure Fn 0.2

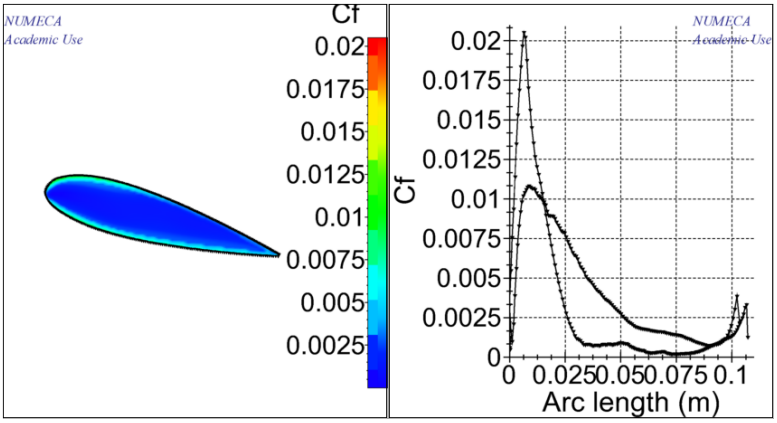

Figure 134. Coefficient Friction Fn 0.2

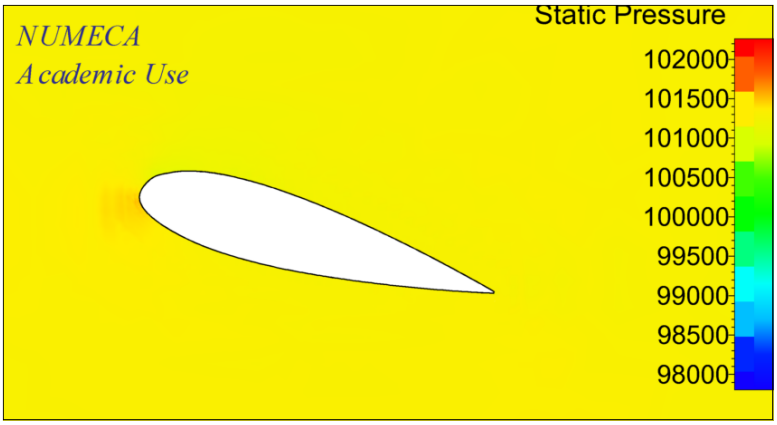

Figure 135. Distribution Static Pressure Fn 0.3

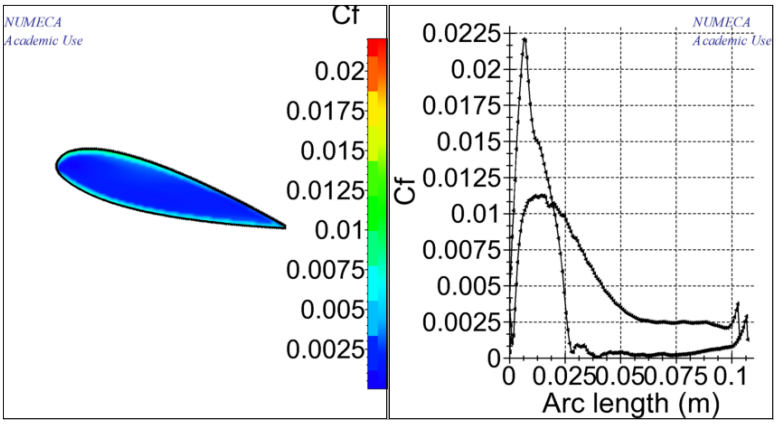

Figure 136. Coefficient Friction Fn 0.3

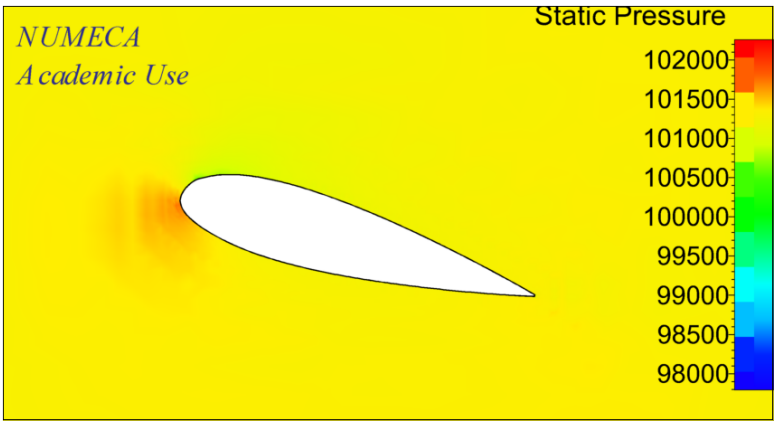

Figure 137. Distribution Static Pressure Fn 0.4

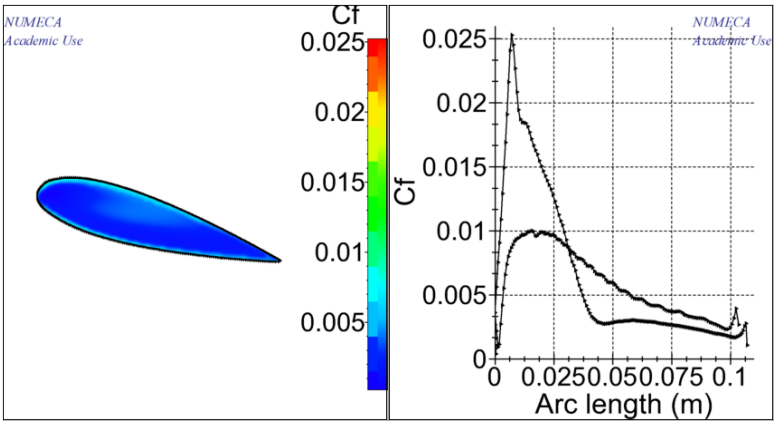

Figure 138. Coefficient Friction Fn 0.4

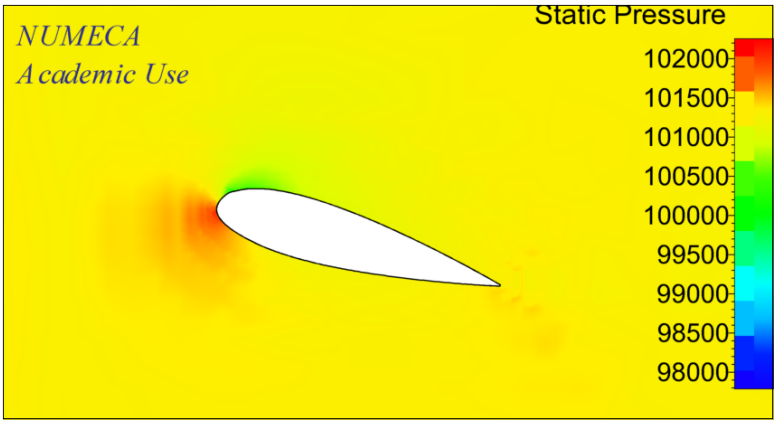

Figure 139. Distribution Static Pressure Fn 0.5

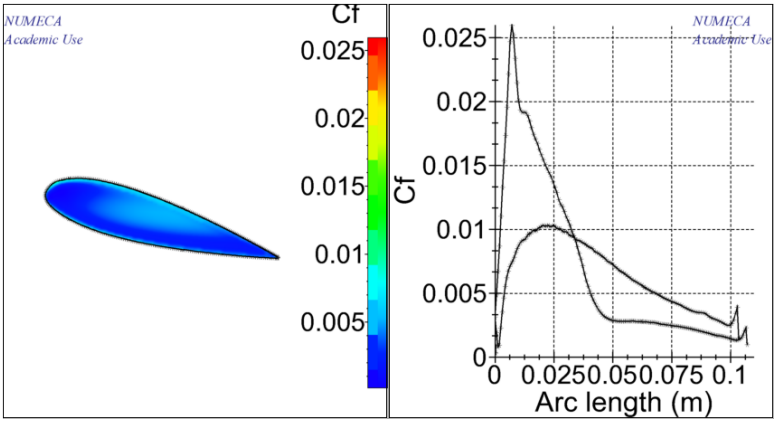

Figure 140. Coefficient Friction Fn 0.5

Lampiran 6. AR 0.85 with angle of attack 15°

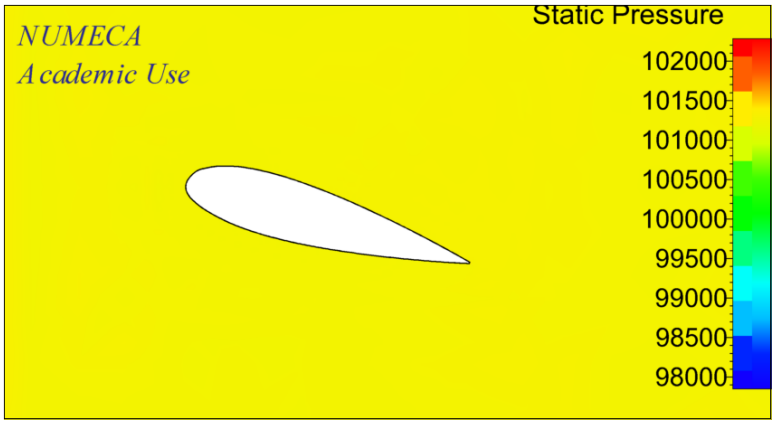

Figure 141. Distribution Static Pressure Fn 0.1

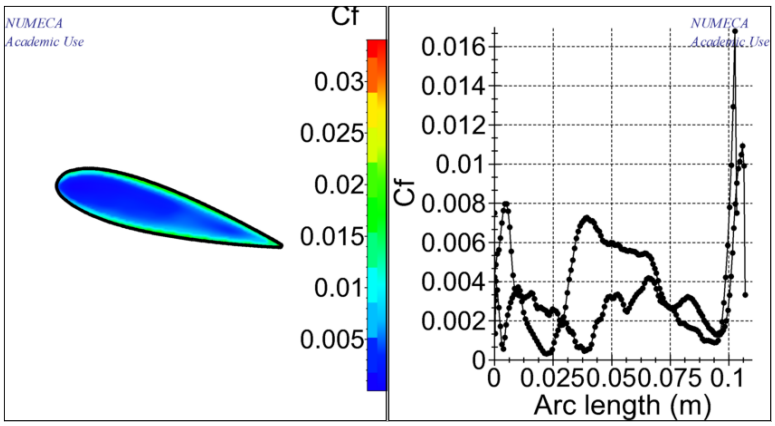

Figure 142. Coefficient Friction Fn 0.1

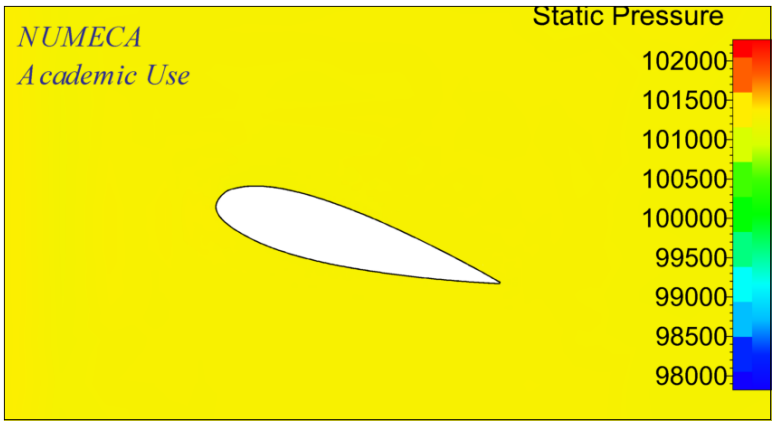

Figure 143. Distribution Static Pressure Fn 0.2

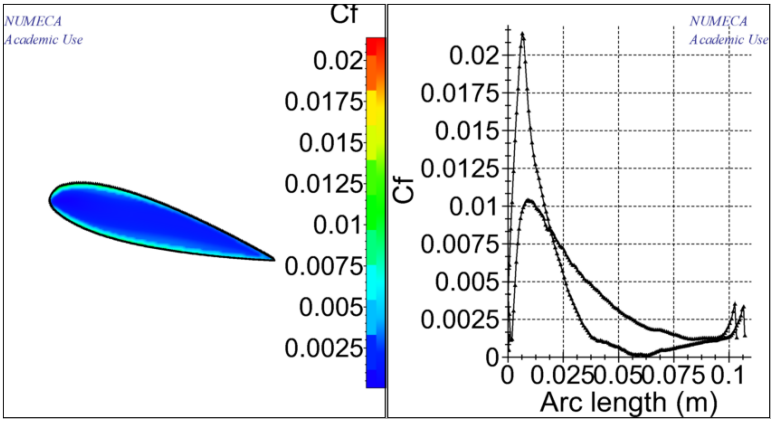

Figure 144. Coefficient Friction Fn 0.2

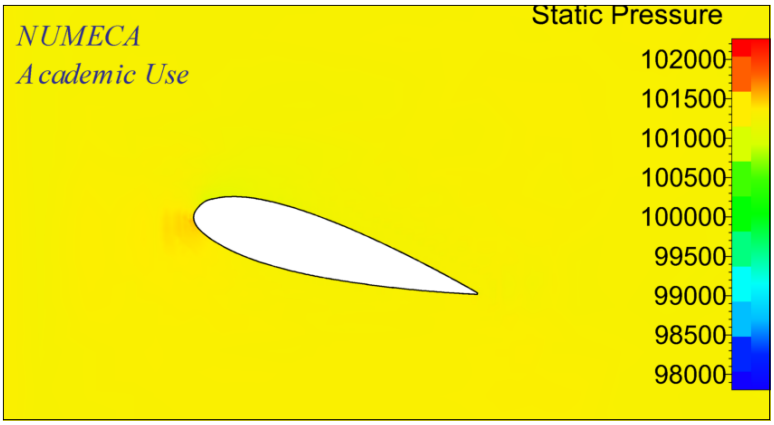

Figure 145. Distribution Static Pressure Fn 0.3

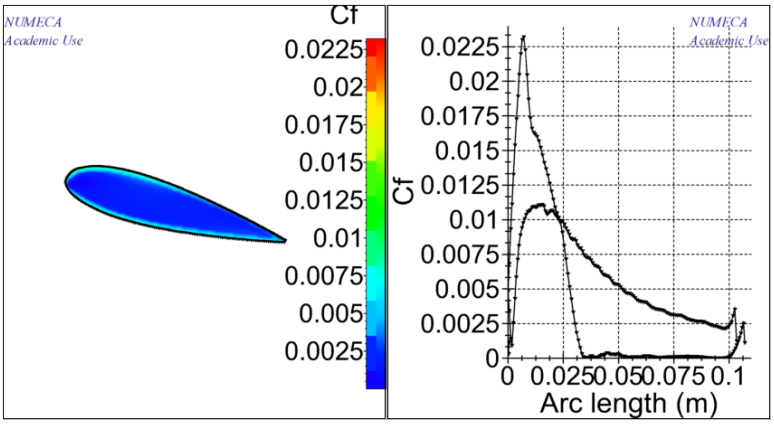

Figure 146. Coefficient Friction Fn 0.3

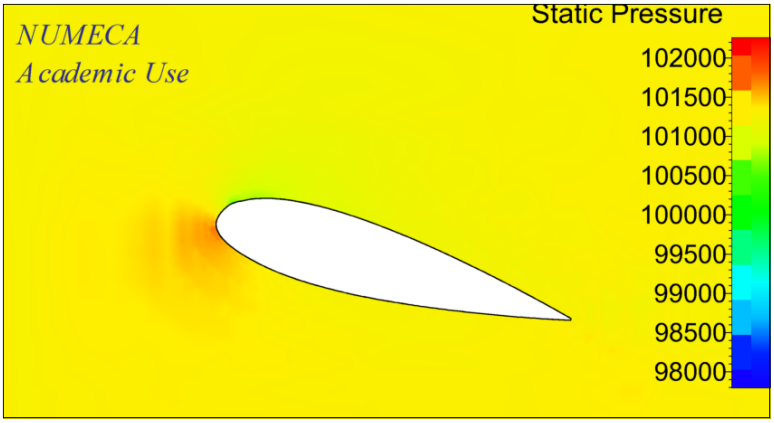

Figure 147. Distribution Static Pressure Fn 0.4

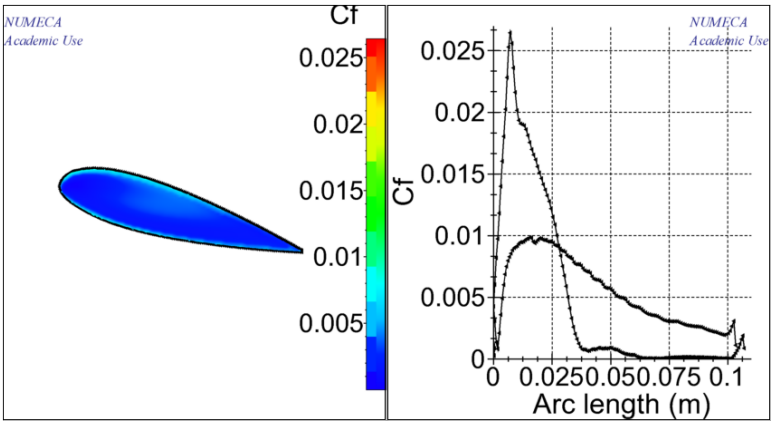

Figure 148. Coefficient Friction Fn 0.4

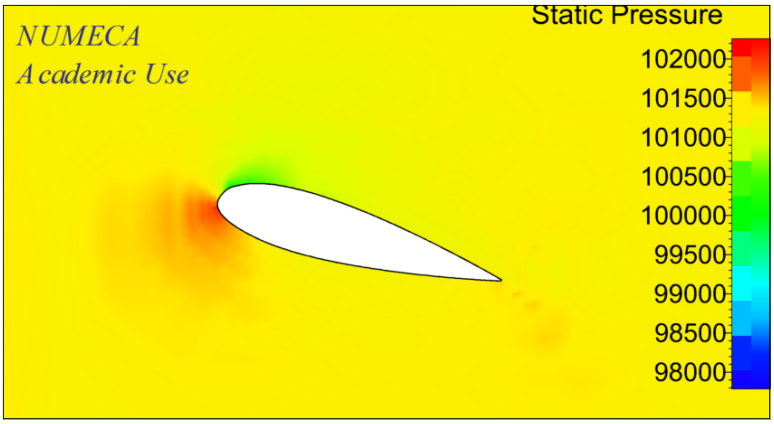

Figure 149. Distribution Static Pressure Fn 0.5

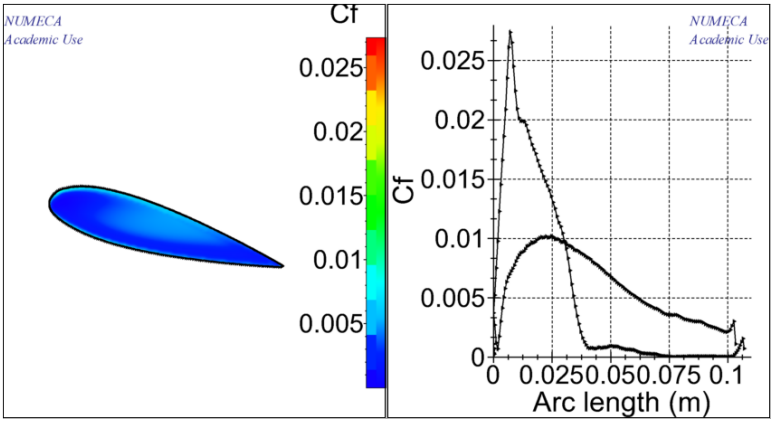

Figure 150. Coefficient Friction Fn 0.5

Lampiran 7. AR 0.05 with angle of attack 20°

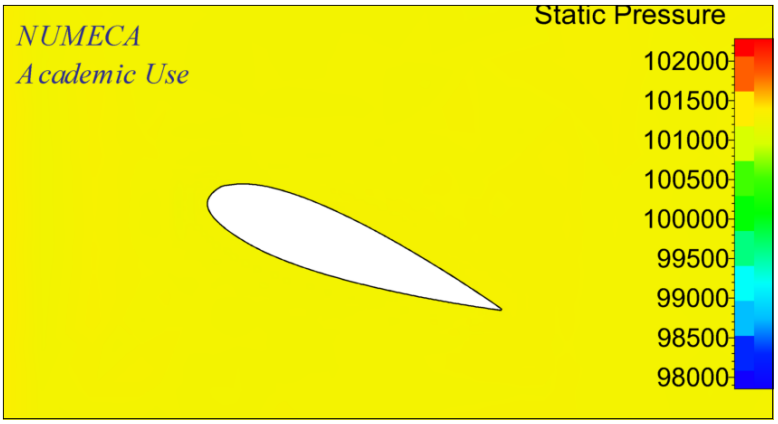

Figure 151. Distribution Static Pressure Fn 0.1

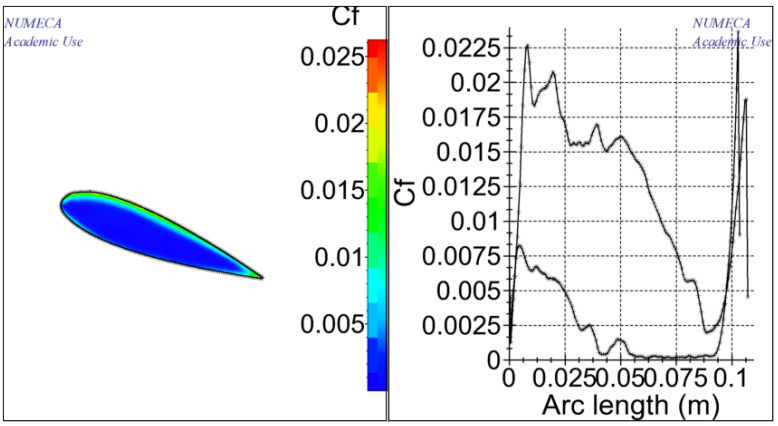

Figure 152. Coefficient Friction Fn 0.1

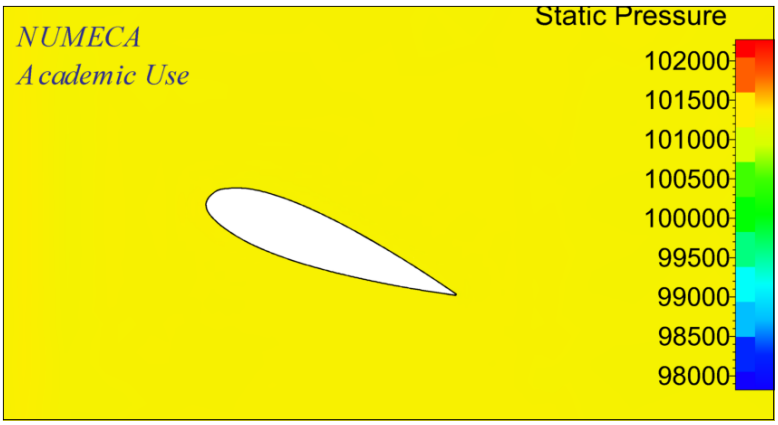

Figure 153. Distribution Static Pressure Fn 0.2

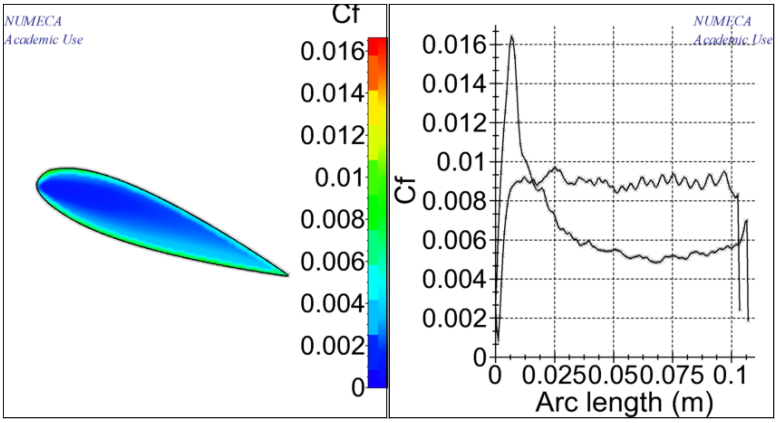

Figure 154. Coefficient Friction Fn 0.2

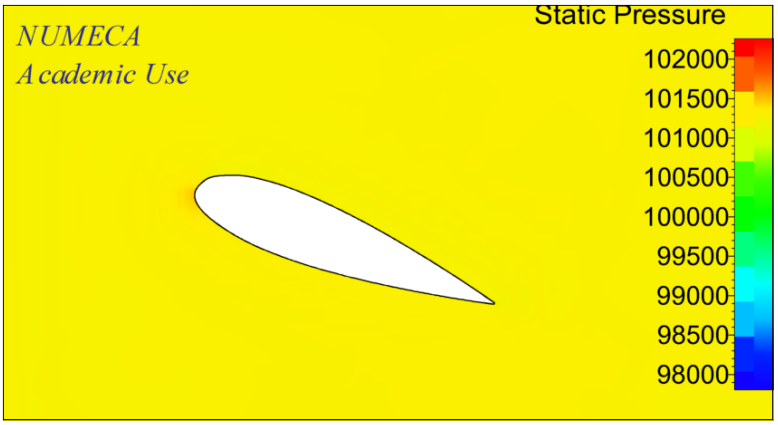

Figure 155. Distribution Static Pressure Fn 0.3

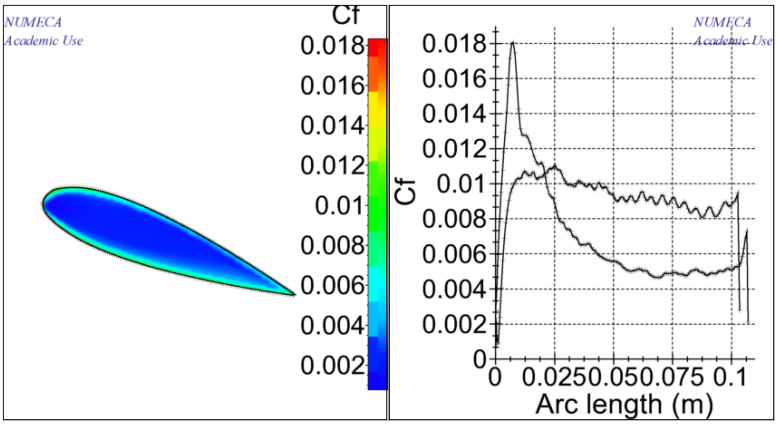

Figure 156. Coefficient Friction Fn 0.3

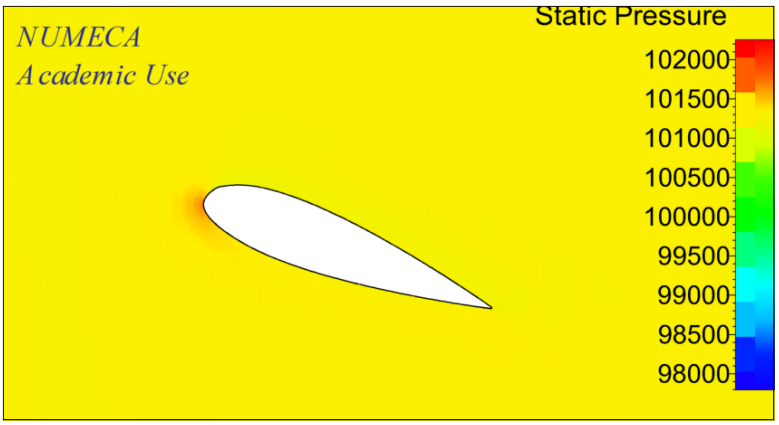

Figure 157. Distribution Static Pressure Fn 0.4

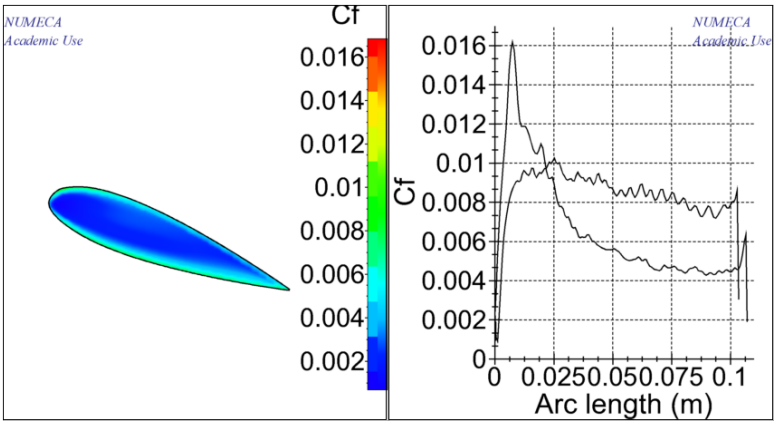

Figure 158. Coefficient Friction Fn 0.4

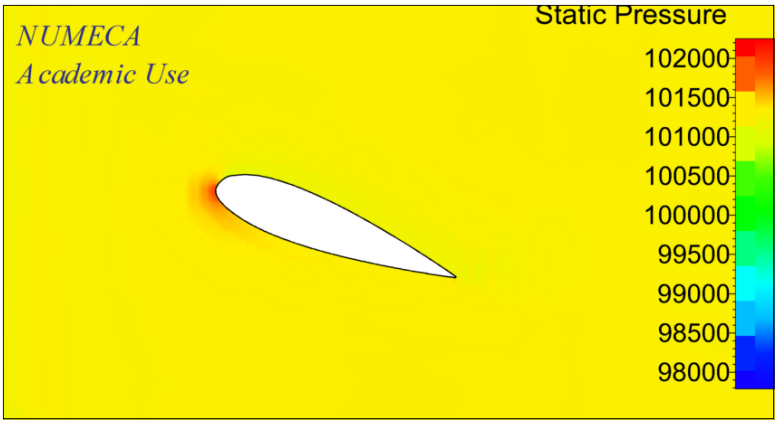

Figure 159. Distribution Static Pressure Fn 0.5

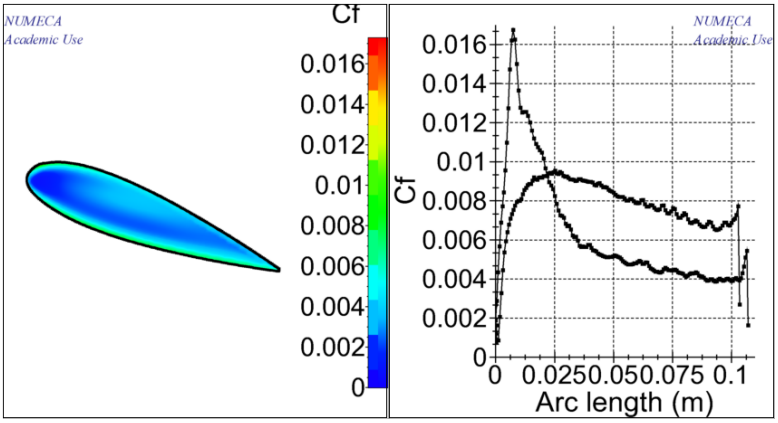

Figure 160. Coefficient Friction Fn 0.5

Lampiran 8. AR 0.25 with angle of attack 20°

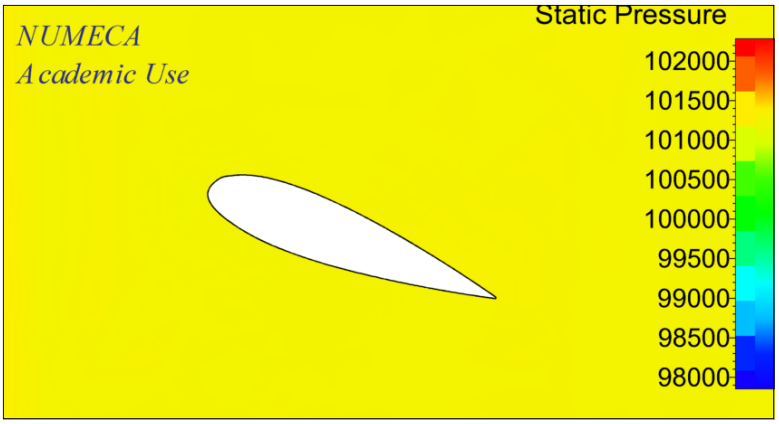

Figure 161. Distribution Static Pressure Fn 0.1

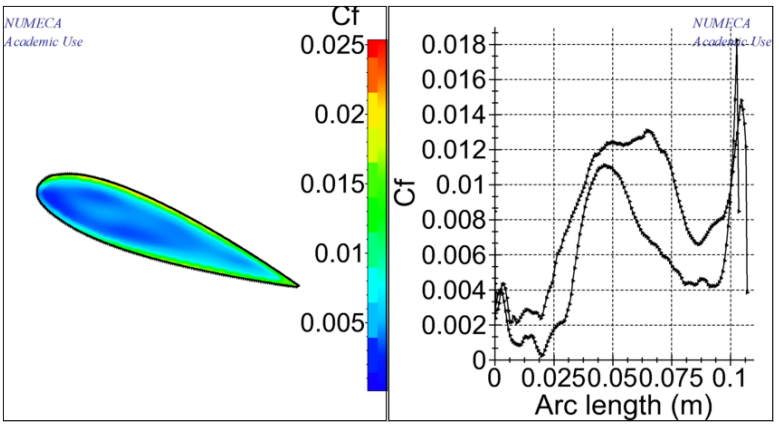

Figure 162. Coefficient Friction Fn 0.1

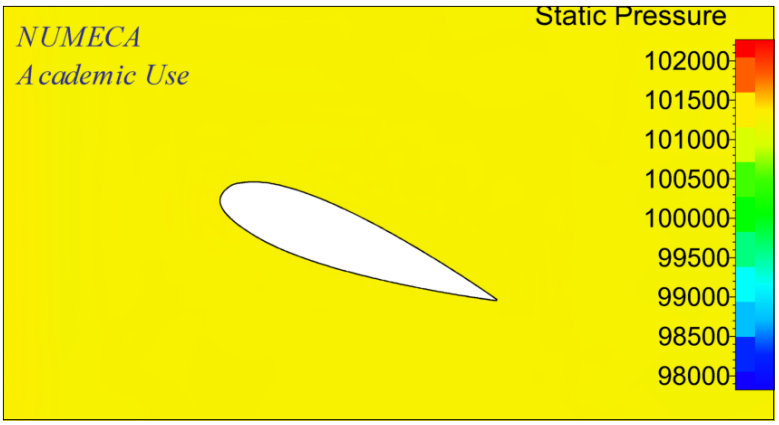

Figure 163. Distribution Static Pressure Fn 0.2

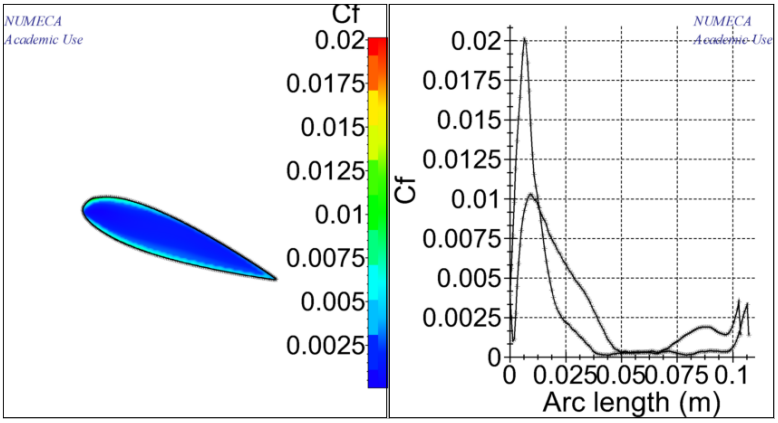

Figure 164. Coefficient Friction Fn 0.2

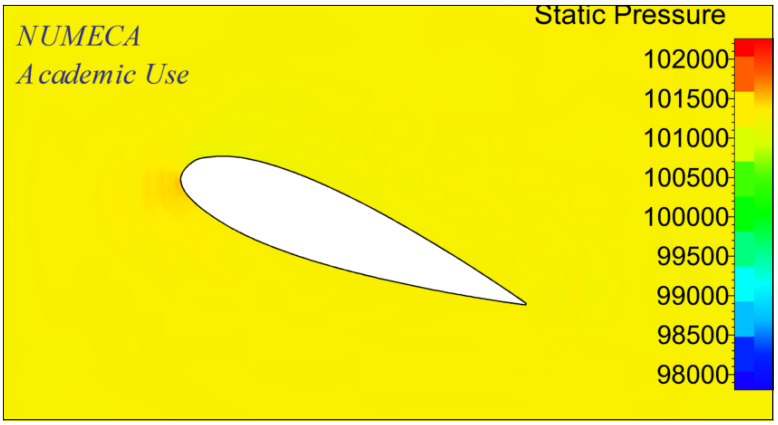

Figure 165. Distribution Static Pressure Fn 0.3

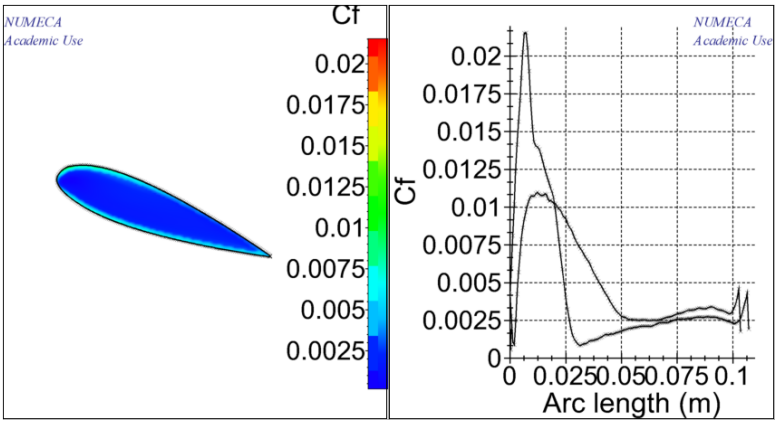

Figure 166. Coefficient Friction Fn 0.3

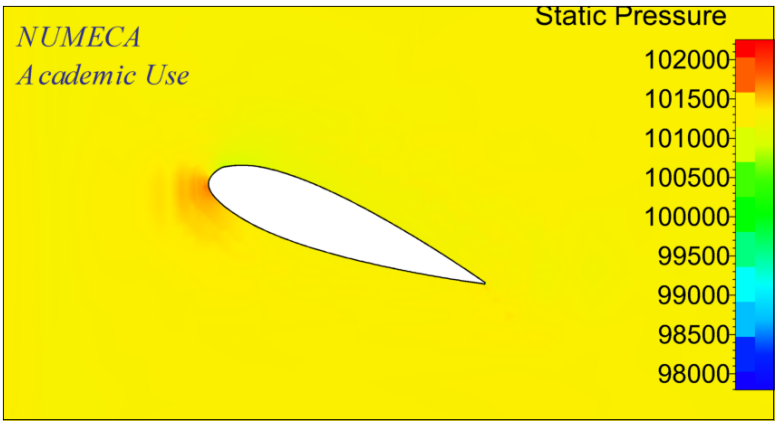

Figure 167. Distribution Static Pressure Fn 0.4

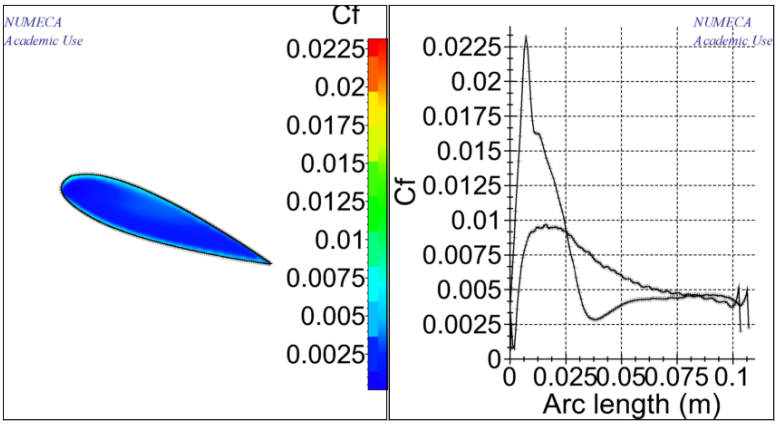

Figure 168. Coefficient Friction Fn 0.4

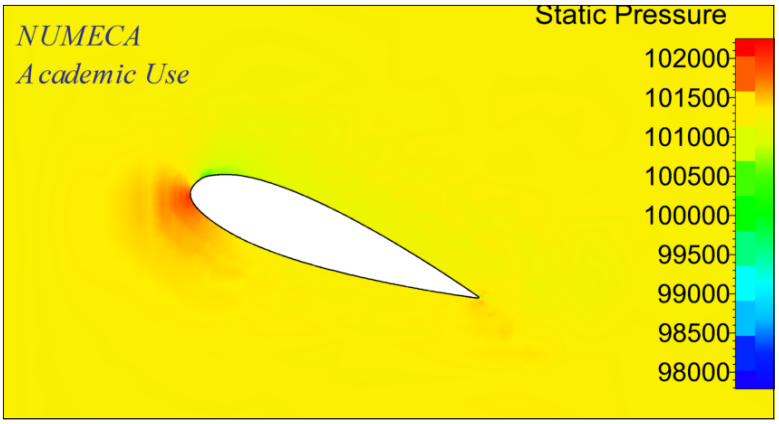

Figure 169. Distribution Static Pressure Fn 0.5

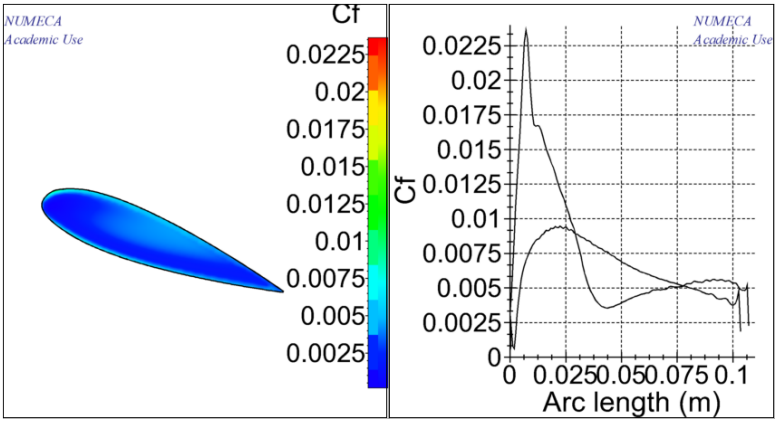

Figure 170. Coefficient Friction Fn 0.5

Lampiran 9. AR 0.45 with angle of attack 20°

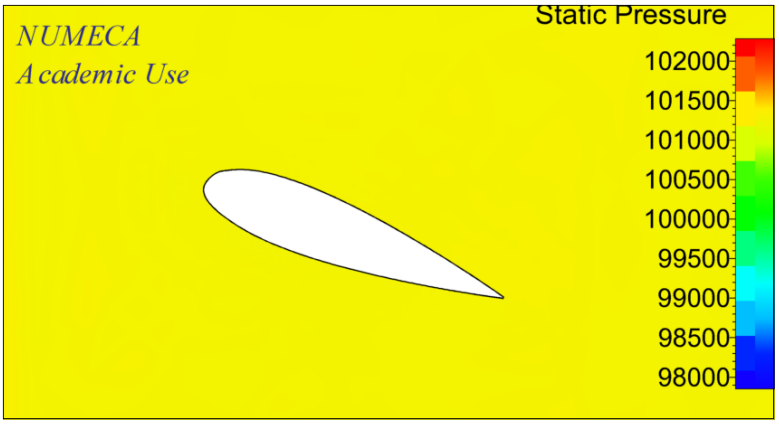

Figure 171. Distribution Static Pressure Fn 0.1

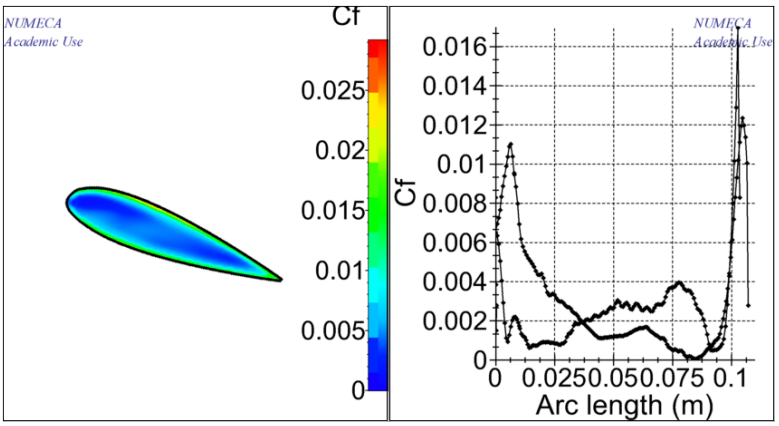

Figure 172. Coefficient Friction Fn 0.1

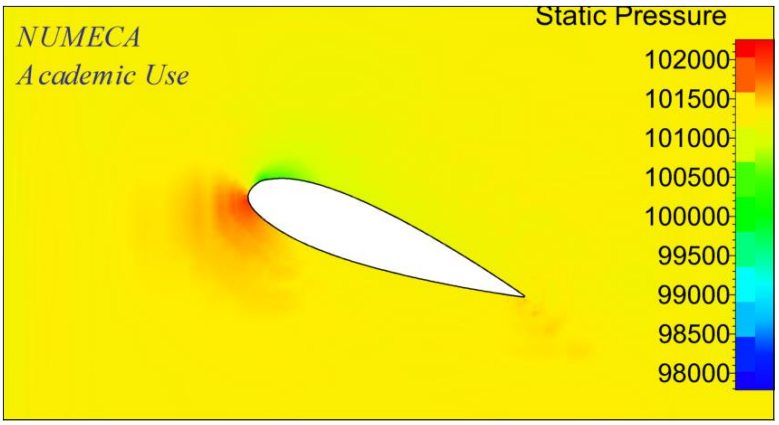

Figure 173. Distribution Static Pressure Fn 0.2

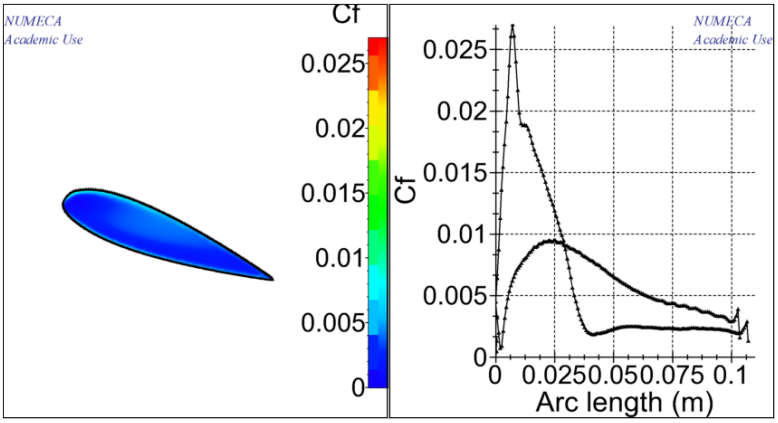

Figure 174. Coefficient Friction Fn 0.2

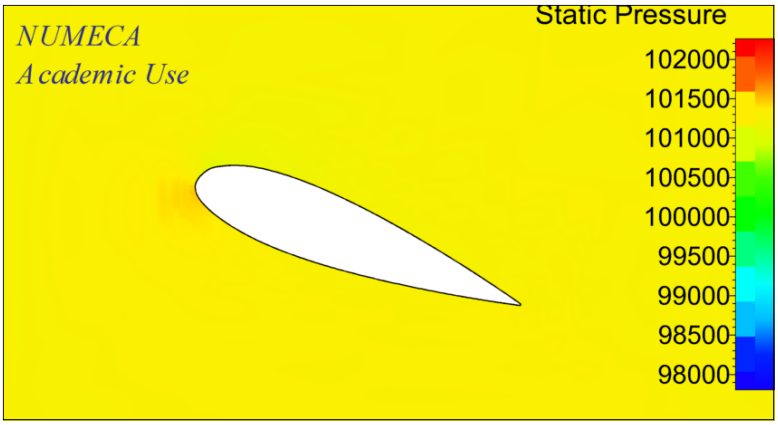

Figure 175. Distribution Static Pressure Fn 0.3

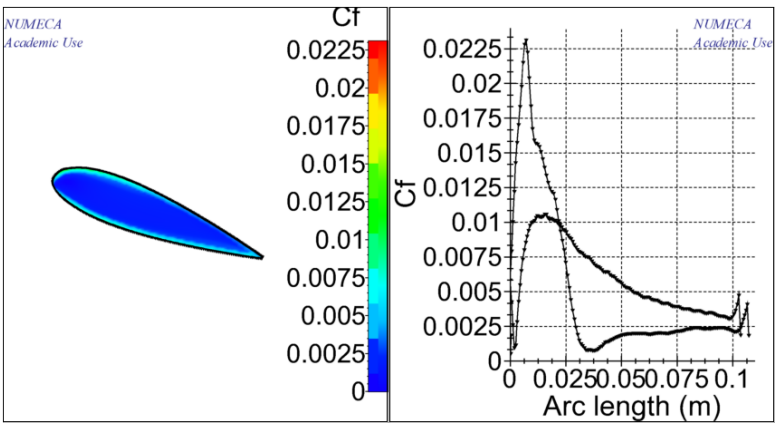

Figure 176. Coefficient Friction Fn 0.3

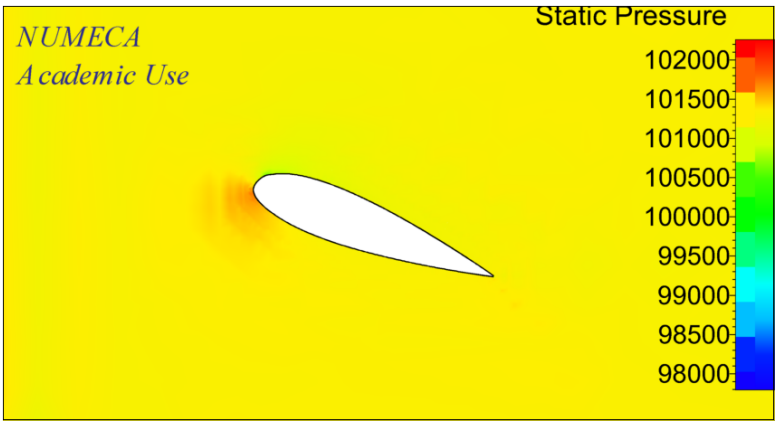

Figure 177. Distribution Static Pressure Fn 0.4

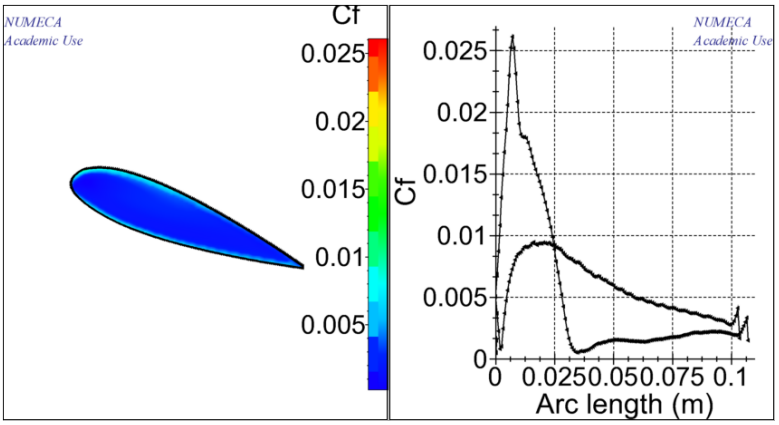

Figure 178. Coefficient Friction Fn 0.4

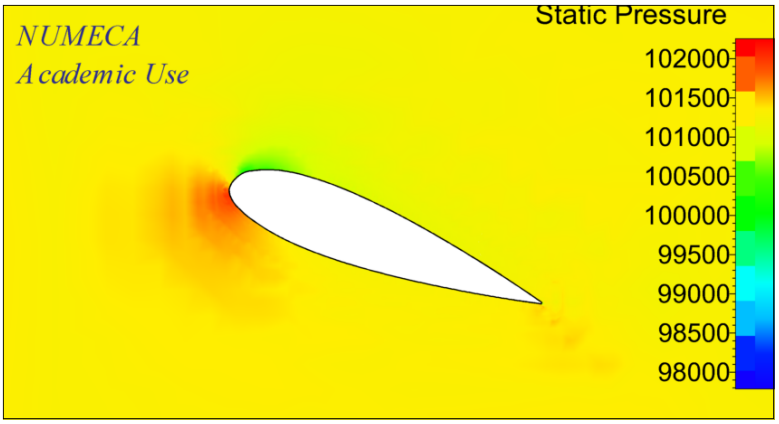

Figure 179. Distribution Static Pressure Fn 0.5

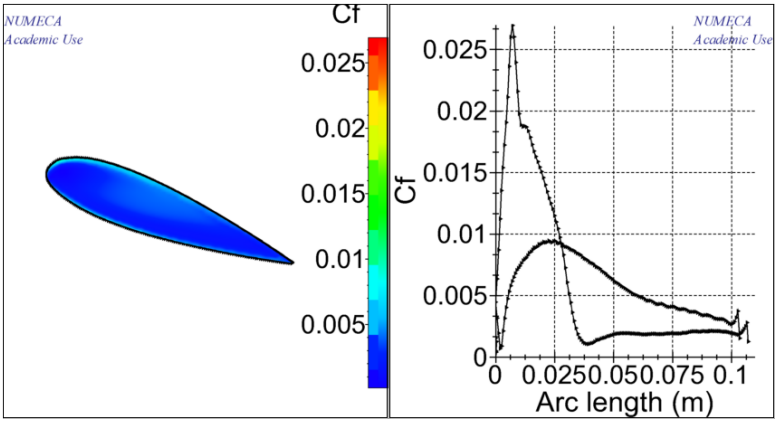

Figure 180. Coefficient Friction Fn 0.5

Lampiran 10. AR 0.65 with angle of attack 20°

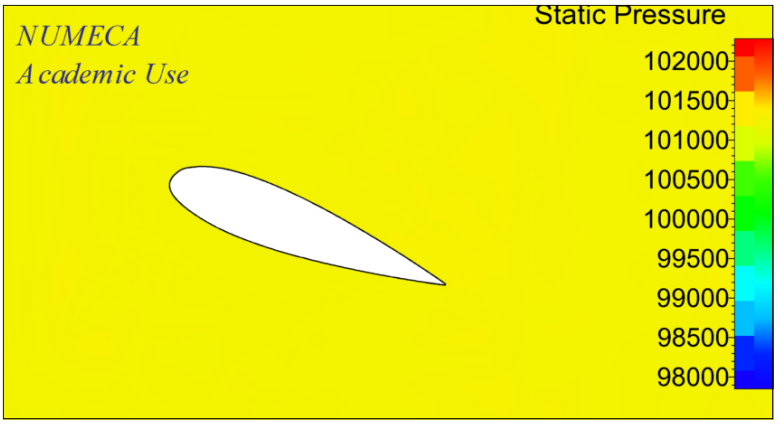

Figure 181. Distribution Static Pressure Fn 0.1

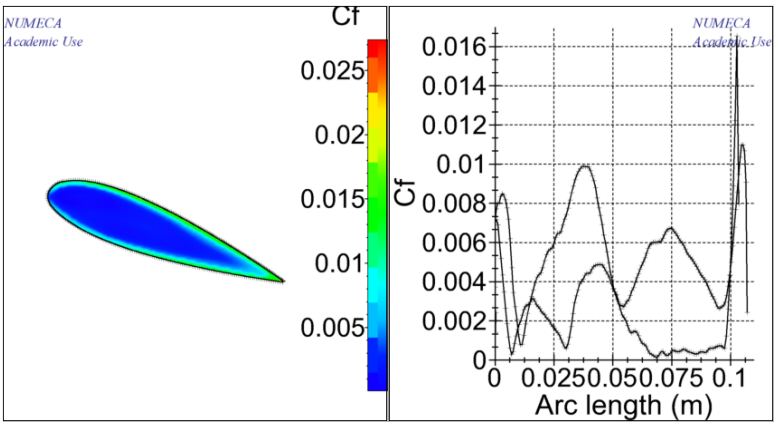

Figure 182. Coefficient Friction Fn 0.1

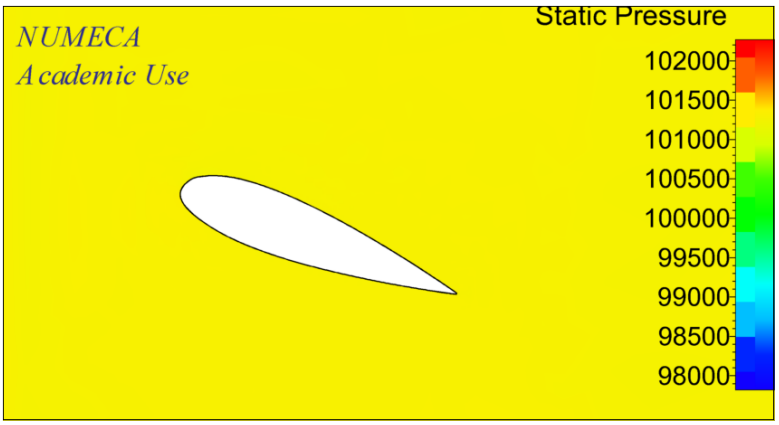

Figure 183. Distribution Static Pressure Fn 0.2

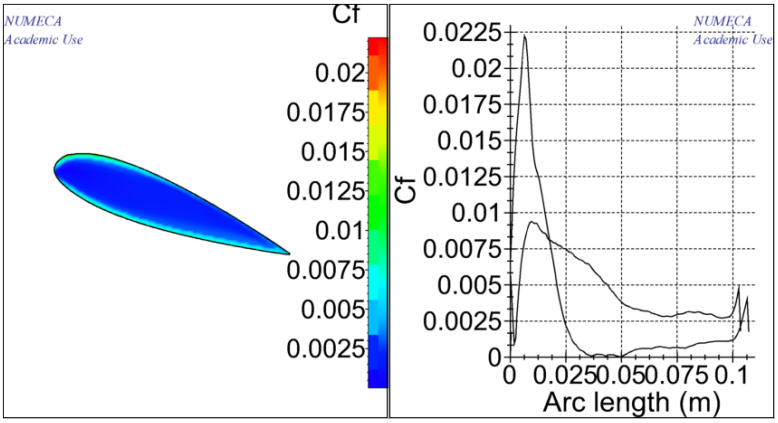

Figure 184. Coefficient Friction Fn 0.2

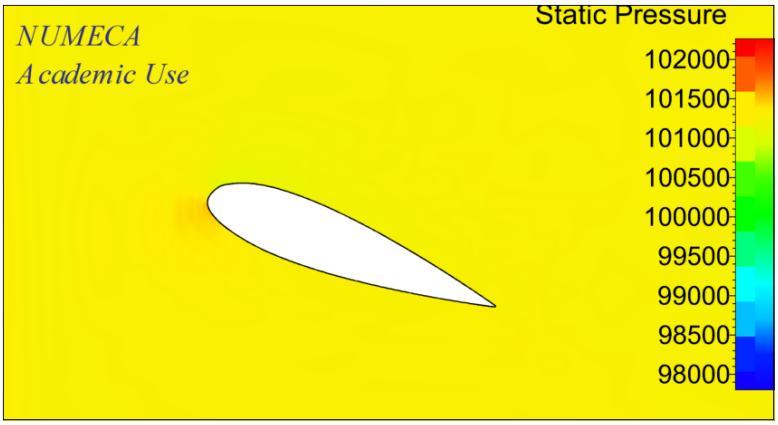

Figure 185. Distribution Static Pressure Fn 0.3

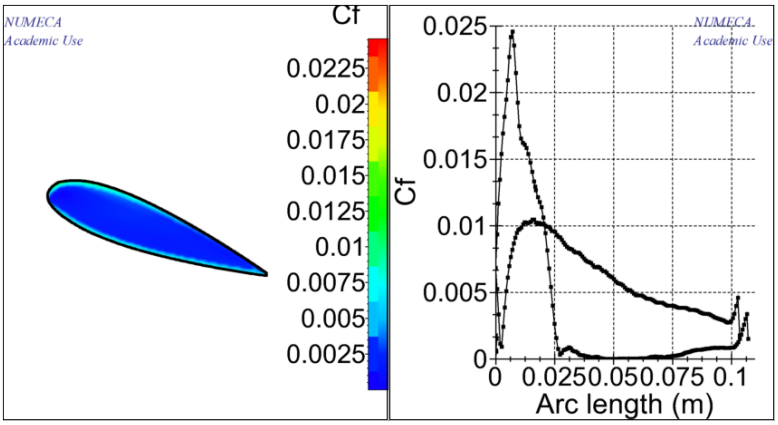

Figure 186. Coefficient Friction Fn 0.3

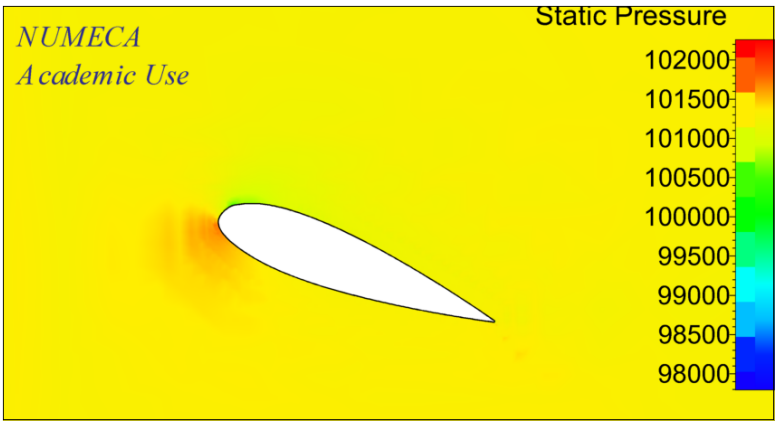

Figure 187. Distribution Static Pressure Fn 0.4

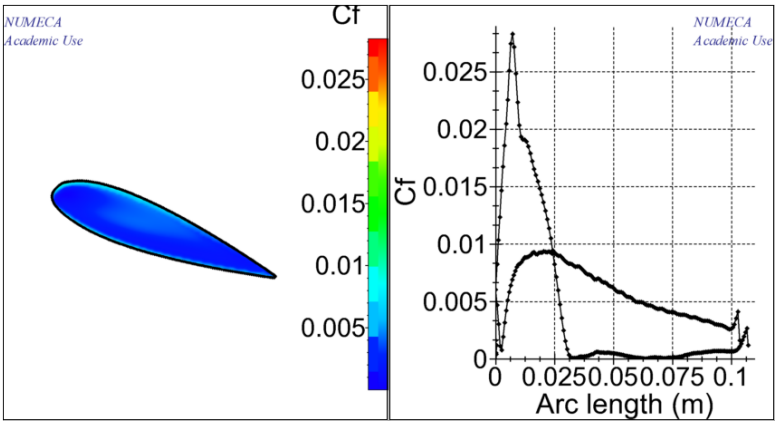

Figure 188. Coefficient Friction Fn 0.4

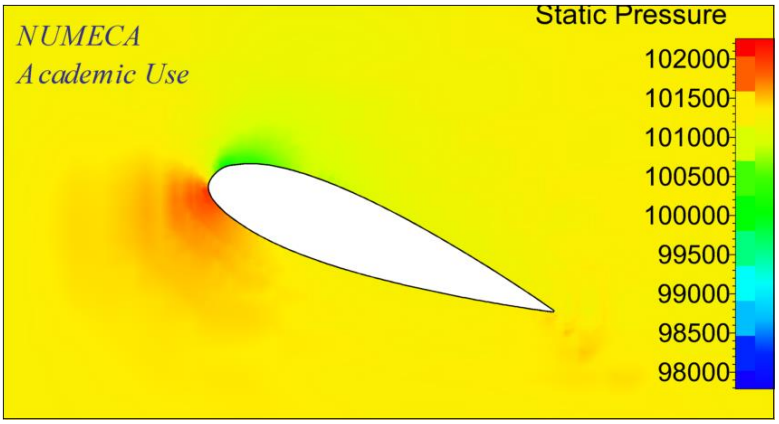

Figure 189. Distribution Static Pressure Fn 0.5

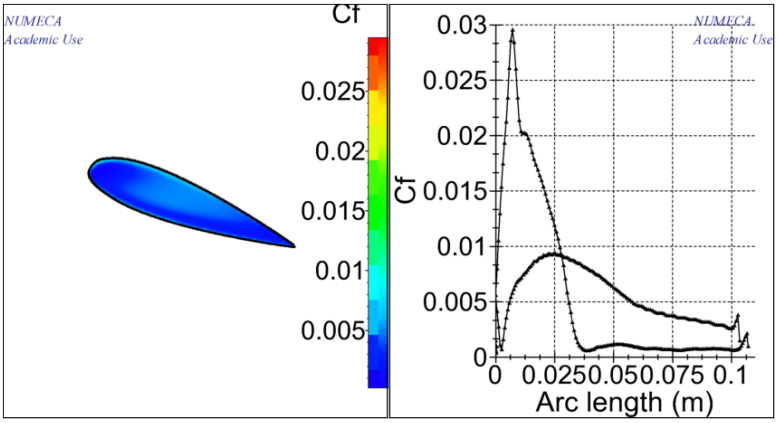

Figure 190. Coefficient Friction Fn 0.5

Lampiran 11. AR 0.85 with angle of attack 20°

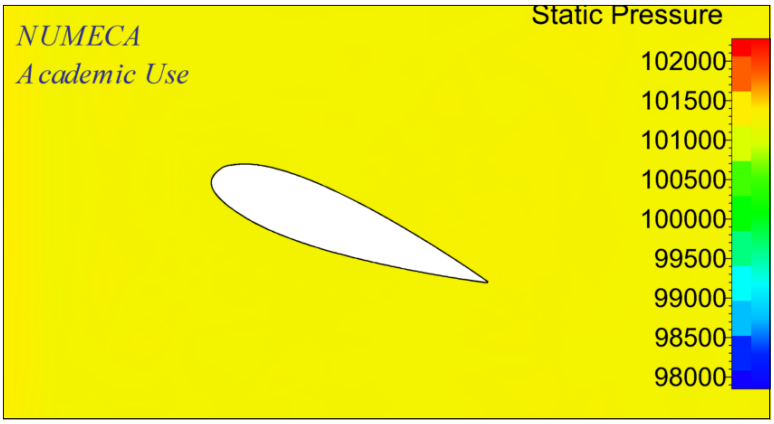

Figure 191. Distribution Static Pressure Fn 0.1

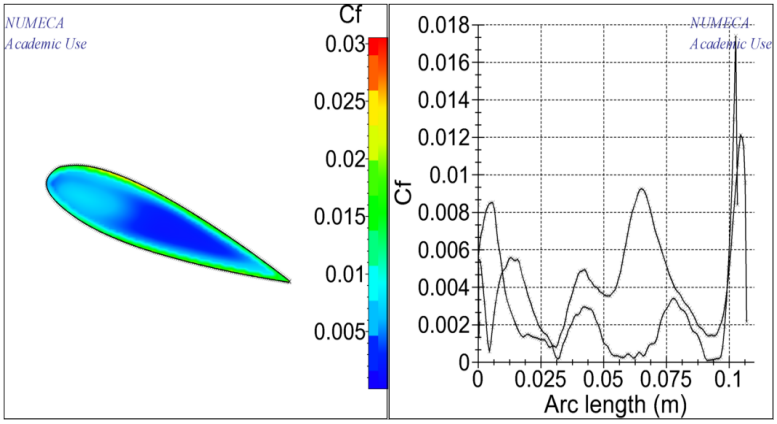

Figure 192. Coefficient Friction Fn 0.1

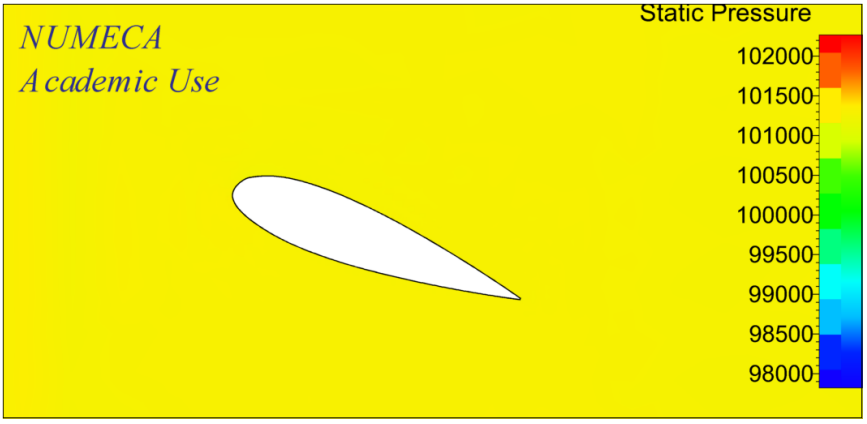

Figure 193. Distribution Static Pressure Fn 0.2

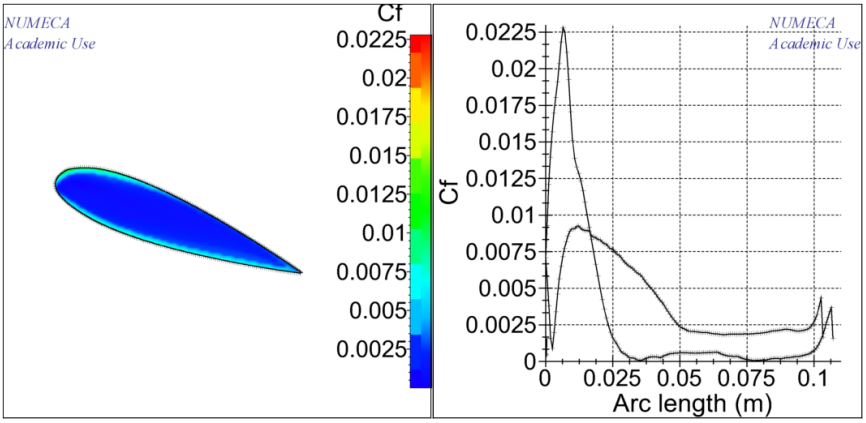

Figure 194. Coefficient Friction Fn 0.2

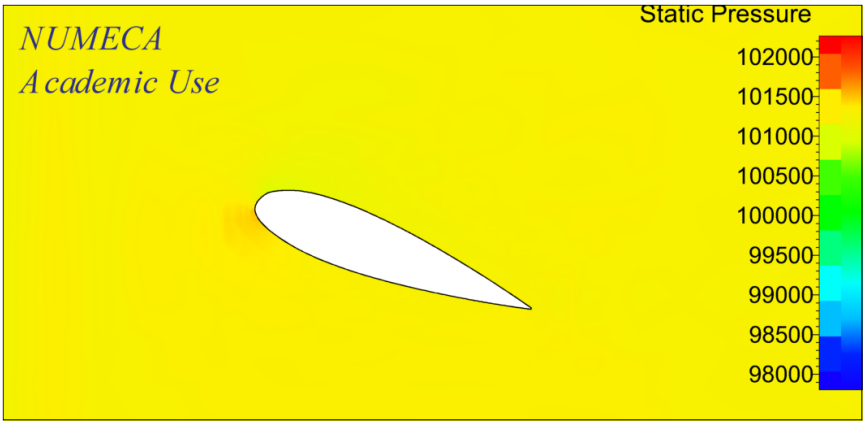

Figure 195. Distribution Static Pressure Fn 0.3

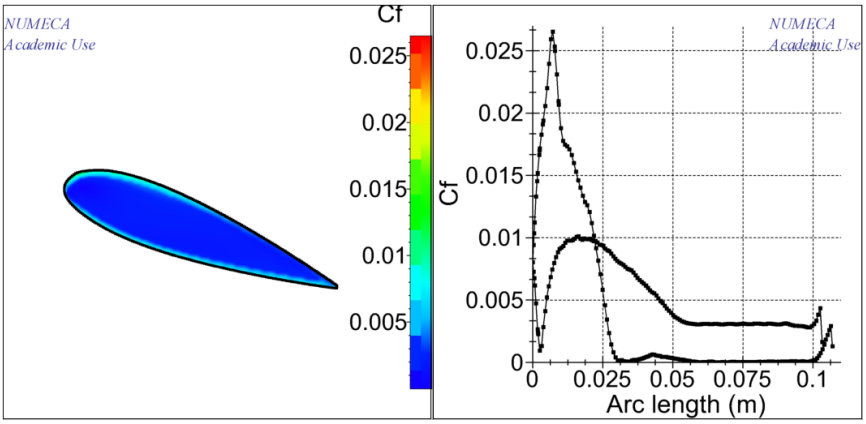

Figure 196. Coefficient Friction Fn 0.3

Figure 197. Distribution Static Pressure Fn 0.4

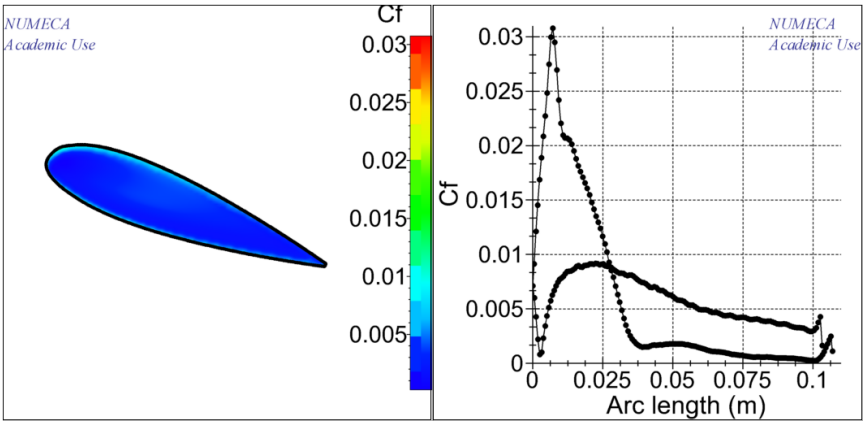

Figure 198. Coefficient Friction Fn 0.4

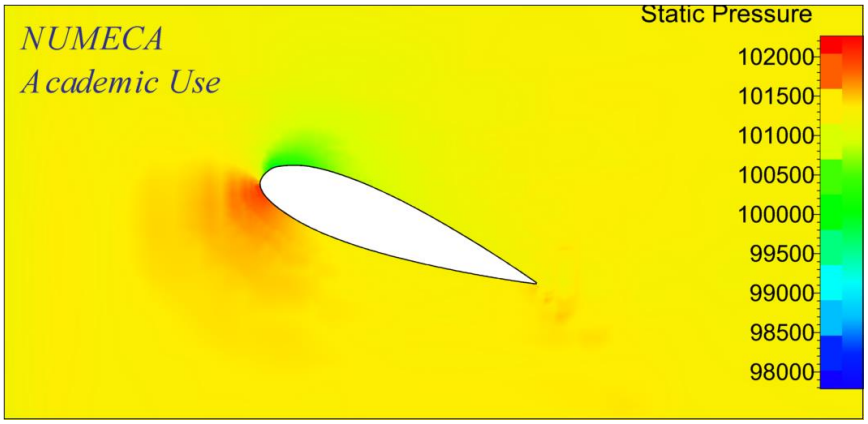

Figure 199. Distribution Static Pressure Fn 0.5

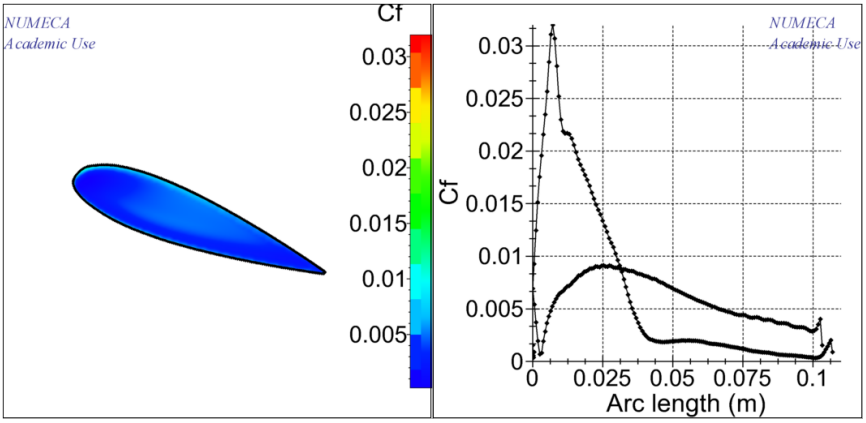

Figure 200. Coefficient Friction Fn 0.5

Attachment 210. AR 0.05 with angle of attack 25°

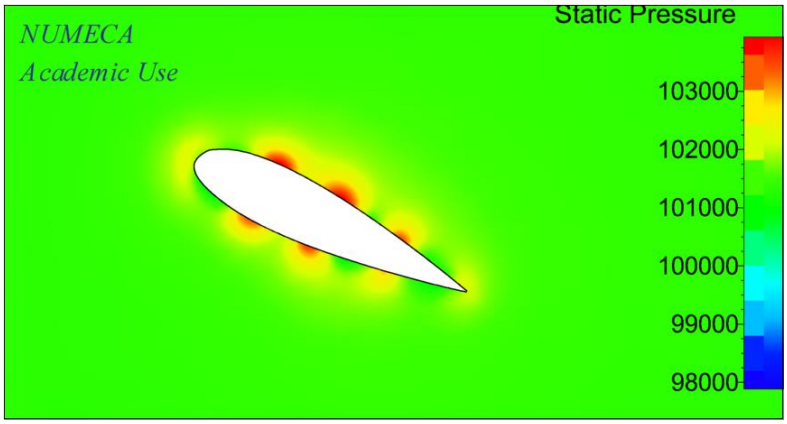

Figure 201. Distribution Static Pressure Fn 0.1

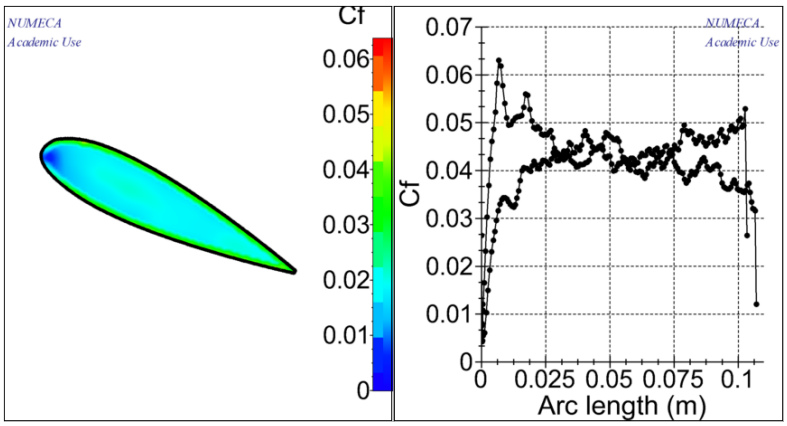

Figure 202. Coefficient Friction Fn 0.1

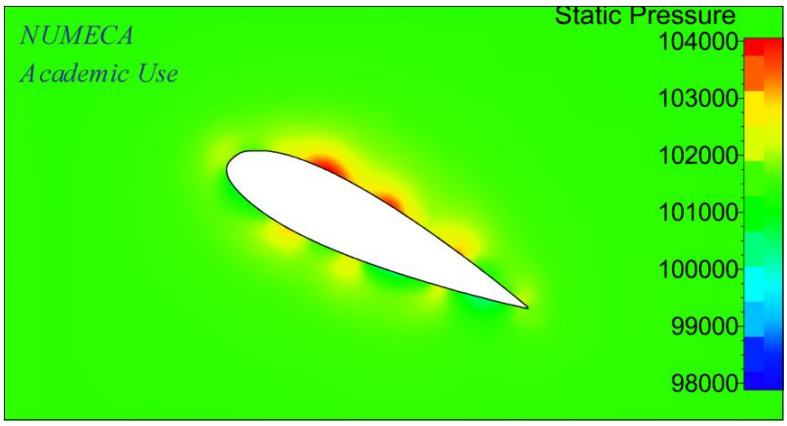

Figure 203. Distribution Static Pressure Fn 0.2

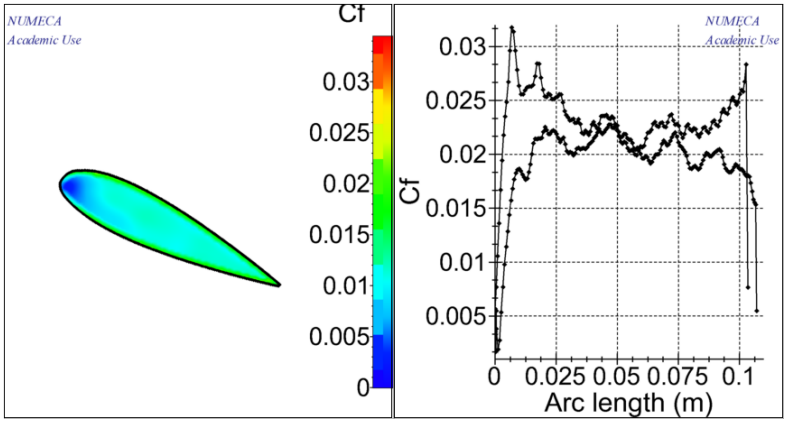

Figure 204. Coefficient Friction Fn 0.2

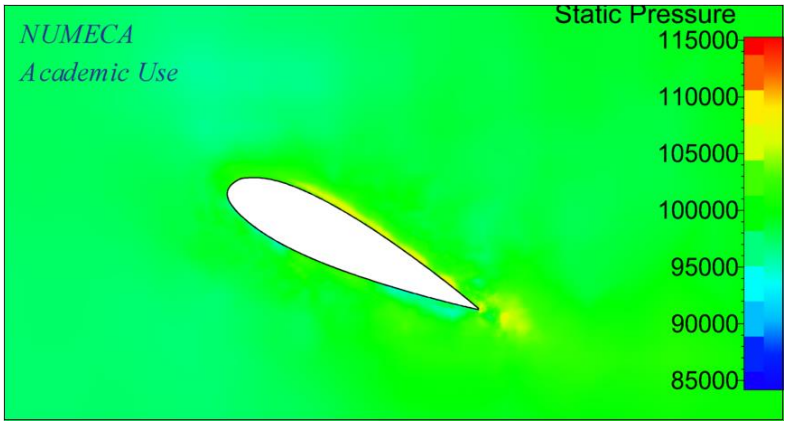

Figure 205. Distribution Static Pressure Fn 0.3

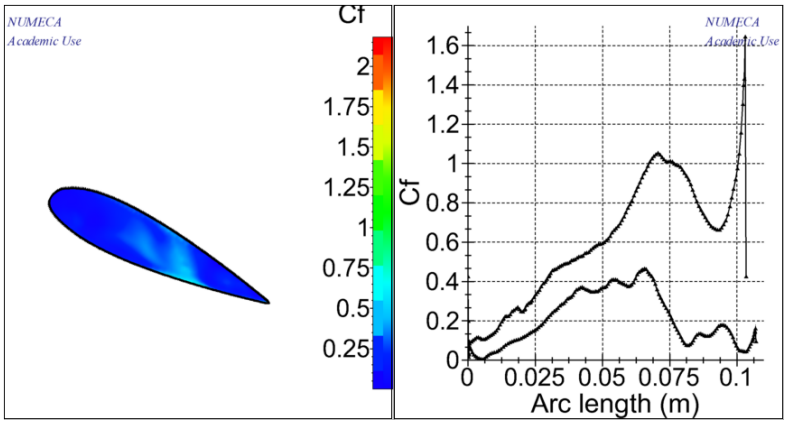

Figure 206. Coefficient Friction Fn 0.3

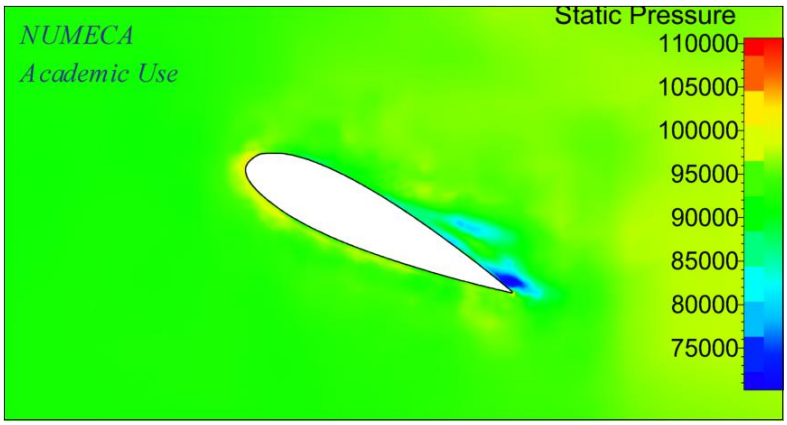

Figure 207. Distribution Static Pressure Fn 0.4

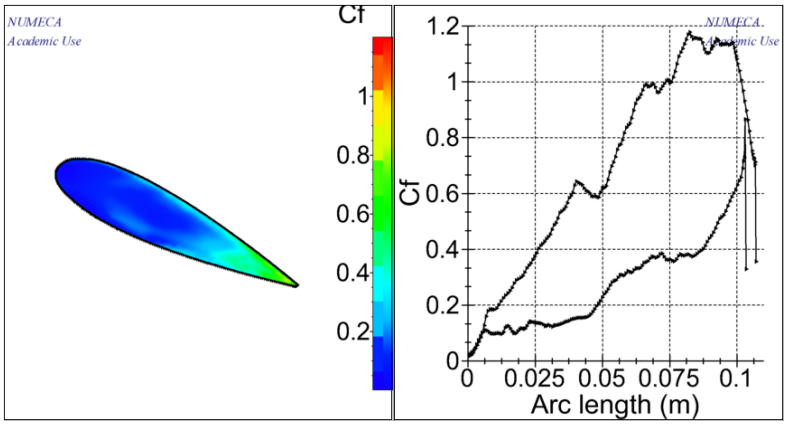

Figure 208. Coefficient Friction Fn 0.4

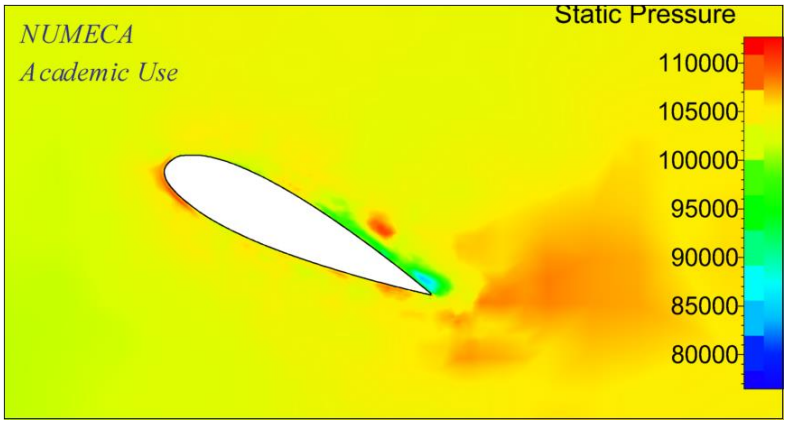

Figure 209. Distribution Static Pressure Fn 0.5

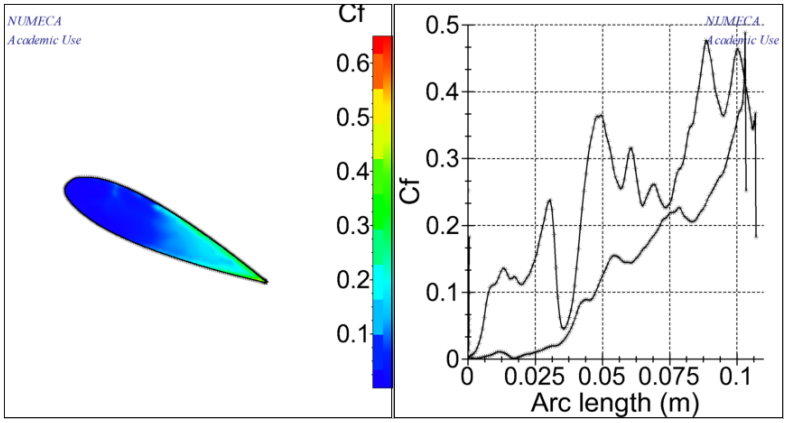

Figure 210. Coefficient Friction Fn 0.5

Attachment 211. AR 0.25 with angle of attack 25°

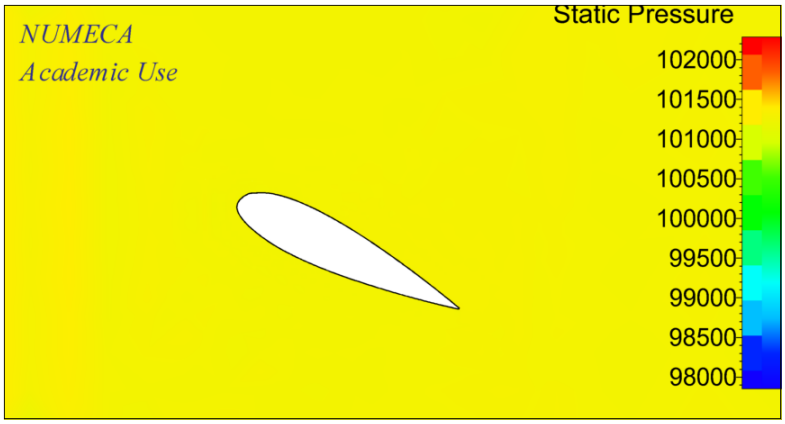

Figure 211. Distribution Static Pressure Fn 0.1

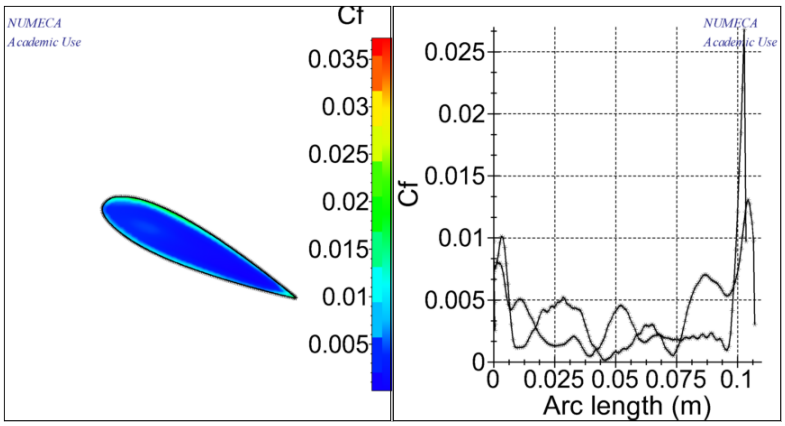

Figure 212. Coefficient Friction Fn 0.1

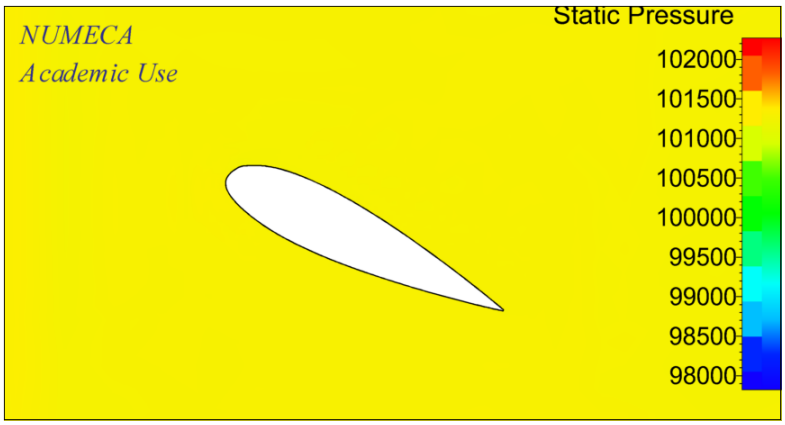

Figure 213. Distribution Static Pressure Fn 0.2

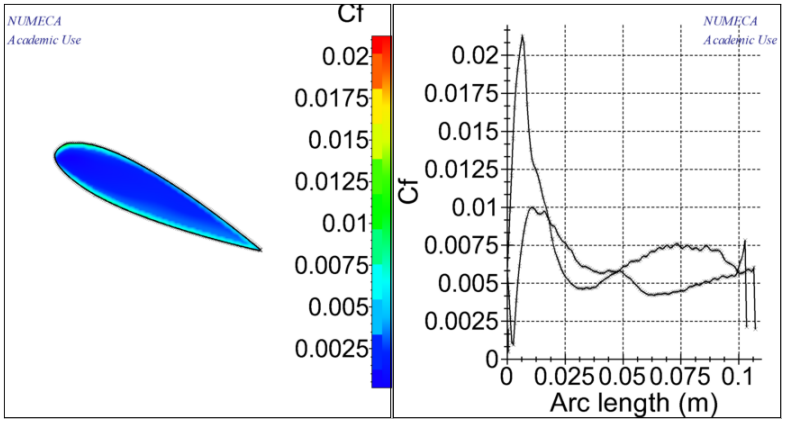

Figure 214. Coefficient Friction Fn 0.2

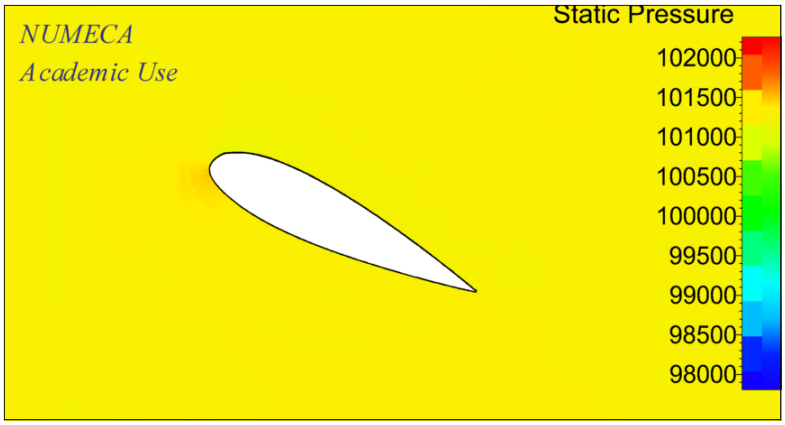

Figure 215. Distribution Static Pressure Fn 0.3

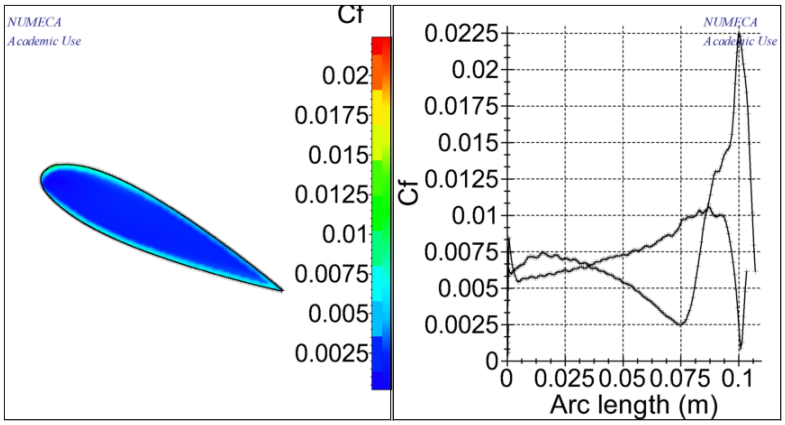

Figure 216. Coefficient Friction Fn 0.3

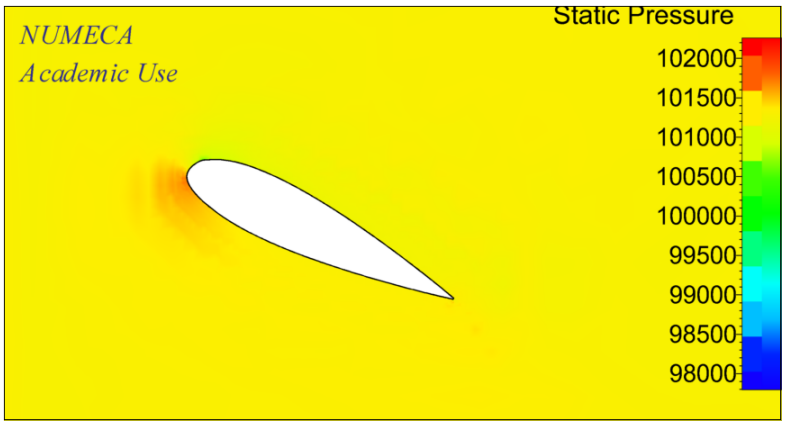

Figure 217. Distribution Static Pressure Fn 0.4

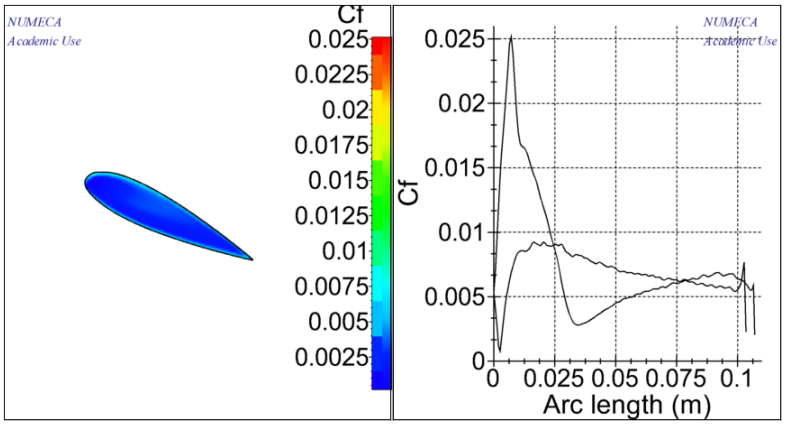

Figure 218. Coefficient Friction Fn 0.4

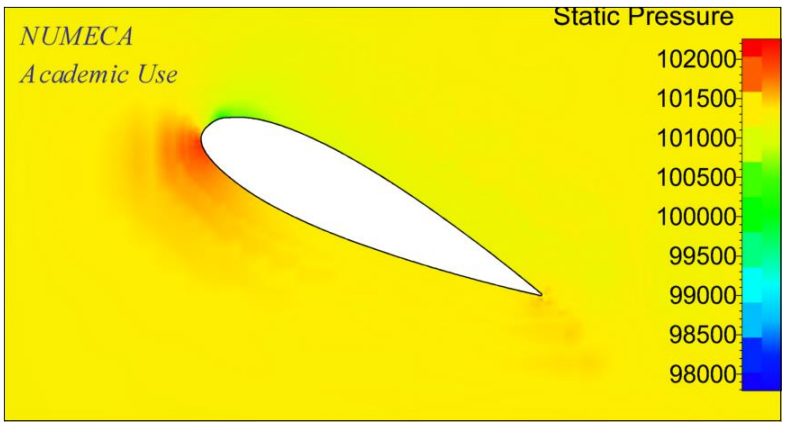

Figure 219. Distribution Static Pressure Fn 0.5

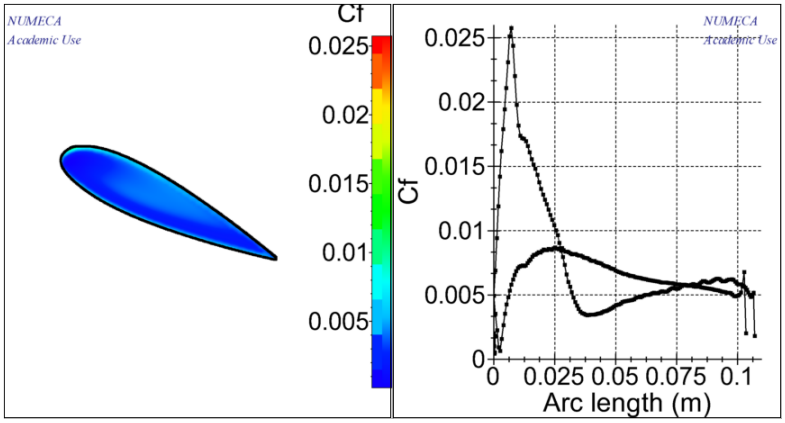

Figure 220. Coefficient Friction Fn 0.5

Attachment 212. AR 0.45 with angle of attack 25°

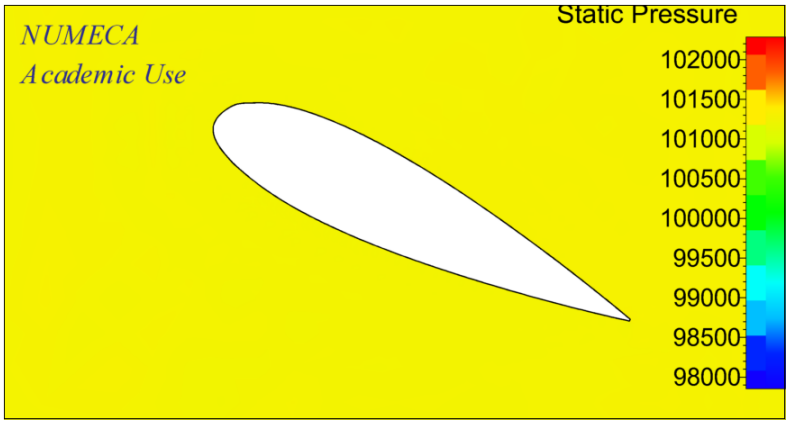

Figure 221. Distribution Static Pressure Fn 0.1

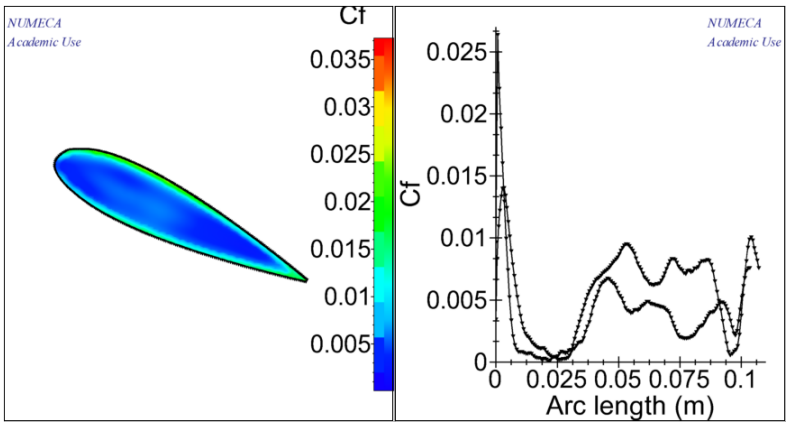

Figure 222. Coefficient Friction Fn 0.1

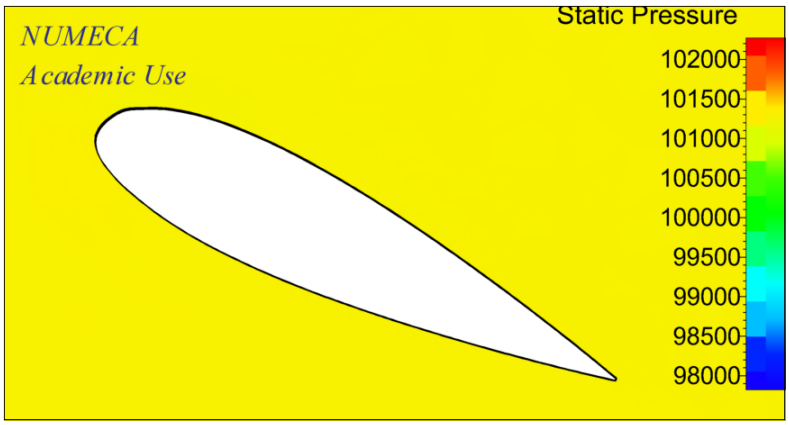

Figure 223. Distribution Static Pressure Fn 0.2

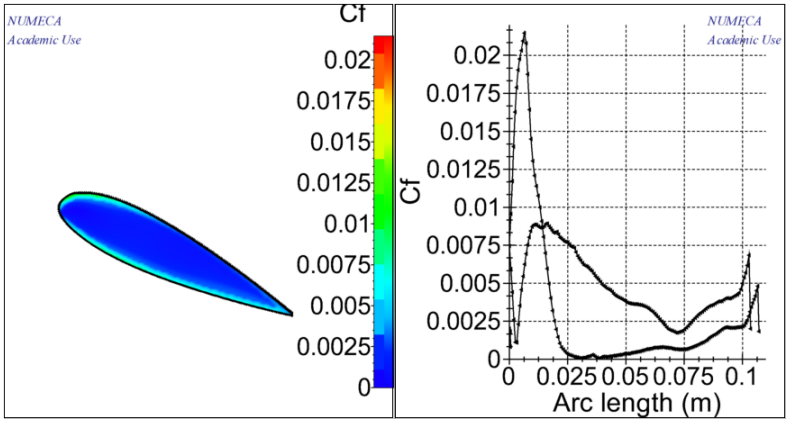

Figure 224. Coefficient Friction Fn 0.2

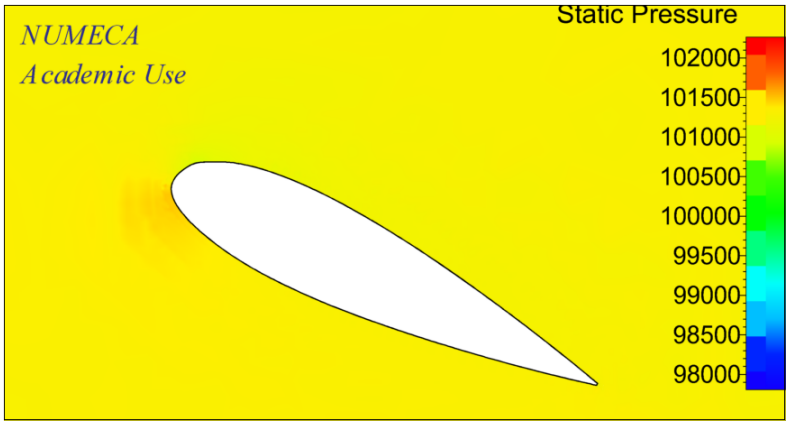

Figure 225. Distribution Static Pressure Fn 0.3

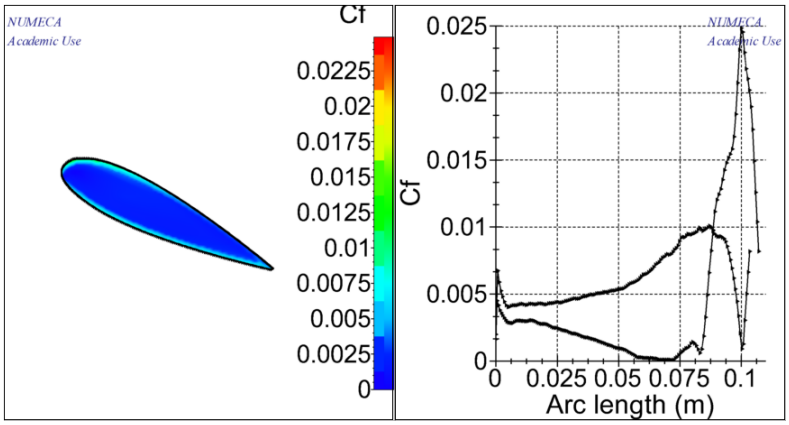

Figure 226. Coefficient Friction Fn 0.3

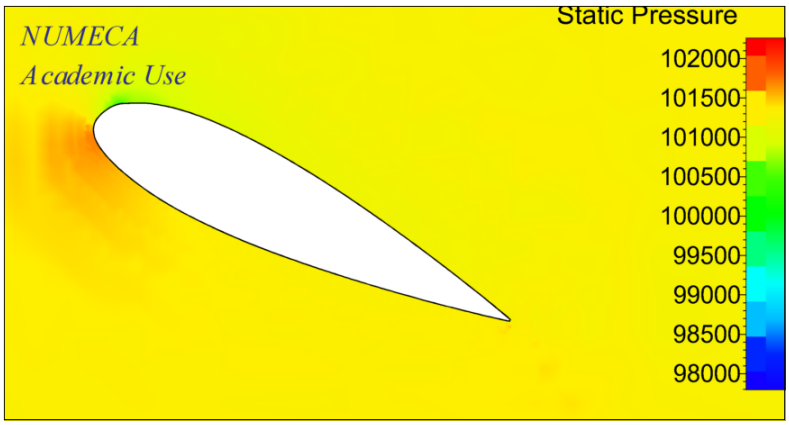

Figure 227. Distribution Static Pressure Fn 0.4

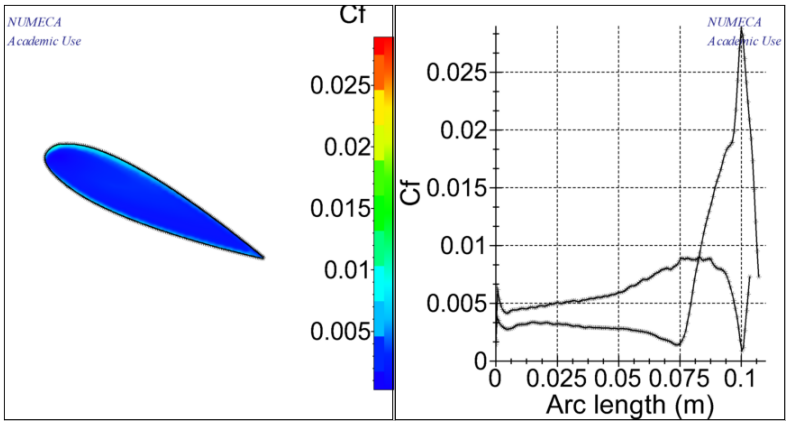

Figure 228. Coefficient Friction Fn 0.4

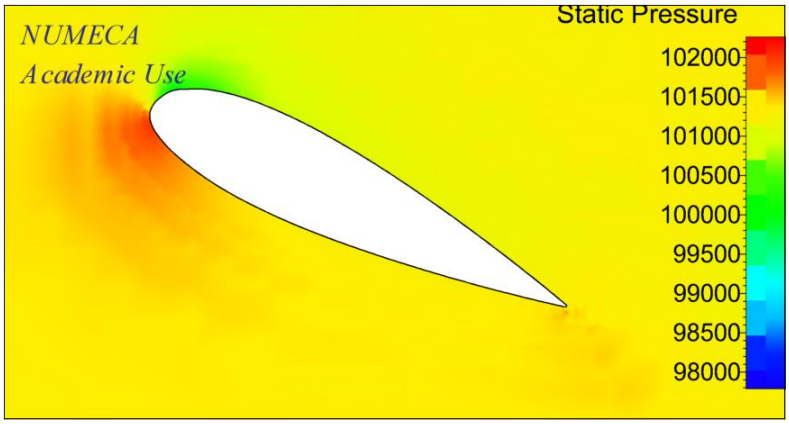

Figure 229. Distribution Static Pressure Fn 0.5

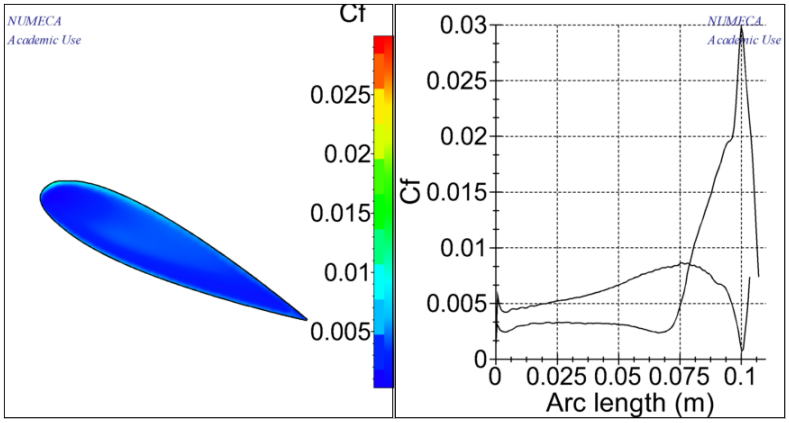

Figure 230. Coefficient Friction Fn 0.5

Attachment 213. AR 0.65 with angle of attack 25°

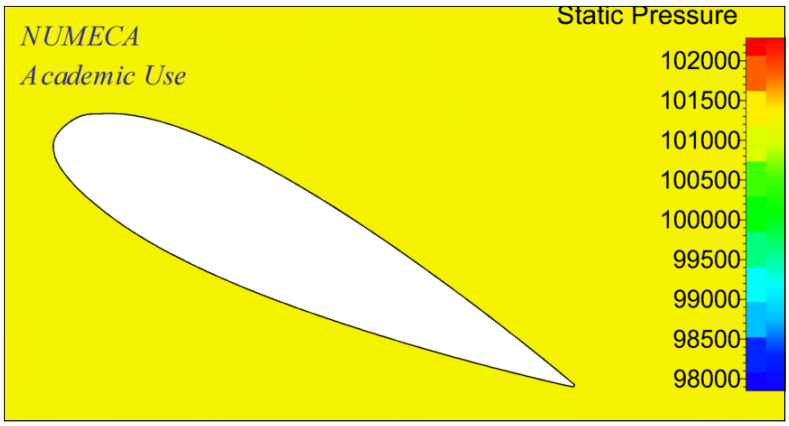

Figure 231. Distribution Static Pressure Fn 0.1

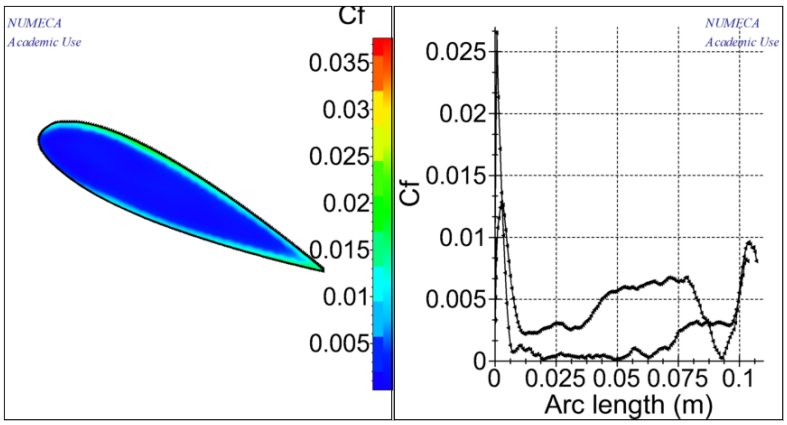

Figure 232. Coefficient Friction Fn 0.1

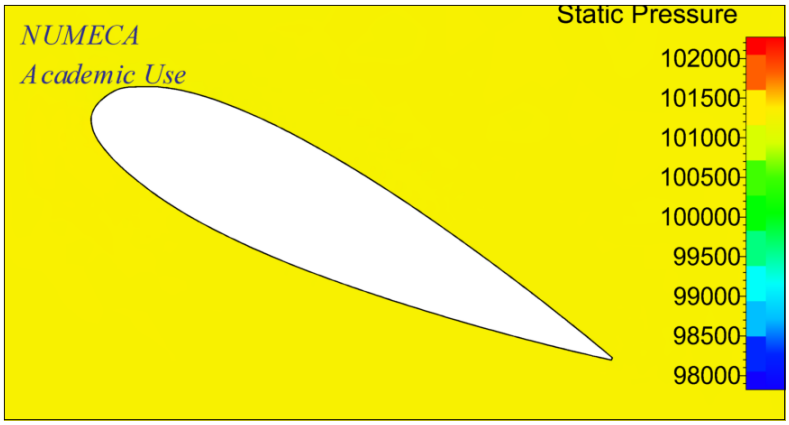

Figure 233. Distribution Static Pressure Fn 0.2

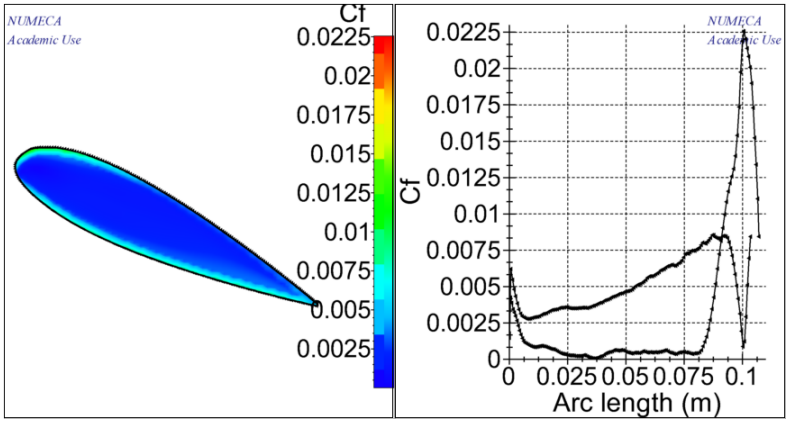

Figure 234. Coefficient Friction Fn 0.2

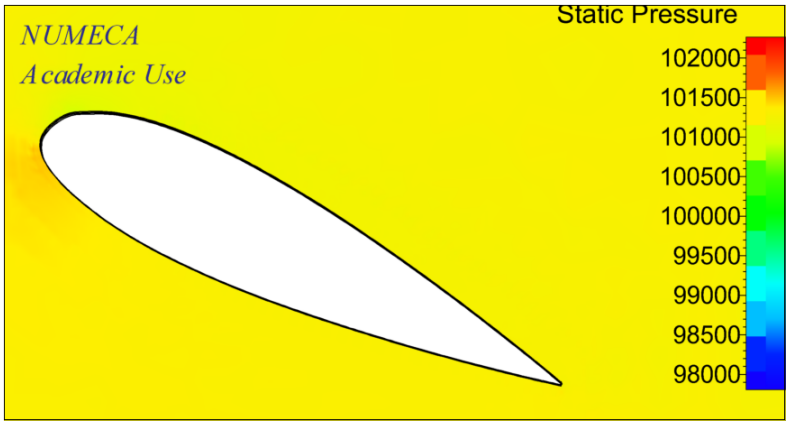

Figure 235. Distribution Static Pressure Fn 0.3

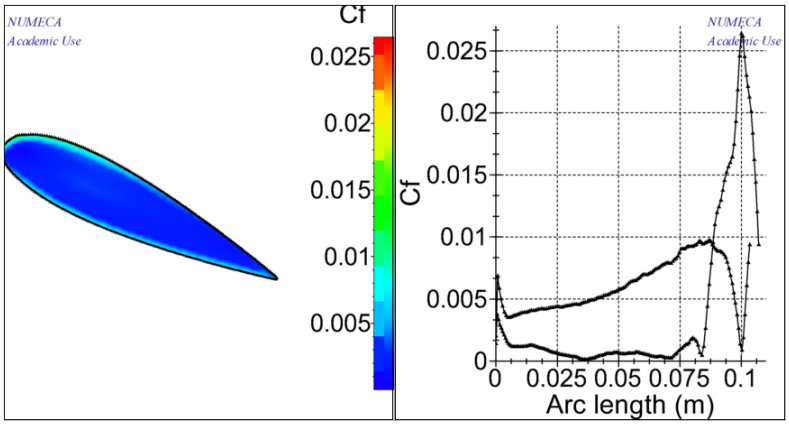

Figure 236. Coefficient Friction Fn 0.3

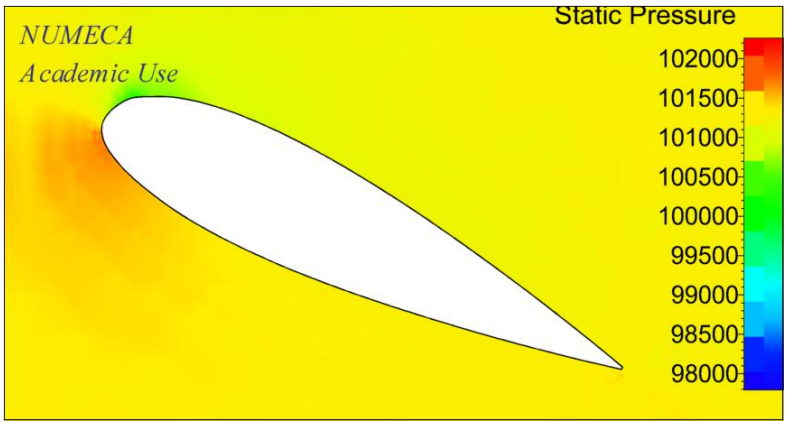

Figure 237. Distribution Static Pressure Fn 0.4

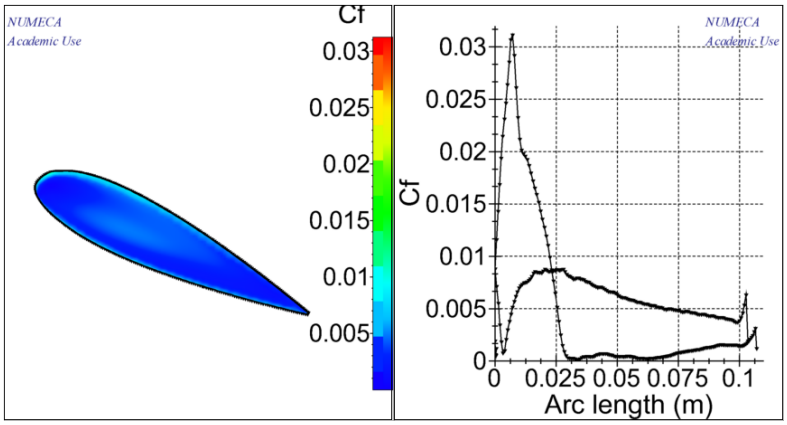

Figure 238. Coefficient Friction Fn 0.4

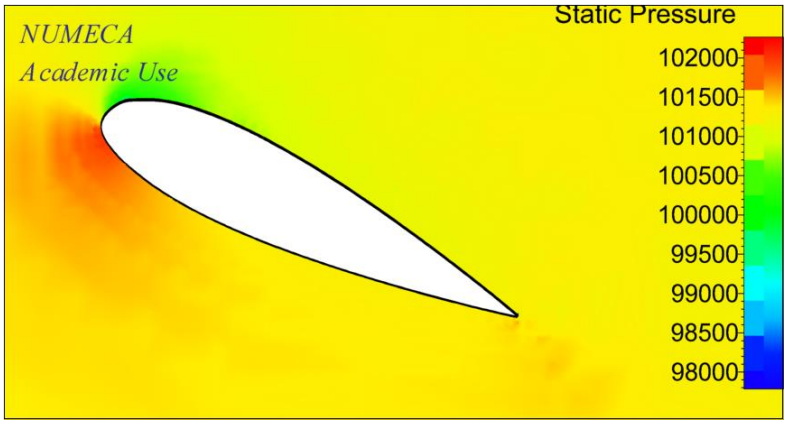

Figure 239. Distribution Static Pressure Fn 0.5

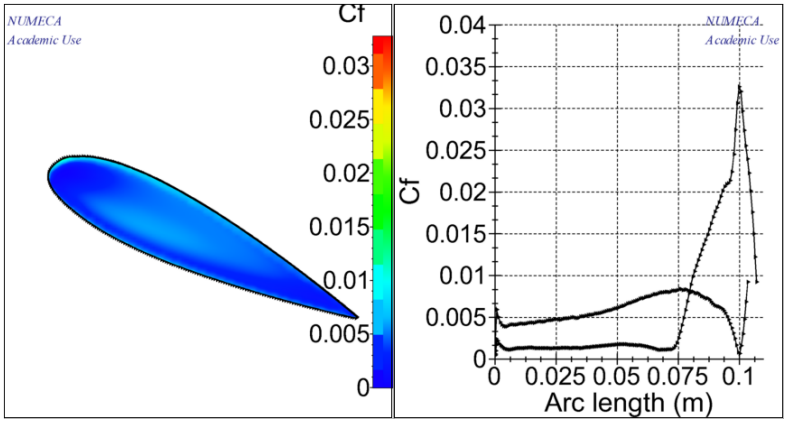

Figure 240. Coefficient Friction Fn 0.5

Attachment 214. AR 0.85 with angle of attack 25°

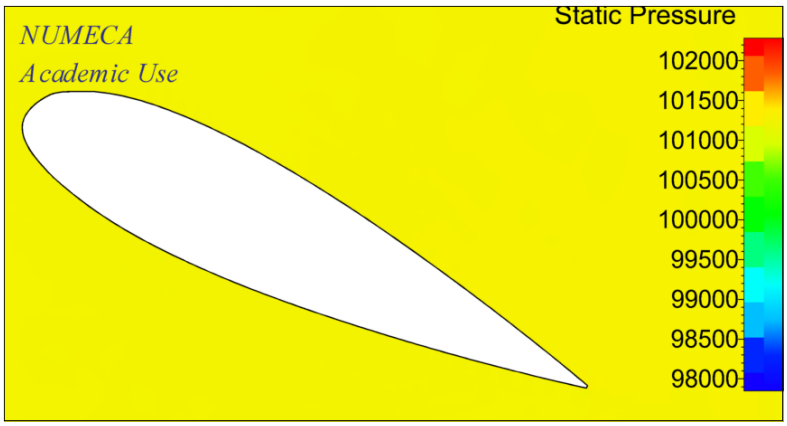

Figure 241. Distribution Static Pressure Fn 0.1

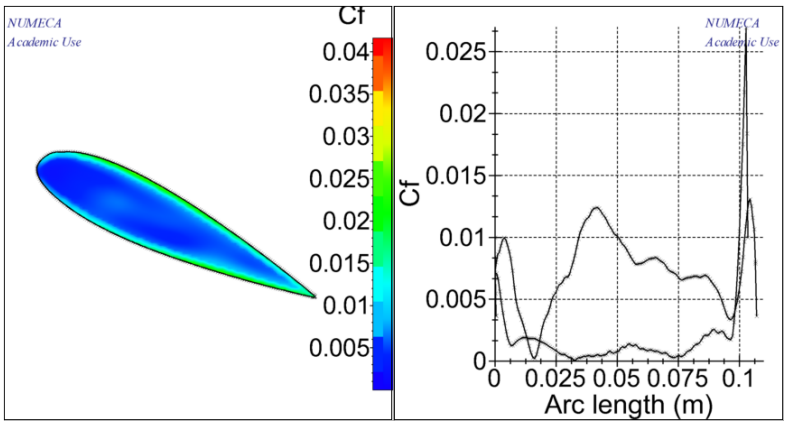

Figure 242. Coefficient Friction Fn 0.1

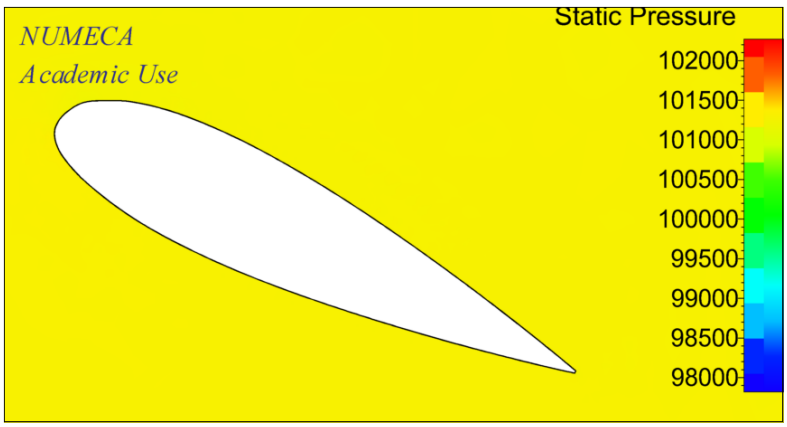

Figure 243. Distribution Static Pressure Fn 0.2

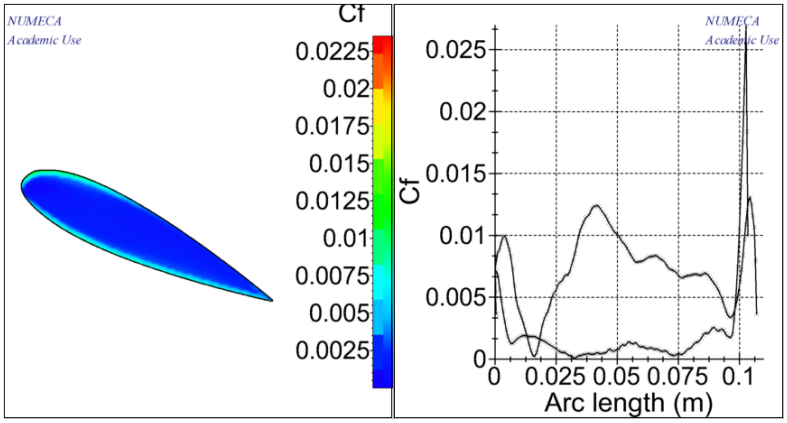

Figure 244. Coefficient Friction Fn 0.2

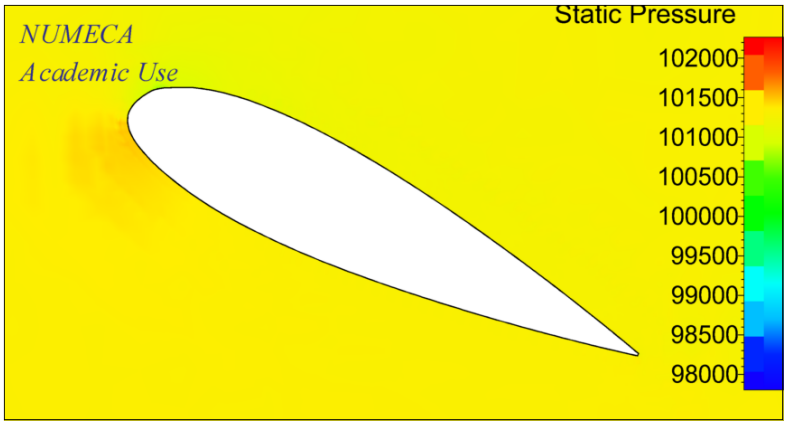

Figure 245. Distribution Static Pressure Fn 0.3

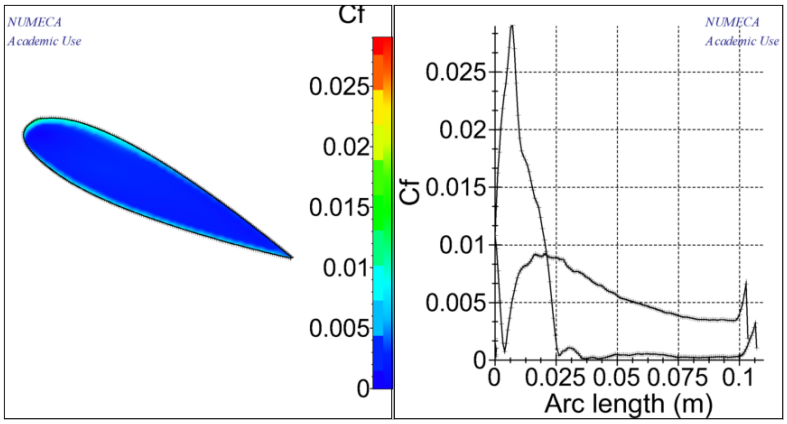

Figure 246. Coefficient Friction Fn 0.3

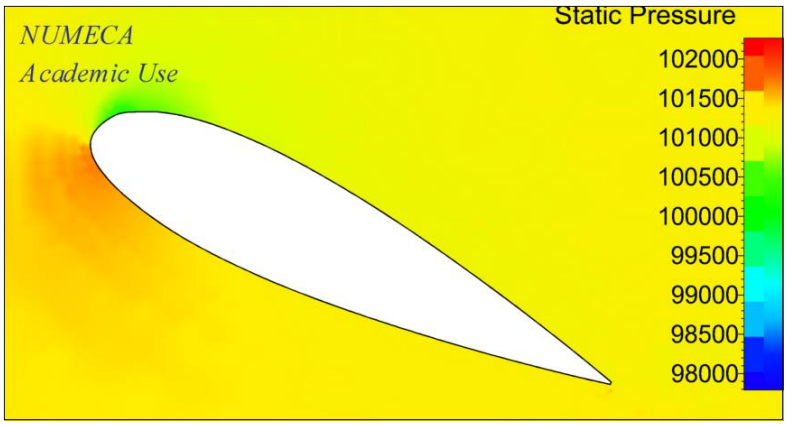

Figure 247. Distribution Static Pressure Fn 0.4

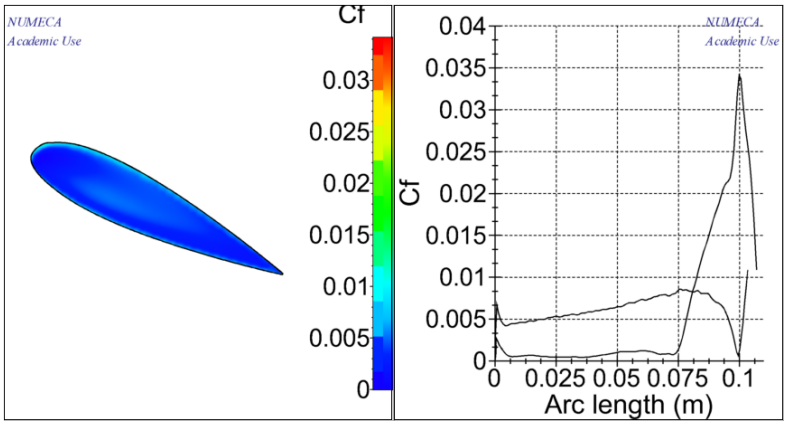

Figure 248. Coefficient Friction Fn 0.4

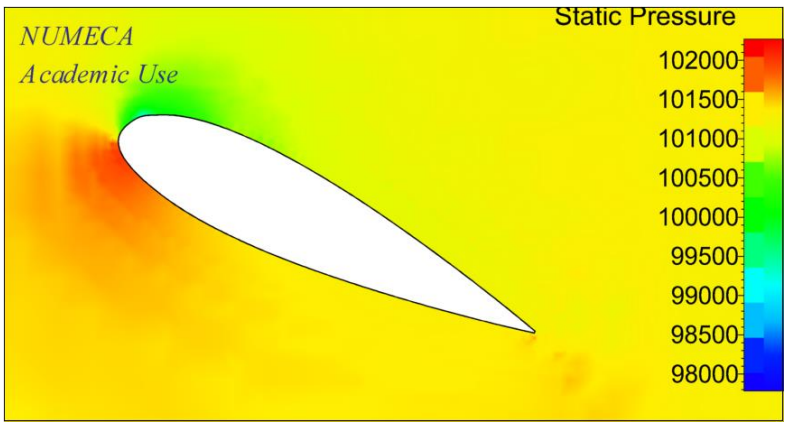

Figure 249. Distribution Static Pressure Fn 0.5

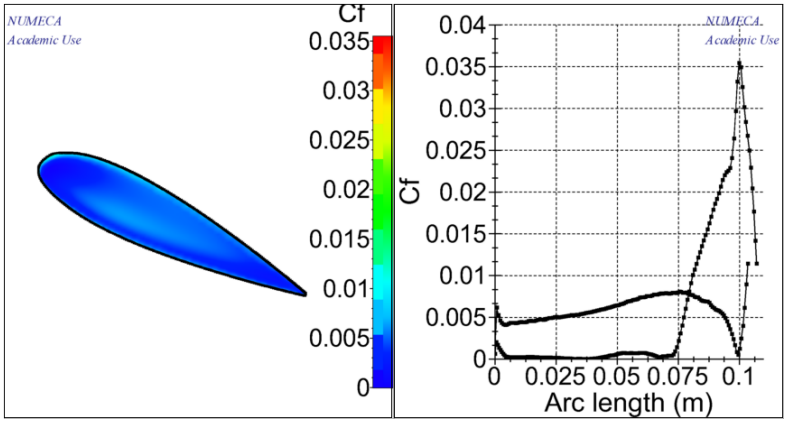

Figure 250. Coefficient Friction Fn 0.5

Fitri Puspita Dewi <fitri13@mhs.ne.its.ac.id>

Your free NUMECA student version

1 message

NUMECA Academic Group <academic@numeca.be> Fri, Mar 31, 2017 at 8:51 PM
To: fitri13@mhs.ne.its.ac.id

Hello,

Thanks for choosing *NUMECA* and its Student Version!

Please find below your login and password to access the Customer Area on www.numeca.com.

Customer Area ID
*Username: *fitri13@mhs.ne.its.ac.id
*Password: *[redacted]

*In order to ensure the security of your access,
please reset your password according to the following rules: minimum 8 characters, 1 uppercase letter, 1 lowercase letter and 1 number.*

From the Products page of the Customer Area, get started with your free *Student Version
v6.1* and download:

- the documentation archive with detailed information on the system requirements and installation notes,
- the installation archive for the selected OS,
- the tutorials archive with necessary files for the tutorials in the documentation,
- the demo cases archive with the files needed to run the demo cases described in the documentation.

Install your Student Version on the machine of your choice. At the end of the installation you will see a message suggesting to send the machine information to NUMECA. You do NOT need to do so as you may use the following *activation ID *in NUMECA's Administration Tool to activate your license:

ActivationID: [redacted]

NOTE: the license activation is based on the machine characteristics. Before changing the machine configuration (e.g. upgrade OS version, change network card...), the activation should be returned (see the installation note). Only after the return, the same activation ID can be used again to re-activate the license.

Get started with our recommended tutorials, videos and best practices for first time use:

- Beginner level Tutorial 1 of FINE™/Open with OpenLabs™: Automotive Manifold.
- Beginner level Tutorial 2 of IGG™: 2D NACA Airfoil.
- Videos for FINE™/Open with OpenLabs™: 2D Cylinder case

BIOGRAPHY

The author was born in Banjarmasin, 12 February 1995, the author is the first child of two in her family and taken formal education at MIN Teluk Dalam Banjarmasin Elementary School, SMPN 2 Banjarmasin Junior High School, and SMAN 1 Banjarmasin Senior High School. The author was graduated from SMAN 1 Banjarmasin in 2013, then continuing to bachelor degree and accepted at Institut Teknologi Sepuluh Nopember (ITS), Faculty of Marine Technology, Department of Marine Engineering in Double Degree Program with Hochschule Wismar Germany in 2013 and registered with student number 4213101005.

The author has keen of learning, not only in classes but also by doing job training, proved by job training at shipyard company, PT. IMS Indonesia (Persero) in 2015 and reliability engineering company, PT. Antakusuma Inti Raharja in 2016. The author take the Marine Manufacturing and Design (MMD) Laboratory for her concern to do research for this final project. During studying in Department of Marine Engineering, the author expect to be patient person, having good personality, friendly to everyone, and to helpful for the family, country, and community.

The author contact :

Phone : +628978703631

Email : fitripuspita95@gmail.com